1976

Two electron bond-orbital model

Chuping. Huang
College of William & Mary - Arts & Sciences

TWO ELECTRON BOND-ORBITAL MODEL

A Thesis

Presented to

The Faculty of the Department of Physics

The College of William and Mary in Virginia

In Partial Fulfillment

Of the Requirements for the Degree of

Doctor of Philosophy

---

by

Chuping Huang

June 1976

APPROVAL SHEET

This dissertation is submitted in partial fulfillment of

the requirements for the degree of

Doctor of Philosophy

Chuping Huang

Author

Approved, March 1976

Arden Sher

Arden Sher

Kenneth G. Petzinger

Kenneth G. Petzinger

Jon F. Soest

Jon F. Soest

John A. Moriarty

John A. Moriarty

R. M. White

R. M. White

Xerox Palo Alto Research Center

To my parents, Tong and Lai-Fung Wang Huang

TABLE OF CONTENTS

ACKNOWLEDGMENTS

I wish to express my gratitude to the following persons:

My advisor, Professor Arden Sher, not only for his initiating this research topic and his guidance throughout the course of work, but also for his invaluable assistance in many respects;

Dr. John A. Moriarty for his invaluable discussions and help in this work, and also for his assistance with the computer programs;

Professors Kenneth G. Petzinger, Jon F. Soest and Dr. Robert M. White for their time and care in reading of this dissertation, and for their valuable comments;

Professor Walter A. Harrison for a helpful conversation; and

Mrs. Sylvia Stout for her expert typing of this dissertation.

I would also like to give my thanks for the instructive education from the faculty of the Department of Physics in my years of graduate study.

LIST OF FIGURES

LIST OF TABLES

ABSTRACT

Harrison's one-electron bond-orbital model of tetrahedrally-coordinated solids is extended to a full two-electron model and is applied to calculate several important physical properties. All intra-bond matrix elements entering the formalism are explicitly retained, including the direct overlap integral S between anion and cation $\underline{sp}^3$ hybrid wavefunctions. Complete analytic results are obtained for the six two-electron eigenvalues and eigenstates of the anion-cation bond in terms of S, one-electron parameters V_2 and V_3, and two-electron correlation parameters V_4, V_5 and V_6. A refined formula for the dielectric constant as well as new expressions for the nuclear exchange and pseudo-dipolar coefficient, valence electron density, polarity of the bond and the cohesive energy, are then derived. A scheme for evaluating the basic parameters of the model is established, in which V_2 is fitted to the E_2 optical absorption peak of group-IV elements in the manner of Harrison and Ciraci. The remaining quantities are calculated using Hartree-Fock free-atom wavefunctions and term values. For the twenty group IV and III-V semiconductors, we find $V_5 \sim V_6 \sim 0$, but $V_4/V_2 \sim 1/2$, leading to significant correlation effects in most physical properties. The theory gives a good account of the experimentally observed trends in all properties considered, and approximate quantitative agreement is achieved for the pseudodipolar coefficient. Good agreement is also obtained for the

E_2 optical-absorption peak, the dielectric constant, the nuclear exchange coefficient and the cohesive energy of the binary compounds by scaling to experiment for the group IV elements. Calculations of the cohesive energy suggest that the intrabond overlap energy, discarded by Harrison and Ciraci, is an essential source of positive cohesion and probably rules out any major role by the interbond van der Waals interaction suggested by them. The valence electron density is found to be dominated by the polarity and the shape of the sp^3 hybrids. The preliminary indication is that long-range tails of the free-atom s and p wavefunctions must be contracted to account for the observed bond density in Si.

TWO ELECTRON BOND-ORBITAL MODEL

I. INTRODUCTION

The description of the valence bands of tetrahedrally-coordinated solids in terms of sp^3 hybrid wavefunctions has been considered at various times by a number of different workers. Among them, a model based on a linear combination of atomic orbitals (LCAO) for diamond was proposed many years ago by Hall[1] and was elaborated further by Lehman and Friedel,[2] and Coulson, Redei and Stocker[3]. More recently Weaire and Thorpe[4] generalized the model to treat topologically disordered tetrahedrally-coordinated solids in order to study the electronic structure of amorphous group IV elements.

In a recent paper Harrison[5] has introduced what he named the bond-orbital model. The important aspect of the model, which distinguishes it from previous LCAO studies, is an extra simplifying approximation that will be discussed in detail presently. Harrison and Ciraci[6] (hereafter referred to as HC) have reformulated the problem by explicitly taking into account the overlap between the anion and cation hybrids. They also have a prescription different from Harrison's[5] for determining the parameters of the model by comparison with experiments.

The bond-orbital model is able to treat a wide range of physical properties in a rather straightforward way. The properties calculated to date are: dielectric constants,[5,6,7] elastic constants,[8,9] transverse electric charges,[6,10,11,12] piezoelectric charges,[6,10,13] photoelectric thresholds,[6] magnetic susceptibilities,[14,15] x-ray core shifts,[16] surface

effects,[17,18] and energy band structure.[5,6,19,20] It has also proven to be useful in studying the 4:2-coordinated materials,[21] such as SiO_2.

In the bond-orbital model context the band structure becomes a separate question[19] and a large number of physical properties can be calculated from only a knowledge of the local properties of the anion and cation bond. Formally, the bond is equivalent to a two-electron diatomic molecule. Harrison[5] and his predecessors have treated this effective molecule in the usual one-electron molecular-orbital approximation. In a step toward a more complete treatment of the bond, Huang, Moriarty, Sher and Breckenridge[22] (hereafter referred to as HMSB) introduced a direct two-electron bond-orbital formalism. This two-electron bond-orbital model was an extension of the method of Falicov and Harris[23] for treating the hydrogen molecule. In HMSB the simplest special case of the theory was considered, i.e., the wavefunction overlap and related parameters were neglected. The theory was applied to calculate the dielectric constant, and the nuclear exchange and pseudodipolar coefficients. In this dissertation the two-electron bond-orbital model is generalized to a full quantitative theory and its application is extended to several additional physical properties. The importance of two-electron correlations is assessed in each case.

The simplicity of any bond-orbital approach rests with three approximations. First, the appropriate anion and cation $\underline{sp}^3$ hybrids are assumed to form a complete set for the description of the bond. If the $\underline{s}$ and $\underline{p}$ wavefunctions making up these hybrids are atomic-like states, this set is technically under-complete, although the choice of states can be

optimized. In a one-electron description, one then has a simple two-state eigenvalue problem and the ground-state or bond-orbital is a symmetric linear conbination of two sp^3 hybrids. In a two-electron description, a six-state eigenvalue problem must be solved. However, an exact analytic solution is still possible for the two-electron bond-orbital, as well as for all the excited states. In either case, the bond-orbitals obtained are then assumed to be orthogonal to one another in the solid. This is approximately true because the four sp^3 hybrids sharing a common atomic site are orthogonal by construction. Finally, all matrix elements linking the ground state of one bond to the excited states of its neighbors are discarded. The only interbond matrix elements permitted, and the ones that give rise to the band structure,[5,6,19] are those connecting neighboring bond-orbitals through the Hamiltonian. Then, because the valence band is full, one can make a unitary transformation from extended Bloch states to the localized bond-orbitals in calculating both the total energy and the total valence electron density of the solid. These latter quantities are then given, respectively, as a sum of the total energies and as a sum of the total electron densities of the individual bonds. They are exactly independent of the remaining interbond terms. Thus physical properties that depend only on the total energy or electron density can be calculated entirely in terms of intrabond matrix elements.

In this dissertation, after a brief review of the previous work, we obtain a complete solution of the full two-electron problem. The direct overlap matrix element between anion and cation hybrids, and the two-center Coulomb, exchange and transfer integrals, all of which were

dropped in HMSB, are included here without approximation. In Sec. III exact analytic results for the singlet and triplet eigenvalues and eigenstates are obtained. We then proceed to develop a full formal theory of several important physical properties. In addition to the dielectric constant and indirect nuclear interactions, we consider the valence electron density, the polarity of the bond and the cohesive energy. In Sec. IV a procedure for quantatively evaluating the basic parameters of the theory is established and an application of the formal results of Sec. III is made to twenty tetrahedrally-bonded solids.

II. REVIEW OF PREVIOUS WORK*

We shall now briefly summarize the bond-orbital model method as originally structured by Harrison[5] and extended by HC and HMSB. First, in the one-electron picture a bond-orbital $|b\rangle$ is constructed from a linear combination of the sp^3 hybrids $|a\rangle$ and $|c\rangle$ on adjacent anion and cation sites respectively (see Fig. 1):

$$|b\rangle = u_a|a\rangle + u_c|c\rangle . \tag{II.1}$$

The coefficients u_a and u_c are determined by minimizing the bonding energy, given by

$$E_b = \langle b|H|b\rangle / \langle b|b\rangle , \tag{II.2}$$

where H is the total Hamiltonian of the system. This process yields

$$E_b = \tfrac{1}{2}(\varepsilon_a^{HC} + \varepsilon_c^{HC}) + V_2^{HC} S - (V_2^{HC\,2} + V_3^{HC\,2})^{1/2} \tag{II.3}$$

and

$$\begin{aligned} u_a^2 &= \tfrac{1}{2}\left[(1-S\alpha_c^{HC})/(1-S^2) + \alpha_p^{HC}/(1-S^2)^{1/2}\right] \\ u_c^2 &= \tfrac{1}{2}\left[(1-S\alpha_c^{HC})/(1-S^2) - \alpha_p^{HC}/(1-S^2)^{1/2}\right] , \end{aligned} \tag{II.4}$$

where S is the overlap matrix element between $|a\rangle$ and $|c\rangle$,

---

*The content of this section is based on Ref. 5, 6, and 22. However, for coherence, the symbols used here are sometimes different from those in the original papers.

$$S = \langle a|c \rangle , \tag{II.5}$$

and

$$V_2^{HC} \equiv \left[-\langle a|H|c\rangle + \tfrac{1}{2} S \left(\varepsilon_a^{HC} + \varepsilon_c^{HC} \right) \right] / (1-S^2) \tag{II.6}$$

$$\begin{aligned} 2\, V_3^{HC} &\equiv \left(\langle c|H|c\rangle - \langle a|H|a\rangle \right) / (1-S^2)^{1/2} \\ &= \left(\varepsilon_c^{HC} - \varepsilon_a^{HC} \right) / (1-S^2)^{1/2} \end{aligned} \tag{II.7}$$

are the covalent and polar energies respectively. Also, Harison,[5] followed by HC, defined

$$\alpha_p^{HC} \equiv V_3^{HC} / \left(V_2^{HC^2} + V_3^{HC^2} \right)^{1/2} \tag{II.8}$$

and

$$\alpha_c^{HC} \equiv V_2^{HC} / \left(V_2^{HC^2} + V_3^{HC^2} \right)^{1/2} \tag{II.9}$$

as the polarity and covalency respectively. The polarity is a measure of the ionic character of the bond. For purely covalent semiconductors, such as group IV elements in the Periodic Table, $\alpha_p^{HC} = 0$ and $\alpha_c^{HC} = 1$. An antibonding state $|\bar{b}\rangle$ can also be obtained as

$$|\bar{b}\rangle = u_a |a\rangle - u_c |c\rangle , \tag{II.10}$$

with energy

$$E_{\bar{b}} = \tfrac{1}{2} \left(\varepsilon_a^{HC} + \varepsilon_c^{HC} \right) + V_2^{HC} S + \left(V_2^{HC^2} + V_3^{HC^2} \right)^{1/2} . \tag{II.11}$$

A wide range of physical properties can be predicted once V_2^{HC} and V_3^{HC} (or α_c^{HC} and α_p^{HC}) are determined. Among the calculated properties of the model, the expression for the static dielectric constant is of central importance.

$$\epsilon = 1 + \pi N (\gamma^{HC} e d)^2 \; V_2^{HC\,2} / 3 (V_2^{HC\,2} + V_3^{HC\,2})^{3/2}, \qquad \text{(II.12)}$$

where N is the average electron density, e is the electron charge, and d is the bond length. Formally, γ^{HC} enters the theory as the ratio of the distance between the center of charge of the two hybrids to the distance between the ion centers. However, it is used by Harrison[5] as a free parameter to take account of local field, d-state polarization, and other corrections to the bond-orbital model. In HC, the parameters V_2^{HC}, V_3^{HC} γ^{HC} are fitted to experiment. The energy difference between bonding and antibonding states is set equal to the principal optical absorption peak E_2

$$E_2 = E_{\bar{b}} - E_b = 2 (V_2^{HC\,2} + V_3^{HC\,2})^{1/2}. \qquad \text{(II.13)}$$

In their procedure, $2V_2^{HC}$ is fitted to experimental values of E_2 for group-IV elements. Then V_2^{HC} values are assumed to be the same for isoelectronic materials (e.g. Ge, GaAs, ZnSe . . .). For skew (cross-row) compounds, V_2^{HC} is set equal to the geometric mean of the corresponding group-IV values. γ^{HC} in Eq. (II.12) is fitted for the group-IV elements by equating the dielectric constant, with V_2^{HC} fit to E_2, to the experimental values. Then the γ^{HC} values for the other materials are found in the same way as for V_2^{HC}. Finally, V_3^{HC} is fitted for each binary compound so ϵ in Eq. (II.12) is equal to the experimental value.

HC and subsequent workers used the parameters found this way to calculate the other physical properties discussed in Sec. I with fair success. However, HC obtained negative values for the cohesive energy of most solids. This, as we shall see, resulted from some important overlap terms and the effects of correlations that were not included in their one-electron model.

Instead of treating this problem via the variational method, it is instructive to formulate the one-electron bond-orbital model as a two level eigenvalue problem of the Hamiltonian matrix

$$(H) = \begin{pmatrix} \varepsilon_a^{HC} & -V_2^{HC} \\ -V_2^{HC} & \varepsilon_c^{HC} \end{pmatrix}, \tag{II.14}$$

with $|a\rangle$ and $|c\rangle$ used as the basis functions. The two eigenvalues and eigenstates of (H) can be determined in the usual way and are exactly the same as the energies and wavefunctions of the bonding and antibonding states obtained from the variational method. In the two-electron picture this generalizes to a six-state problem, corresponding to the six ways consistent with the Pauli principle, that two spin 1/2 particles can be put into two single particle states. Then the correlation between the two electrons within one bond can be considered explicitly.

The two-electron bond-orbital model[22] is most simply and transparently formulated in the language of second quantization for the special case when the anion and cation $\underline{sp^3}$ hybrids are assumed to be orthogonal, i.e., when S = 0.

Following Falicov and Harris,[33] the Hamiltonian operator can be written

$$
\begin{aligned}
H = {} & \varepsilon_{a0}\left(n_{a\uparrow} + n_{a\downarrow}\right) + \varepsilon_{c0}\left(n_{c\uparrow} + n_{c\downarrow}\right) \\
& - V_{20}\left(c_{a\uparrow}^{+} c_{c\uparrow} + c_{a\downarrow}^{+} c_{c\downarrow} + c_{c\uparrow}^{+} c_{a\uparrow} + c_{c\downarrow}^{+} c_{a\downarrow}\right) \\
& + U_a\, n_{a\uparrow} n_{a\downarrow} + U_c\, n_{c\uparrow} n_{c\downarrow} \\
& + K\left(n_{a\uparrow} n_{c\uparrow} + n_{a\uparrow} n_{c\downarrow} + n_{a\downarrow} n_{c\uparrow} + n_{a\downarrow} n_{c\downarrow}\right) ,
\end{aligned}
\tag{II.15}
$$

where $c_{a\uparrow}^{+}$ and $c_{a\uparrow}$ etc. are the usual creation and annihilation operators and $n_{a\uparrow} = c_{a\uparrow}^{+} c_{a\uparrow}$ is the number operator. The a,c and $\uparrow,\downarrow$ subscripts denote whether an electron is on the anion or the cation and whether the spin state is up and down. Also, in Eq. (II.15) ε_{a0} (ε_{c0}) is the energy associated with an electron when it is on the anion (cation). V_{20} is the transfer or hopping energy needed for an electron to hop from anion (cation) to cation (anion). $U_{a,c}$ and K are the Coulomb repulsion energies of the two electrons when they are on the same ion or on different ions respectively.

By using the fact that there are two electrons in a bond, Eq. (II.15) can be simplified to

$$
H = \varepsilon_{a0} + \varepsilon_{c0} + K + V_{20} H' \quad , \tag{II.16}
$$

where

$$
H' = X_a\, n_{a\uparrow} n_{a\downarrow} + X_c\, n_{c\uparrow} n_{c\downarrow} - \left(c_{a\uparrow}^{+} c_{c\uparrow} + c_{a\downarrow}^{+} c_{c\downarrow} + c_{c\uparrow}^{+} c_{a\uparrow} + c_{c\downarrow}^{+} c_{a\downarrow}\right) ; \tag{II.17}
$$

and

$$
\begin{aligned}
X_a &= \left(U_a - K\right)/V_{20} - \left(\varepsilon_{c0} - \varepsilon_{a0}\right)/V_{20} \quad , \\
X_c &= \left(U_c - K\right)/V_{20} + \left(\varepsilon_{c0} - \varepsilon_{a0}\right)/V_{20} \quad .
\end{aligned}
\tag{II.18}
$$

If $\varepsilon_{a0} = \varepsilon_{c0}$ and $U_a = U_c$, then the Hamiltonian H given by Eq. (II.17) is formally equivalent to that considered by Falicov and Harris.[23] This corresponds to homopolar solids, and is called the Falicov-Harris limit (hereafter referred to as the FH limit).

There are six linearly independent two-electron states in terms of which all the eigenstates of H can be expressed. They are $|a\uparrow c\uparrow\rangle$, $|a\downarrow c\downarrow\rangle$, $|a\uparrow a\downarrow\rangle$, $|c\uparrow c\downarrow\rangle$, $|a\uparrow c\downarrow\rangle$, and $|c\uparrow a\downarrow\rangle$; where $|a\uparrow c\uparrow\rangle$ means $C_{a\uparrow}^{+} C_{c\uparrow}^{+} |0\rangle$. The eigenvalues and eigenfunctions can be obtained by solving the six by six secular equation

$$\begin{vmatrix} -E_M' & 0 & 0 & 0 & 0 & 0 \\ 0 & -E_M' & 0 & 0 & 0 & 0 \\ 0 & 0 & X_a - E_M' & 0 & -1 & -1 \\ 0 & 0 & 0 & X_c - E_M' & -1 & -1 \\ 0 & 0 & -1 & -1 & -E_M' & 0 \\ 0 & 0 & -1 & -1 & 0 & -E_M' \end{vmatrix} = 0 \quad , \tag{II.19}$$

where E_M' is defined by the expression

$$E_M = \varepsilon_{a0} + \varepsilon_{c0} + K + V_{20} E_M' . \tag{II.20}$$

One then finds three triplet energies that are degenerate, with energy

$$E_M = \varepsilon_{a0} + \varepsilon_{c0} + K \quad , \qquad M = \text{I}, \text{II}, \text{III} \tag{II.21}$$

and three singlet energies

$$E_M = \varepsilon_{a0} + \varepsilon_{c0} + K + V_{20} E_M' \quad , \qquad M = \text{IV}, \text{V}, \text{VI} \quad , \tag{II.22a}$$

where the E'_M are the solutions of the cubic equation

$$E'^3_M - (X_a + X_c) E'^2_M + (X_c X_a - 4) E'_M + 2(X_a + X_c) = 0 \,. \qquad \text{(II.22b)}$$

In the limit (hereafter called the Harrison limit) where the correlation energies are set to zero, the Harrison one-electron results[5,6] are regained. Then, Eq. (II.22b) can be factorized

$$E_{IV} = \varepsilon_{a0} + \varepsilon_{c0}$$

and (II.23)

$$E_{V,\,VI} = \varepsilon_{a0} + \varepsilon_{c0} \pm 2(V_{20}^2 + V_{30}^2) \,,$$

where

$$2V_{30} = \varepsilon_{c0} - \varepsilon_{a0} \,. \qquad \text{(II.24)}$$

The energies E_{VI} and E_V equal twice the bonding and antibonding energies of HC for S = 0.

For the homopolar case the subscripts a and c are dropped and the three roots of Eq. (II.22b) become

$$E_{IV} = 2\varepsilon_0 + K + 2V_{40}$$

and (II.25)

$$E_{V,\,VI} = 2\varepsilon_0 + K + V_{40} \pm (4V_{20}^2 + V_{40}^2)^{1/2} \,,$$

where

$$2V_{40} = U - K \,. \qquad \text{(II.26)}$$

Comparing Eq. (II.25) and Eq. (II.23) with $\varepsilon_{a0} = \varepsilon_{c0}$ $(V_{30} = 0)$, makes the effect of correlation transparent. The details of the energy shifts due to correlation and overlap effects are discussed in Sec. III.

Given the eigenvalues, the eigenfunctions can be found. For the three triplet states they are

$$|I\rangle = |a\uparrow c\uparrow\rangle$$

$$|II\rangle = |a\downarrow c\downarrow\rangle \tag{II.27}$$

$$|III\rangle = \frac{1}{\sqrt{2}}\left(|a\uparrow c\downarrow\rangle - |c\uparrow a\downarrow\rangle\right) ,$$

and for the singlet states they are

$$|M\rangle = [1/D'(E'_M)]\left[(X_c - E'_M)|a\uparrow a\downarrow\rangle + (X_a - E'_M)|c\uparrow c\downarrow\rangle + \tfrac{1}{2}(X_a - E'_M)(X_c - E'_M)\left(|a\uparrow c\downarrow\rangle + |c\uparrow a\downarrow\rangle\right)\right] , \tag{II.28}$$

$$M = IV, V, VI ,$$

where

$$D'(E'_M) = \left[(X_c - E'_M)^2 + (X_a - E'_M)^2 + \tfrac{1}{2}(X_c - E'_M)^2(X_a - E'_M)^2\right]^{1/2} . \tag{II.29}$$

The dielectric constant and the indirect nuclear interaction coefficients will now be obtained by perturbation theory.

Because of the tetrahedral symmetry the dielectric constant is isotropic. Thus one can suppose for simplicity that the electric field $\vec{\mathcal{E}}$ is along the positive x-axis in the [100] direction. Then the perturbing Hamiltonian is

$$H_{\mathcal{E}} = \left[-(\bar{x}_c - \bar{x}_a) - (d\gamma'/2\sqrt{3})(n_{a\uparrow} + n_{a\downarrow}) + (d\gamma'/2\sqrt{3})(n_{c\uparrow} + n_{c\downarrow})\right] e\mathcal{E} , \tag{II.30}$$

where

$$\bar{x}_n = \left|\langle \phi_{n\uparrow} | x_n | \phi_{n\uparrow}\rangle\right| , \qquad n = a, c , \tag{II.31}$$

and

$$\gamma' = 1 - \sqrt{3}\,(\bar{x}_a + \bar{x}_c)/d \,. \tag{II.32}$$

Carrying out perturbation theory to second order one finds the electric susceptibility

$$\chi = -Ne^2 \sum_{M=I,\Gamma} \frac{\langle G|H_\varepsilon|M\rangle\langle M|H_\varepsilon|G\rangle}{E_G - E_M} \,, \tag{II.33}$$

where N is the average electron density. Equation (II.33) reduces to the HC expression for the dielectric constant, i.e. Eq. (II.12) in the Harrison limit. In the FH limit one finds

$$\epsilon = 1 + \tfrac{1}{3}\pi N (\gamma' e d)^2 (1/V_{20}\beta_0) \,, \tag{II.34}$$

where

$$\begin{aligned}\beta_0 &= \tfrac{1}{32}\left[X_0(X_0^2+16) + (X_0^2+8)(X_0^2+16)^{1/2}\right] \\ &= 1 + \tfrac{1}{2}X_0 + \tfrac{5}{32}X_0^2 + \cdots\end{aligned} \tag{II.35}$$

with

$$X_0 = 2V_{40}/V_{20} \,. \tag{II.36}$$

There are two kinds of indirect interactions between neighboring nuclear moments that are coupled through the electrons. The first called the indirect exchange interaction is isotropic. The second, called the pseudodipolar interaction, has the angular dependence of a dipole-dipole interaction. For the forms of these indirect interactions see Eq. (II.45).

To calculate the indirect nuclear magnetic interactions, one starts from the perturbing Hamiltonian that couples the nuclear and electron magnetic moments:

$$H_A = \Delta_a (n_{a\uparrow} - n_{a\downarrow}) + \Delta_c (n_{c\uparrow} - n_{c\downarrow}) + \delta'_a c^+_{a\uparrow} c_{a\downarrow} + \delta'^*_a c^+_{a\downarrow} c_{a\uparrow} + \delta'_c c^+_{c\uparrow} c_{c\downarrow} + \delta'^*_c c^+_{c\downarrow} c_{c\uparrow} \quad , \tag{II.37}$$

where

$$\Delta_a = \vec{I}_a \cdot \overleftrightarrow{A}_a \cdot \hat{z}$$

and

$$\delta'_a = \vec{I}_a \cdot \overleftrightarrow{A}_a \cdot (\hat{x} - i\hat{y}) \tag{II.38}$$

with

$$\overleftrightarrow{A}_n = \langle \phi_{n\uparrow} | \mu_B \hbar \gamma_n \left[\frac{8}{3} \pi \delta(\vec{r}) \overleftrightarrow{1} + \frac{1}{r^3} \left(\frac{3 \hat{r} \hat{r}}{r^2} - \overleftrightarrow{1} \right) \right] | \phi_{n\uparrow} \rangle, \quad n = a, c. \tag{II.39}$$

In Eq. (II.39) $|\phi_{n\uparrow}\rangle$ is an $\underline{sp}^3$ hybrid wavefunction on site n. The ground state energy shift calculated to second order is

$$\Delta E = - \left[(\delta'_a - \delta'_c)(\delta'^*_a - \delta'^*_c) + (\Delta_a - \Delta_c)^2 \right] / E_o' \quad , \tag{II.40}$$

where

$$E_o'^{-1} = -\tfrac{1}{2} (X_a - E'_G)^2 (X_c - E'_G)^2 / V_{20} E'_G D'^2(E'_G) \quad . \tag{II.41}$$

Eq. (II.40) can be expressed more explicitly as

$$\Delta E = - \left(\vec{I}_a \cdot \overleftrightarrow{A}_a \cdot \overleftrightarrow{A}_a \cdot \vec{I}_a + \vec{I}_c \cdot \overleftrightarrow{A}_c \cdot \overleftrightarrow{A}_c \cdot \vec{I}_c - 2 \vec{I}_a \cdot \overleftrightarrow{A}_a \cdot \overleftrightarrow{A}_c \cdot \vec{I}_c \right) / E_o' \tag{II.42}$$

$$= - \Delta E_{aa} - \Delta E_{cc} + \Delta E_{ac} \quad .$$

If one inserts $\underline{sp}^3$ hybrids for $|\phi_{at}\rangle$ and $|\phi_{ct}\rangle$ and lets $\hat{r}_{ac}$ be a unit vector directed from the anion to the cation, one has

$$\overleftrightarrow{A}_a = \tfrac{1}{2}\mu_B \hbar \gamma_a \left[\tfrac{1}{3} \delta^a_{aa} \overleftrightarrow{1} + \tfrac{3}{5} \rho^a_{aa} \left(3 \hat{r}_{ac} \hat{r}_{ac} - \overleftrightarrow{1}\right)\right] , \qquad \text{(II.43)}$$

where all the overlap terms have been discarded. Retaining only

$$\delta^a_{aa} = 4\pi \langle \underline{S}_a | \delta(\vec{r}) | \underline{S}_a \rangle = R_S^2(0) \qquad \text{(II.44a)}$$

and

$$\rho^a_{aa} = \langle \underline{P}_a | r^{-3} | \underline{P}_a \rangle , \qquad \text{(II.44b)}$$

the energy shift ΔE_{ac} becomes

$$\Delta E_{ac} = \Gamma_e \vec{I}_a \cdot \vec{I}_c + \Gamma_{Pd} \left[3(\vec{I}_a \cdot \hat{r}_{ac})(\hat{r}_{ac} \cdot \vec{I}_c) - \vec{I}_a \cdot \vec{I}_c\right] . \qquad \text{(II.45)}$$

In Eq. (II.45) Γ_e and Γ_{Pd} are the nuclear exchange and pseudodipolar interaction coefficients, respectively. These have the form

$$\Gamma_e = \mu_B^2 \hbar^2 \gamma_a \gamma_c \left(\tfrac{1}{18} \delta^a_{aa} \delta^c_{cc} + \tfrac{9}{25} \rho^a_{aa} \rho^c_{cc}\right) / E_o' ,$$

and $\qquad \text{(II.46)}$

$$\Gamma_{Pd} = \mu_B^2 \hbar^2 \gamma_a \gamma_c \left[\tfrac{1}{10} \left(\delta^a_{aa} \rho^c_{cc} + \delta^c_{cc} \rho^a_{aa}\right) + \tfrac{9}{50} \rho^a_{aa} \rho^c_{cc}\right] / E_o' .$$

Notice that all the intrabond dependence is in E_o' . In the FH limit $E_o'^{-1}$ is given as

$$E_o'^{-1} = \left(1/4 V_{20}\right) \xi_0 , \qquad \text{(II.47)}$$

where

$$\xi_0 = \tfrac{1}{2}\left[X_0^2 + 8 + X_0 (X_0^2 + 16)^{1/2} \right] / (X_0^2 + 16)^{1/2}$$
$$= 1 + \tfrac{1}{2} X_0 + \tfrac{3}{32} X_0^2 + \cdots \quad . \tag{II.48}$$

While in the Harrison limit it is given by

$$E_0'^{-1} = \tfrac{1}{4} V_{20}^2 / (V_{20}^2 + V_{30}^2)^{3/2} \quad . \tag{II.49}$$

It is interesting to notice that in the Harrison limit one finds both the expressions for the dielectric constant and the indirect nuclear interaction coefficients have the same dependence on V_{20} and V_{30}. Using this fact, one may obtain a simple relationship between ϵ and Γ_e or Γ_{Pd}

$$\epsilon - 1 = C \Gamma_e / d \quad , \tag{II.50}$$

where

$$C = \sqrt{3}\,\pi (\gamma' e)^2 / \left[\mu_B^2 \hbar^2 \gamma_a \gamma_c \left(\tfrac{1}{18} \delta^a_{aa} \delta^c_{cc} + \tfrac{9}{25} P^a_{aa} P^c_{cc} \right) \right] . \tag{II.51}$$

We reserve a detailed discussion of this point as well as the other special cases reviewed above until the full theory ($S \neq 0$) is developed in the following section.

III. FORMULATION OF THE FULL TWO ELECTRON BOND-ORBITAL MODEL

A. Eigenvalues and Eigenstates

When the overlap between anion and cation hybrids is retained, the second-quantization formalism described in Sec. II loses its simplicity and elegance. Thus we revert to a spatial representation.

It is possible to continue to use $|a\uparrow c\uparrow\rangle$, $|a\downarrow c\downarrow\rangle$, $|a\uparrow a\downarrow\rangle$, $|c\uparrow c\downarrow\rangle$, $|a\uparrow c\downarrow\rangle$ and $|c\uparrow a\downarrow\rangle$ as the six basis states. However both the physics and the mathematics are simplified if we make linear combinations of the six states and choose a basis set of three singlet and three triplet states from the outset. Then the six-by-six Hamiltonian matrix block diagonalizes into two three-by-three blocks. One of these two blocks, that associated with the triplet states, is also diagonal with all three diagonal elements equal.

We begin by defining three orthonomal triplet states in the coordinate representation:

$$
\begin{aligned}
|1\rangle &= \frac{1}{\sqrt{1-S^2}}\,|a\uparrow c\uparrow\rangle = \Phi_A(\vec{r}_1,\vec{r}_2)\,\sigma_\uparrow(1)\,\sigma_\uparrow(2)\,, \\
|2\rangle &= \frac{1}{\sqrt{1-S^2}}\,|a\downarrow c\downarrow\rangle = \Phi_A(\vec{r}_1,\vec{r}_2)\,\sigma_\downarrow(1)\,\sigma_\downarrow(2)\,, \\
|3\rangle &= \frac{1}{\sqrt{2(1-S^2)}}\left(|a\uparrow c\downarrow\rangle - |c\uparrow a\downarrow\rangle\right) = \frac{1}{\sqrt{2}}\,\Phi_A(\vec{r}_1,\vec{r}_2)\left[\sigma_\uparrow(1)\sigma_\downarrow(2) + \sigma_\uparrow(2)\sigma_\downarrow(1)\right],
\end{aligned}
\tag{III.1}
$$

where $\Phi_A(\vec{r}_1,\vec{r}_2)$ is the anti-symmetric spatial function

$$
\Phi_A(\vec{r}_1,\vec{r}_2) = \frac{1}{\sqrt{2(1-S^2)}}\left[\phi_a(\vec{r}_1)\phi_c(\vec{r}_2) - \phi_c(\vec{r}_1)\,\phi_a(\vec{r}_2)\right]. \tag{III.2}
$$

Again S is the overlap integral

$$S = \int \phi_a^*(\vec{r})\, \phi_c(\vec{r})\, d\vec{r} \ . \qquad \text{(III.3)}$$

In Eqs. (III.1), (III.2) and (III.3) $\phi_a(\vec{r})$ and $\phi_c(\vec{r})$ are, respectively, the anion and cation hybrid wavefunctions. We next define three normalized singlet states:

$$\begin{aligned} |4\rangle &= |a\uparrow a\downarrow\rangle = \phi_a(\vec{r}_1)\,\phi_a(\vec{r}_2)\,\Sigma_A \ , \\ |5\rangle &= |c\uparrow c\downarrow\rangle = \phi_c(\vec{r}_1)\,\phi_c(\vec{r}_2)\,\Sigma_A \ , \\ |6\rangle &= \frac{1}{\sqrt{2(1+S^2)}}\left(|a\uparrow c\downarrow\rangle + |c\uparrow a\downarrow\rangle\right) = \frac{1}{\sqrt{2(1+S^2)}}\left[\phi_a(\vec{r}_1)\phi_c(\vec{r}_2) + \phi_c(\vec{r}_1)\phi_a(\vec{r}_2)\right]\Sigma_A \ , \end{aligned} \qquad \text{(III.4)}$$

where Σ_A is the antisymmetric spin function

$$\Sigma_A = \frac{1}{\sqrt{2}}\left[\sigma_\uparrow(1)\,\sigma_\downarrow(2) - \sigma_\uparrow(2)\,\sigma_\downarrow(1)\right] . \qquad \text{(III.5)}$$

The singlets are automatically orthogonal to the triplets because of the orthogonality of $\sigma_\uparrow$ and $\sigma_\downarrow$, but the singlets are not mutually orthogonal to one another:

$$\langle 4|5\rangle = S^2 \ ,$$

and

$$\langle 4|6\rangle = \langle 5|6\rangle = \sqrt{\frac{2S^2}{1+S^2}} \ . \qquad \text{(III.6)}$$

1. Eigenvalues

The two-electron Hamiltonian operator has the form

$$H(\vec{r}_1,\vec{r}_2) = H_0(\vec{r}_1) + H_0(\vec{r}_2) + \frac{e^2}{|\vec{r}_1 - \vec{r}_2|} \ , \qquad \text{(III.7)}$$

where H_0 is the sum of a kinetic energy operator T and an external potential V_{ext}

$$H_o(\vec{r}) = T(\vec{r}) + V_{ext}(\vec{r}) \, . \qquad \text{(III.8)}$$

The quantity V_{ext} includes the bare-ion potential from the anion and the cation plus the potential associated with all other bonds in the crystal. Because the full Hamiltonian H has no spin-operator dependence, all matrix elements coupling singlet and triplet states vanish, and the secular determinant has the simple block structure

$$\left| \begin{array}{c|c} E_T - E & \\ \hline & \langle i|H|j\rangle - \langle i|j\rangle E \\ & i, j = 4, 5, 6 \end{array} \right| = 0 \, , \qquad \text{(III.9)}$$

where $E_T = \langle 1|H|1\rangle = \langle \Phi_A|H|\Phi_A\rangle$. We may write out the matrix elements entering Eq. (III.9) explicitly in terms of familiar one- and two-center integrals. We define the one-electron expectation values

$$\varepsilon_{no} = \int \phi_n^*(\vec{r}) \, H_o(\vec{r}) \, \phi_n(\vec{r}) \, d\vec{r} \, , \qquad n = a, c \, , \qquad \text{(III.10)}$$

and the (positive) transfer or hopping integral

$$V_{2o} = - \int \phi_a^*(\vec{r}) \, H_o(\vec{r}) \, \phi_c(\vec{r}) \, d\vec{r} \, . \qquad \text{(III.11)}$$

Note ε_{no} and V_{20} are defined in the same way in Sec. II. All of the two-center Coulomb integrals have the form

$$I(nn'|mm') = \int \phi_n^*(\vec{r}_1) \, \phi_{n'}(\vec{r}_2) \, \frac{e^2}{|\vec{r}_1 - \vec{r}_2|} \, \phi_m(\vec{r}_1) \, \phi_{m'}(\vec{r}_2) \, d\vec{r}_1 \, d\vec{r}_2 \, , \qquad \text{(III.12)}$$

$$m, m', n, n' = a, c \, .$$

The Coulomb repulsive energy of two electrons on the same ion site is

$$U_n = I(nn|nn), \quad n = a, c, \tag{III.13}$$

while the corresponding energy with one electron on each site is

$$K = I(ac|ac), \tag{III.14}$$

The exchange energy is

$$J = I(ac|ca), \tag{III.15}$$

and finally the transfer energy (analogous to V_{20}) is

$$H_n = I(nn|ac), \quad n = a, c. \tag{III.16}$$

Note that H_n is called the hybrid integral in Ref. (24). It is easily seen from Eq. (III.12) that J and H_n, unlike U_n and K, will vanish as $S \to 0$, so that they can be neglected together with S in the limit that S is small. In the real semiconductors of interest, the overlap is large, $S \sim 0.6$, and J and H_n will have comparable magnitudes to U_n and K. Our calculations which are discussed in Sec. IV, show that for homopolar solids like the group IV elements

$$U > K > H > J \tag{III.17}$$

with $J \sim \frac{1}{2} U$. Similar trends exist for the binary compounds, where in addition

$$U_a > U_c \quad \text{and} \quad H_a > H_c, \tag{III.18}$$

because the anion hybrid is usually less spacially extended than the

cation hybrid. In our calculations Eq. (III.18) holds for all III-V compounds except BP and BAs where the inequalities are reversed, as discussed in Sec. IV.

The block in Eq. (III.9) associated with the singlet states with the parameters defined above becomes

$$\begin{vmatrix} 2\mathcal{E}_{a0}+U_a-E_M & -2SV_{20}+J-S^2E_M & \sqrt{\frac{2}{1+S^2}}(S\mathcal{E}_{a0}-V_{20}+H_a-SE_M) \\ -2SV_{20}+J-S^2E_M & 2\mathcal{E}_{c0}+U_c-E_M & \sqrt{\frac{2}{1+S^2}}(S\mathcal{E}_{c0}-V_{20}+H_c-SE_M) \\ \sqrt{\frac{2}{1+S^2}}(S\mathcal{E}_{a0}-V_{20}+H_a-SE_M) & \sqrt{\frac{2}{1+S^2}}(S\mathcal{E}_{c0}-V_{20}+H_c-SE_M) & \frac{1}{1+S^2}(\mathcal{E}_{a0}+\mathcal{E}_{c0}-2SV_{20}+K+J)-E_M \end{vmatrix} = 0 \quad \text{(III.19)}$$

$$M = \text{IV}, \text{V}, \text{VI} ,$$

and the energy for the degenerate triplet states is immediately given by

$$E_M = E_T = \frac{1}{1-S^2}(\mathcal{E}_{a0}+\mathcal{E}_{c0}+K+2SV_{20}-J), \quad M = \text{I}, \text{II}, \text{III} . \quad \text{(III.20)}$$

In order to simplify the analysis and to make contact with HC and HMSB, it is useful to define the following combinations of the above quantities:

$$\begin{aligned} \mathcal{E}_n &\equiv \mathcal{E}_{n0}+K , \qquad n = a, c , \\ V_2^\circ &\equiv V_{20}-\tfrac{1}{2}(H_a+H_c)+\tfrac{1}{2}S(\mathcal{E}_a+\mathcal{E}_c) , \\ V_3^\circ &\equiv \tfrac{1}{2}[(\mathcal{E}_c-\mathcal{E}_a)-\tfrac{1}{2}(U_a-U_c)], \\ V_4^\circ &\equiv \tfrac{1}{2}[\tfrac{1}{2}(U_a+U_c)-K] , \\ V_5^\circ &\equiv \tfrac{1}{2}[\tfrac{1}{2}S(U_a-U_c)-(H_a-H_c)] , \end{aligned} \quad \text{(III.21)}$$

and

$$V_6^\circ \equiv S(H_a+H_c)-J-S^2K .$$

Because of the overall charge neutrality of the solid, its energy levels will depend only on absolute differences of the one- and two-center Coulomb integrals defined in Eqs. (III.10)-(III.16). The energies defined in Eq. (III.21) correctly reflect this fact. For example, the addition of K to ε_{a0} has the effect of screening the bare-ion potential arising from the cation and gives ε_a a magnitude close to a Hartree-Fock expectation value. To see this one writes

$$\varepsilon_a = \varepsilon_{a0} + K = \int \phi_a^*(\vec{r})\,(T(\vec{r}) + V_a(\vec{r}))\,\phi_a(\vec{r})\,d\vec{r}$$
$$+ \int \phi_a^*(\vec{r}) \left[V_c(\vec{r}) + \int (e^2 \phi_c^*(\vec{r}')\phi_c(\vec{r}')/|\vec{r}-\vec{r}'|)\,d\vec{r}' \right] \phi_a(\vec{r})\,d\vec{r} \qquad \text{(III.22)}$$
$$+ \sum_{i \neq a,c} \int \phi_a^*(\vec{r})\, V_i(\vec{r})\, \phi_a(\vec{r})\,d\vec{r} \ .$$

The first term on the right-hand side of Eq. (III.22) is just the Hartree-Fock expectation value of $(T + v_a(\vec{r}))$. The second and third terms vanish identically in the limit that $\phi_a(\vec{r})$ and $\phi_c(\vec{r})$ do not overlap. Then $\frac{1}{2}(\varepsilon_a + \varepsilon_c)$ is the center of gravity of the one-electron band structure and the term $\frac{1}{2} S(\varepsilon_a + \varepsilon_c)$ in Eq. (III.21) removes exactly the dependence of V_{20} on the zero of energy. The energies V_2^0 and V_3^0 are conceptually similar to the one-electron HC parameters which we denoted as V_2^{HC} and V_2^{HC}. The quantities $\frac{1}{2}(H_a + H_c)$ and $\frac{1}{2}(U_a - U_c)$ are appropriate average values of the electron-electron interaction, which physically screen V_{ext} and reduces the magnitudes of V_2^0 and V_3^0. More specifically, V_2^0 and V_3^0 are derivable from the one-electron Hamiltonian

$$H_{one}(\vec{r}) = H_0(\vec{r}) + \tfrac{1}{2} \int \frac{[\phi_a^*(\vec{r}')\phi_a(\vec{r}') + \phi_c^*(\vec{r}')\phi_c(\vec{r}')]}{|\vec{r} - \vec{r}'|} d\vec{r}' - \tfrac{1}{2}(\varepsilon_a + \varepsilon_c) \qquad \text{(III.23)}$$

by the tight-binding formulas (also see in Sec. II).

$$V_2^0 = -\langle \phi_a | H_{one} | \phi_c \rangle,$$
$$V_3^0 = \tfrac{1}{2}\left[\langle \phi_c | H_{one} | \phi_c \rangle - \langle \phi_a | H_{one} | \phi_a \rangle\right]. \qquad \text{(III.24)}$$

We emphasize, however, that V_2^0 and V_3^0 enter the present theory only as definitions. All the two-electron correlation corrections to the screening are included exactly through the remaining parameters V_4^0, V_5^0 and V_6^0. The quantity V_4^0 is the difference between the average repulsive energy when both electrons are on one ion and the repulsive energy when the two electrons are on different ions. V_4^0 remains finite even in the limit $S \to 0$, while V_5^0 and V_6^0 vanish in this limit. Interestingly, even for large values of S, our calculated values of V_5^0 and V_6^0 always turn out to be negligible (see Table III), and the dominant correlation parameter is V_4^0 (as in the case when $S \to 0$).

Finally, we should point out the symmetry properties of our new quantities. The energies V_2^0, V_4^0 and V_6^0 involve symmetric quantities V_{20}, S, K and J. Consequently, V_2^0, V_4^0 and V_6^0 are covalent energies that depend primarily on bond length and not on the polarity of the bond. The energies V_3^0 and V_5^0, on the other hand, are antisymmetric in ε_n, U_n and H_n and thus vanish identically for homopolar solids. We may already anticipate that for negligible V_5^0 and V_6^0 the effect of two-electron correlation will be to increase the covalency and decrease the polarity of the bond in binary compounds, because $V_4^0 > 0$ $(U_a + U_c > 2K)$.

The eigenvalue E_T, Eq. (III.20), associated with the degenerate triplet states can be rewritten as

$$E_M = E_T = \varepsilon_a + \varepsilon_c - K + (2S V_2^\circ + V_6^\circ)/(1-S^2), \quad M = \text{I}, \text{II}, \text{III}. \qquad \text{(III.25)}$$

By making changes in Eq. (III.19) the eigenvalues associated with the three singlet states may be written now as

$$E_M = \varepsilon_a + \varepsilon_c - K + E_M^\circ, \quad M = \text{IV}, \text{V}, \text{VI}, \qquad \text{(III.26)}$$

where E_M^0 is a solution of the determinantal equation

$$\begin{vmatrix} 2V_4^\circ - 2V_3^\circ - E_M^\circ & 2SV_2^\circ - V_6^\circ - S^2E_M^\circ & -V_2^\circ - SV_3^\circ - V_5^\circ - SE_M^\circ \\ -2SV_2^\circ - V_6^\circ - S^2E_M^\circ & 2V_4^\circ + 2V_3^\circ - E_M^\circ & -V_2^\circ + SV_3^\circ + V_5^\circ - SE_M^\circ \\ -V_2^\circ - SV_3^\circ - V_5^\circ - SE_M^\circ & -V_2^\circ + SV_3^\circ + V_5^\circ - SE_M^\circ & \tfrac{1}{2}[-2SV_2^\circ - V_6^\circ - (1+S^2)E_M^\circ] \end{vmatrix} = 0 \qquad \text{(III.27)}$$

Equation (III.27) is a cubic equation in E_M^0. The physical content of the solutions of Eq. (III.27) is most transparent in the two special cases where this equation factors. These cases are: (1) $V_3^0 = V_5^0 = 0$, which is the appropriate solution for the group IV elements, and (2) $V_4^0 = V_5^0 = V_6^0 = 0$, which is the limit of no two-electron correlation. We again denote the former case as the Falicov-Harris limit (hereafter referred to as the FH limit) and the latter as the Harrison limit.

In the FH limit the energy eigenvalues and the splittings between them may be expressed as

$$\begin{aligned} E_{\text{I, II, III}} &= 2\varepsilon - K + 2SV_2 + V_6 - 2S^2(V_4 - V_6)/(1-S^2), \\ E_{\text{IV}} &= 2\varepsilon - K + 2SV_2 + 2V_4 + V_6 - 2S^2(V_4 - V_6)/(1-S^2), \\ E_{\text{V, VI}} &= 2\varepsilon - K + 2SV_2 + V_4 - V_6 \pm \sqrt{4V_2^2 + V_4^2}, \end{aligned} \qquad \text{(III.28)}$$

and

$$E_{IV} - E_{VI} = 2V_6/(1-S^2) + V_4(1-3S^2)/(1-S^2) + \sqrt{4V_2^2+V_4^2} \ ,$$
$$E_{III} - E_I = 2V_4 \ , \qquad \text{(III.29)}$$
$$E_I - E_{IV} = 2V_6/(1-S^2) - V_4(1+S^2)/(1-S^2) + \sqrt{4V_2^2+V_4^2} \ .$$

In Eq. (III.29) we have dropped the subscript a and c on ε and have introduced the renormalized variables:

$$V_2 \equiv [V_2^0 + S(V_4 - V_6)]/(1-S^2) \ ,$$
$$V_3 \equiv V_3^0/(1-S^2)^{1/2} \ ,$$
$$V_4 \equiv V_4^0/(1-S^2) \ , \qquad \text{(III.30)}$$
$$V_5 \equiv V_5^0/(1-S^2)^{1/2} \ ,$$

and

$$V_6 \equiv V_6^0/(1-S^2) \ ,$$

that facilitate comparison with HC and HMSB (see Sec. II). These new variables will be used throughout the remainder of this dissertation. The renormalization factors, $(1-S^2)^{-1}$ and $(1-S^2)^{-1/2}$, are precisely the same as those used by HC in defining V_2^{HC} and V_3^{HC}, respectively. The term added to V_2^0 may be viewed as the subtraction of the constant $(V_4 - V_6)$ from H_{one} in Eq. (III.23).

The qualitative ordering of the energy levels in Eq. (III.28) is shown in Fig. (2), where E_{VI} is the ground state energy, and the triplet levels and the first excited singlet E_{IV} are separated by $2V_4$. Note that overlap has shifted all six states upward in energy by an

amount $2SV_2$. This term, however, will contribute only to properties which depend on the absolute positions of the levels, such as the cohesive energy. For $V_6 = 0$ the triplet energy and V_{IV} are also shifted downward from the center of gravity by $-2S^2V_4/(1 - S^2)$. This means that if one fits $E_{IV} - E_{VI}$ to the energy of the principal optical absorption peak for a fixed V_4, as we do in Sec. IV, one requires a larger value of V_2 than with $S = 0$.

In the Harrison limit the energy levels and splittings are found to be

$$\begin{aligned} E_{I,II,III} &= E_{IV} = \varepsilon_a + \varepsilon_c - K + 2SV_2 \ , \\ E_{V,VI} &= \varepsilon_a + \varepsilon_c - K + 2SV_2 \pm 2\sqrt{V_2^2 + V_3^2} \ , \end{aligned} \tag{III.31}$$

and

$$\begin{aligned} E_{IV} - E_{VI} &= E_I - E_{VI} = 2\sqrt{V_2^2 + V_3^2} \ , \\ E_I - E_{IV} &= 0 \ . \end{aligned} \tag{III.32}$$

Again all levels are shifted by the amount $2SV_2$, which is consistent with the shift of SV_2 in the one-electron energy levels of HC, Eqs. (II.3) and (II.11). Otherwise, overlap has not altered the formal structure of the eigenvalues, and Eqs. (III.31) and (III.32) are completely equivalent to the HC results. One can relate the six two-electron eigenvalues in the Harrison limit to E_b and $E_{\bar{b}}$, the one-electron bonding and antibonding energy levels. This correspondence is also illustrated in Fig. (2). The six two-electron energy levels represent the six unique ways that two electrons can occupy E_b and $E_{\bar{b}}$. Thus E_{VI} corresponds to having two electrons (one with spin up and one with spin down) in E_b. The four degenerate

levels E_I, E_{II}, E_{III} and E_{IV} arise from the four possible spin combinations with one electron in E_b and the other in $E_{\bar{b}}$. Finally, E_V corresponds to two electrons occupying $E_{\bar{b}}$.

2. Eigenstates

We next consider the calculation of the eigenfunctions of the Hamiltonian H. It is evident from Eq. (III.9) that the three triplet basis states are already eigenstates of H:

$$\begin{aligned} |\mathrm{I}\rangle &= |1\rangle , \\ |\mathrm{II}\rangle &= |2\rangle , \\ |\mathrm{III}\rangle &= |3\rangle . \end{aligned} \tag{III.33}$$

The singlet eigenstates can be written as a linear combination of the three singlet basis states

$$|M\rangle = \sum_{i=4,5,6} a_{iM} |i\rangle \quad , \qquad M = \mathrm{IV}, \mathrm{V}, \mathrm{VI} , \tag{III.34}$$

setting

$$a_{iM} = A_{iM} / D , \tag{III.35}$$

where D is the normalization constant

$$D = \left[A_{4M}^2 + A_{5M}^2 + A_{6M}^2 + 2S^2 A_{4M} A_{5M} + 2S \sqrt{\frac{2}{1+S^2}} (A_{4M} + A_{5M}) A_{6M} \right]^{1/2} . \tag{III.36}$$

The coefficients A_{iM} are obtained in the usual way and may be expressed as

$$\begin{Bmatrix} A_{4M} \\ A_{5M} \end{Bmatrix} = \sqrt{\frac{2}{1+S^2}} \left\{ \left[(-2SV_2 - V_6)(1-S^2) + 2S^2(V_4 - V_6) - S^2 E_M^0 \right] \left[-V_2(1-S^2) \right.\right.$$
$$\left. + S(V_4 - V_6) \pm (SV_3 + V_5)(1-S^2)^{1/2} - SE_M^0 \right] - \left[2V_4(1-S^2) \pm 2V_3(1-S^2)^{1/2} - E_M^0 \right]$$
$$\left. \cdot \left[-V_2(1-S^2) + S(V_4 - V_6) \mp (SV_3 + V_5)(1-S^2)^{1/2} - SE_M^0 \right] \right\} ,$$

and

$$A_{6M} = \left[2V_4(1-S^2) - E_M^0 \right]^2 - 4V_3^2(1-S^2) - \left[(-2SV_2 - V_6)(1-S^2) \right.$$
$$\left. + 2S^2(V_4 - V_6) - S^2 E_M^0 \right] . \qquad \text{(III.37)}$$

In the general case once the roots of the cubic equation (III.27) are found, they can be inserted into Eq. (III.37) to find the A_{iM}.

In the FH limit, $A_{iM} = D = 0$ for M = IV, so the general solution Eq. (III.37) cannot be used. In this case, the proper coefficients can be shown to be

$$\begin{Bmatrix} a_{4\,IV} \\ a_{5\,IV} \end{Bmatrix} = \pm 1/\sqrt{2(1-S^2)} ,$$

and $\qquad \text{(III.38)}$

$$a_{6\,IV} = 0 .$$

For M = V, VI, on the other hand, Eq. (III.28) may be used directly in Eq. (III.37) to obtain

$$a_{4M} = a_{5M} = 4\left[2(1+S^2) + \theta SQ \right] / D_0 ,$$

and

$$a_{6M} = 4\sqrt{\frac{1+S^2}{2}} \left[X(1-S^2) - \theta Q(1+S^2) - 8S \right] / D_0 , \qquad \text{(III.39)}$$

with

$$D_0 \equiv [Q(Q+X)]^{1/2}[4+\theta S(Q+\theta X)](1-S^2), \tag{III.40}$$

where $\theta = +1$ for M = V and $\theta = -1$ for M = VI. As in Sec. II, we have defined

$$X = 2V_4/V_2, \tag{III.41}$$

and also

$$Q = (X^2+16)^{1/2}. \tag{III.42}$$

Note that all explicit dependence on V_6 has cancelled out in this limit.

In the Harrison limit the coefficients are most conveniently expressed in terms of Harrison's polarity and convalency parameters[5,6] α_p and α_c, respectively:

$$\alpha_p = V_3/(V_2^2+V_3^2)^{1/2}, \tag{III.43}$$

and

$$\alpha_c = V_2/(V_2^2+V_3^2)^{1/2}. \tag{III.44}$$

One then finds

$$\left\{\begin{matrix} a_{4\,IV} \\ a_{5\,IV}\end{matrix}\right\} = \frac{1}{\sqrt{2}}\left[\pm\alpha_c(1-S^2)^{1/2}+S\alpha_p\right]/(1-S^2), \tag{III.45}$$

$$a_{6\,IV} = -\frac{2}{\sqrt{2}}\sqrt{\frac{1+S^2}{2}}\,\alpha_p/(1-S^2),$$

and

$$\left\{\begin{matrix} a_{4M} \\ a_{5M}\end{matrix}\right\} = \frac{1}{2}\left[\pm\alpha_p(1-S^2)^{1/2}-(S\alpha_c+\theta)\right]/(1-S^2), \tag{III.46}$$

$$a_{6M} = \sqrt{\frac{1+S^2}{2}}\,[\alpha_c+S\theta]/(1-S^2),$$

$$M = V,\ VI.$$

It is straightforward to show that Eq. (III.38) through (III.46) reduce to the corresponding expressions of HMSB in the limit $S = V_6 = 0$.

B. Physical Properties

The full effect of two-electron correlation and overlap on a wide range of physical properties can be assessed using the eigenvalues and eigenstates obtained above. We shall concentrate here, however, on only a small select number of such properties. For the purposes of comparison with HC and HMSB we derive generalized formulas for the dielectric constant ϵ . As an extension of the method, we also consider the valence-electron density, polarity of the bond, the nuclear exchange and psuedodipolar coefficients Γ_e and Γ_{Pd} , and the cohesive energy.

1. Dielectric constant

The quantities ϵ , Γ_e and Γ_{Pd} are most conveniently calculated in perturbation theory. As we have done previously in Sec. II, apply an electric field $\vec{\mathcal{E}}$ in the + x direction and consider the energy shift ΔE induced in an isolated bond lying in the [111] direction. The origin of the coordinates is chosen at the center of the bond. The potential energy gain by the system is

$$U_\mathcal{E} = (x_1 + x_2)e\mathcal{E} = U_\mathcal{E}^\circ e\mathcal{E} \ , \qquad \text{(III.47)}$$

where x_1 and x_2 are the x coordinate of electron 1 and electron 2. We can also write

$$U_\mathcal{E}^\circ = (-\theta_n d/2\sqrt{3} + x_{1n}) + (-\theta_n d/2\sqrt{3} + x_{2n}) \ , \qquad \text{(III.48)}$$
$$n = a, c \ ,$$

where $\theta_a = +1$ and $\theta_c = -1$, x_{1n} and x_{2n} are measured from the center n. The energy shift due to this potential, to second order in perturbation theory, is then

$$\Delta E = \langle G | U_\varepsilon^\circ | G \rangle e\mathcal{E} + \sum_{M=III,V} \frac{\langle G | U_\varepsilon^\circ | M \rangle \langle M | U_\varepsilon^\circ | G \rangle}{E_G - E_M} , \qquad \text{(III.49)}$$

where we have denoted $|VI\rangle$ as $|G\rangle$ and E_{VI} as E_G, with G denoting the ground state. From elementary electrostatics consideration one has in each unit volume of the solid

$$\sum_{bonds} \Delta E = \sum_{bonds} (\vec{P}_0 \cdot \vec{\mathcal{E}}) - \tfrac{1}{2} \chi \mathcal{E}^2 , \qquad \text{(III.50)}$$

where $\vec{P}_0$ is the (zero-field) polarization of the bond and χ is the dielectric susceptibility. Comparing Eqs. (III.49) and (III.50), one finds

$$\vec{P}_0 = -(\sqrt{3}/d) \langle G | U_\varepsilon^\circ | G \rangle e \vec{d} , \qquad \text{(III.51)}$$

and

$$\chi = -N e^2 \sum_{M=III,V} \frac{\langle G | U_\varepsilon^\circ | M \rangle \langle M | U_\varepsilon^\circ | G \rangle}{E_G - E_M} , \qquad \text{(III.52)}$$

where N is the average valence electron density, and $\vec{d}$ is the vector distance from the anion to the cation. Note that the sum in Eq. (III.52) runs only over the two excited singlet states, because U_ε° cannot couple $|G\rangle$ to the triplet states.

Using Eqs. (III.4) and (III.34), one can derive a general formula for $\langle G | U_\varepsilon^\circ | M \rangle$ in terms of the expansion coefficients a_{iM}:

$$\langle G|U_\varepsilon^\circ|M\rangle = (d/\sqrt{3})\Big[\gamma(1-S^2)^{1/2}\Big\{(a_{5M}a_{5G}-a_{4M}a_{4G})+\tfrac{1}{2}S\sqrt{\tfrac{2}{1-S^2}}$$
$$\cdot[(a_{5G}-a_{4G})a_{6M}+(a_{5M}-a_{4M})a_{6G}]\Big\}-(\delta_c-\delta_a)\Big\{(a_{5G}a_{5M}+a_{4G}a_{4M})$$
$$+a_{6G}a_{6M}/(1+S^2)+\tfrac{1}{2}\sqrt{\tfrac{2}{1+S^2}}\,S[(a_{5G}+a_{4G})a_{6M}+(a_{5M}+a_{4M})a_{6G}]\Big\} \qquad \text{(III.53)}$$
$$-2\delta_{ca}\Big\{S[(a_{4G}a_{5M}+a_{5G}a_{4M})+a_{6G}a_{6M}/(1+S^2)]+\tfrac{1}{2}S\sqrt{\tfrac{2}{1+S^2}}$$
$$\cdot[(a_{5G}+a_{4G})a_{6M}+(a_{5M}+a_{4M})a_{6G}]\Big\}\Big],$$

where we have defined

$$\delta_n \equiv (\sqrt{3}/d)\left|\int \phi_n^*(\vec{r})\,x_n\,\phi_n(\vec{r})\,d\vec{r}\,\right|, \quad n=a,c, \qquad \text{(III.54)}$$

$$\gamma \equiv [1-(\delta_a+\delta_c)]/(1-S^2)^{1/2}, \qquad \text{(III.55)}$$

and

$$\delta_{ca} \equiv -(\sqrt{3}/d)\int \phi_c^*(\vec{r})\times\phi_a(\vec{r})\,d\vec{r}\,. \qquad \text{(III.56)}$$

The quantity $[1-(\delta_a+\delta_c)]$ is the γ' defined in HC, Eq. (II.32). The renormalization factor of $(1-S^2)^{-1/2}$ is again such that our γ is precisely the same as that defined by HC and HMSB. Note that $\delta_n d$ is the center of gravity of the hybrid electron density $\phi_n^*(\vec{r})\,\phi_n(\vec{r})$. A new overlap term δ_{ca}, not considered in HC or HMSB has also appeared. For homopolar solids $\delta_{ca}=0$ and $\delta_c=\delta_a$ by symmetry; for binary compounds one usually has $\delta_c>\delta_a$ and $\delta_{ca}>0$ because of the greater spatial extent of the cation hybrid.

In the FH and Harrison limits, $\vec{P}_\circ$ and χ are given by particularly simple expressions. In the former case the condition $\delta_{ca}=\delta_c-\delta_a=0$ holds, and one finds that only the matrix element $\langle G|U_\varepsilon^\circ|\text{IV}\rangle$ is non-zero.

Thus $\vec{P}_0 = 0$ as expected by symmetry. Using Eqs. (III.38) and (III.40) it is straightforward to show that

$$\epsilon = 1 + 4\pi\chi = 1 + \tfrac{1}{3}\pi N(\gamma e d)^2 (1/V_2\beta), \qquad \text{(III.57)}$$

with

$$\beta \equiv \tfrac{1}{64} Q(Q+X)\left[2Z + X(1-3S^2) + Q(1-S^2)\right]/(1-S^2), \qquad \text{(III.58)}$$

where we have defined

$$Z \equiv 2V_6/V_2 . \qquad \text{(III.59)}$$

Equation (III.57) has the same analytic structure as obtained in HC and HMSB, Eq. (II.34). The factor β reduces to the form in Eq. (II.35) when S = Z = 0. In addition, $\beta = 1$ for X = Z = 0, and $\beta > 0$ for $Z \geq 0$ and $0 < X^2 \ll Q^2$. A further simplification is also possible. In HC the quantity V_2^{HC} is determined by fitting $E_{IV} - E_{VI}$ to the principal optical-absorption peak. If one uses the same prescription to fit V_2, then one has, comparing Eq. (III.29) and Eq. (III.32) with $V_3 = 0$

$$2V_2^{HC} = \tfrac{1}{2} V_2\left[2Z + X(1-3S^2) + Q(1-S^2)\right]/(1-S^2) . \qquad \text{(III.60)}$$

Thus, the effect of the two-electron correlation on the HC result can be expressed in terms of the simpler factor

$$\beta' = V_2\beta / V_2^{HC} = \tfrac{1}{16} Q(Q+X) \qquad \text{(III.61)}$$

which depends on only X and not on either S or Z explicitly. Our calculation suggests $0 < X \lesssim 1$, so that we expect $1 < \beta' \lesssim 1.3$. In addition, if the

quantity γ is determined by fitting ϵ to experiment then the fitted γ will be larger than the HC value by a factor of $(\beta')^{1/2}$.

In the Harrison limit $\langle G|U_\xi^0|\text{III}\rangle$ and $\langle G|U_\xi^0|G\rangle$ are finite and only $\langle G|U_\xi^0|\text{V}\rangle$ vanishes. Thus, from Eqs. (III.32), (III.45) and (III.46) one finds

$$\vec{P}_b = \left\{\gamma^{eff}\alpha_p + \left[(1-S/\alpha_c)(\delta_c-\delta_a) + 2(1/\alpha_c - S)\,\delta_{ca}\right]/(1-S^2)\right\} e\vec{d}, \qquad \text{(III.62)}$$

and

$$\epsilon = 1 + \tfrac{1}{3}\pi N(\gamma^{eff} e d)^2\, V_2^2/(V_2^2+V_3^2)^{3/2}, \qquad \text{(III.63)}$$

where we have defined

$$\gamma^{eff} \equiv \gamma + (\alpha_p/\alpha_c)\left[S(\delta_c-\delta_a) - 2\delta_{ca}\right]/(1-S^2)^{1/2}. \qquad \text{(III.64)}$$

Equations (III.62)-(III.64) reduce to the HC results in the limit $\delta_c = \delta_a$ and $\delta_{ca} = 0$, as was implicitly assumed in their work.

We should stress at this point that the vanishing of the matrix element $\langle G|U_\xi^0|\text{V}\rangle$ is not a general result, but only a property of the FH and Harrison limits. For the binary compounds, there is a non-zero contribution to χ from the additive term $|\langle G|U_\xi^0|\text{V}\rangle|^2/(E_4 - E_\text{V})$ in Eq. (III.52). Thus in the general case the correlation correction to will not simply be a multiplicative factor as in Eq. (III.61).

2. Electron density and polarity

The total valence-electron density in the solid is just a sum of all the individual bond densities. The bond electron density may be

obtained from the two-electron ground state $|G\rangle$ in the following way. If the spatial part of the singlet basis state $|i\rangle$ is written as $\psi_i(\vec{r},\vec{r}')$, then the electron density associated with the ground state obtained from Eq. (III.34), is

$$\rho(\vec{r}) = 2 \sum_{i,j=4,5,6} a_{iG}^{*}\, a_{jG} \int \psi_i^{*}(\vec{r},\vec{r}')\, \psi_j(\vec{r},\vec{r}')\, d\vec{r}' \,. \qquad \text{(III.65)}$$

The factor of 2 arises because there are two electrons per bond, i.e., $\int \rho(\vec{r})\, d\vec{r} = 2$. Also note that $\psi_i(\vec{r},\vec{r}')$ is symmetric under interchange of $\vec{r}$ and $\vec{r}'$, so that it does not matter over which coordinate one integrated in Eq. (III.65). Using Eq. (III.4) it is straightforward to show that

$$\rho(\vec{r}) = u_a^2\, \phi_a(\vec{r}) + u_c^2\, \phi_c(\vec{r}) + 2\, u_{ac}^2\, \phi_a(\vec{r})\, \phi_c(\vec{r}) \qquad \text{(III.66)}$$

with

$$u_a^2 = 2\, a_{4G}^2 + a_{6G}^2/(1+S^2) + 2S\sqrt{\frac{2}{1+S^2}}\; a_{4G}\, a_{6G} \,, \qquad \text{(III.67)}$$

$$u_c^2 = 2\, a_{5G}^2 + a_{6G}^2/(1+S^2) + 2S\sqrt{\frac{2}{1+S^2}}\; a_{5G}\, a_{6G} \,, \qquad \text{(III.68)}$$

and

$$u_{ac}^2 = 2S\, a_{4G}\, a_{5G} + S\, a_{6G}^2/(1+S^2) + \sqrt{\frac{2}{1+S^2}}\; (a_{4G} + a_{5G})\, a_{6G} \,, \qquad \text{(III.69)}$$

where we have noted that $\phi_a(\vec{r})$ and $\phi_c(\vec{r})$ are real. In the FH limit one finds using Eq. (III.39)

$$u_a^2 = u_c^2 = 16\left\{Q(Q-8S)(1+S^2)+32S^2-\left[4S(Q+X)-XQ\right](1-S^2)\right\}(1-S^2)/D_0^2, \quad \text{(III.70)}$$

$$u_{ac}^2 = 16\left\{Q(8-QS)(1+S^2)-32S-\left[4(Q-X)+SXQ\right](1-S^2)\right\}(1-S^2)/D_0^2. \quad \text{(III.71)}$$

In the Harrison limit, on the other hand, one is led from Eq. (III.46) to the results

$$\left\{\begin{matrix} u_a^2 \\ u_c^2 \end{matrix}\right\} = \left[(1-S\alpha_c) \pm \alpha_p(1-S^2)^{1/2}\right]/(1-S^2) \quad \text{(III.72)}$$

which are the same as Eq. (II.4) and

$$u_{ac}^2 = u_a u_c = (\alpha_c - S)/(1-S^2). \quad \text{(III.73)}$$

For X = 0 in Eqs. (III.70), (III.71), or $\alpha_p = 0$ and $\alpha_c = 1$ in Eqs. (III.72), (III.73), then the results $u_a^2 = u_c^2 = u_{ac}^2 = (1+S)^{-1}$ holds, as one might intuitively expect.

We tentatively define a polarity associated with the electron density $\rho(\vec{r})$ as

$$\alpha_p^G \equiv \tfrac{1}{2}\left(u_a^2 - u_c^2\right)(1-S^2)^{1/2} \quad \text{(III.74)}$$

From Eq. (III.72) one clearly has $\alpha_p^G = \alpha_p$ in the Harrison limit, so that Eq. (III.74) is consistent with the HC concept of polarity. In the limit of no overlap, both S = 0 and $\phi_a(\vec{r})\,\phi_c(\vec{r}) = 0$ and this definition is relatively unambiguous. In the case of large overlaps, on the other hand, the definition of α_p^G seems less compelling. Ultimately, an arbitrariness arises from the innumerable ways one can divide up the electron

density in a periodic solid. Nevertheless, there need be no additional uncertainty in any calculation, so long as α_p^G enters solely as a definition.

The concept of polarity is also intimately connected with the polarization of the bond $\vec{P}_0$. Using Eq. (III.53) with M = G in Eq. (III.51) one has in the general case

$$\vec{P}_0 = Z_p e \vec{d} , \tag{III.75}$$

where

$$Z_p \equiv \gamma \alpha_p^G + \tfrac{1}{2}(\delta_c - \delta_a)(u_a^2 + u_c^2) + 2\delta_{ca} u_{ac}^2 . \tag{III.76}$$

The quantity $Z_p e$ is the effective charge connected with the dipole $\vec{P}_0$. It would follow, therefore, that Z_p is also a reasonable measure of polarity. However, this definition has the disadvantage of depending on the additional parameters γ, δ_a, δ_c and δ_{ca}. In HC, the quantities $\delta_c - \delta_a$ and δ_{ca} are set to zero and γ is fitted to experiment through the dielectric constant as described in Sec. II. The fitted γ thus absorbs local-electric-field corrections to ϵ as well as correction to the bond-orbital model itself. Consequently, it is not appropriate to use their γ in any definition of polarity. On the other hand, one may calculate Z_p directly and compare it to α_p^G, and we do this in Sec. III.

We finally point out that one may define a polarity for each of the states $|M\rangle$ by the obvious generalization of Eqs. (III.65)-(III.73). It readily follows from Eqs. (III.39) and (III.46) that $\alpha_p^M = 0$ for all three singlet states in the FH limit and that the polarities $\alpha_p^{IV} = 0$ and $\alpha_p^V = -\alpha_p^G$ in the Harrison limit. These results are in agreement

with HMSB. However, in the general case α_p^{III} is small but not identically zero and α_p^{V} is negative but not equal to $-\alpha_p^{G}$.

3. Indirect nuclear magnetic interactions

To obtain generalized expression for Γ_e and Γ_{pd}, we consider the magnetic interaction between an electron with spin $\frac{1}{2}\hbar\vec{\sigma}$ and a nucleus with spin $\vec{I}$. The system with 2 ions and 2 electrons experiences a magnetic potential

$$U_A(\vec{r}_1,\vec{r}_2) = \sum_{i=1,2}\sum_{n=a,c} \vec{I}_n \cdot \overleftrightarrow{A}_n(\vec{r}_i)\cdot\sigma(\vec{r}_i), \qquad \text{(III.77)}$$

where

$$\overleftrightarrow{A}_n(\vec{r}) = \mu_B\hbar\gamma_n\left[\frac{8\pi}{3}\delta(\vec{r})\overleftrightarrow{1} + \frac{1}{r^3}\left(3\hat{r}\hat{r} - \overleftrightarrow{1}\right)\right]. \qquad \text{(III.78)}$$

In Eq. (III.78) μ_B is the Bohr magneton, γ_n is the gyromagnetic ratio and $\vec{r}$ is the electron coordinate measured relative to the nucleus n. The potential $U_A(\vec{r}_1, \vec{r}_2)$ only couples the singlet and triplet states and to second order gives rise to an energy shift out of the ground state by

$$\Delta E = \frac{1}{E_G - E_T}\sum_{M=I,II,III}\langle G|U_A|M\rangle\langle M|U_A|G\rangle. \qquad \text{(III.79)}$$

The triplet states, as given by Eq. (III.2), have the form $\Phi_A(\vec{r}_1,\vec{r}_2)\Sigma_A$ and the sum over M in Eq. (III.79) can be immediately accomplished by using the sum rule

$$\sum_{M=I,II,III}\langle\Sigma_A|\vec{\sigma}(i)|\Sigma_M\rangle\langle\Sigma_M|\vec{\sigma}(i')|\Sigma_A\rangle = (-1)^{i+i'}\overleftrightarrow{1}. \qquad \text{(III.80)}$$

Then by using Eq. (III.3) and (III.34) and noting that $\Phi_A(\vec{r}_1, \vec{r}_2)$ is antisymmetric in $\vec{r}_1$ and $\vec{r}_2$, one may express ΔE in terms of the expansion coefficient a_{iG}:

$$\Delta E = -\frac{1}{E_0} \sum_{n,n'=a,c} \theta_n \theta_{n'} \vec{I}_n \cdot \overleftrightarrow{Q}_n \cdot \overleftrightarrow{Q}_{n'} \cdot \vec{I}_{n'} \quad , \tag{III.81}$$

where $\theta_a = +1$, $\theta_c = -1$, and we have set

$$\overleftrightarrow{Q}_n = \theta_n \left\{ \langle \phi_a | \overleftrightarrow{A}_n | \phi_a \rangle - \langle \phi_c | \overleftrightarrow{A}_n | \phi_c \rangle + \frac{b_1}{b_2} \left[S(\langle \phi_a | \overleftrightarrow{A}_n | \phi_a \rangle + \langle \phi_c | \overleftrightarrow{A}_n | \phi_c \rangle) - 2 \langle \phi_a | \overleftrightarrow{A}_n | \phi_c \rangle \right] \right\} / (1-S^2)^{1/2} \quad , \tag{III.82}$$

$$b_1 = \tfrac{1}{2} (a_{4G} - a_{5G}) \quad ,$$

$$b_2 = \tfrac{1}{2} S(a_{4G} + a_{5G}) + a_{6G} / \sqrt{2(1+S^2)} \quad , \tag{III.83}$$

and

$$E_0^{-1} = 2 b_2^2 / (E_T - E_G) \quad . \tag{III.84}$$

Equation (III.81) is much more general than the corresponding expression Eq. (II.42) obtained by HMSB. In addition to S, four other overlap matrix elements have appeared, namely $\langle \phi_a | \overleftrightarrow{A}_a | \phi_c \rangle$, $\langle \phi_a | \overleftrightarrow{A}_c | \phi_c \rangle$, $\langle \phi_a | \overleftrightarrow{A}_c | \phi_a \rangle$ and $\langle \phi_c | \overleftrightarrow{A}_a | \phi_c \rangle$. It is not hard to show that all matrix elements of $\overleftrightarrow{A}_n$ have the form

$$\langle \phi_n | A_{n'} | \phi_{n''} \rangle = \tfrac{1}{2} \mu_B \hbar \gamma_{n'} \left[\tfrac{1}{3} \delta_{nn''}^{n'} \overleftrightarrow{1\!\!1} + \tfrac{3}{5} \rho_{nn''}^{n'} \overleftrightarrow{\pi} \right], \quad n, n', n'' = a, c \tag{III.85}$$

with

$$\overleftrightarrow{\pi} = 3 \hat{r}_{ac} \hat{r}_{ac} - \overleftrightarrow{1\!\!1} \quad , \tag{III.86}$$

and where we have defined

$$\delta_{nn''}^{n'} \equiv 16\pi \langle \phi_n | [\delta(\vec{r})]_{n'} | \phi_{n''} \rangle \tag{III.87}$$

and

$$\gamma_{nn''}^{n'} \equiv \frac{5}{3} \langle \phi_n | \left[\frac{3z^2}{r^5} - \frac{1}{r^3}\right]_{n'} | \phi_{n''} \rangle . \tag{III.88}$$

In Eq. (III.86) $\hat{r}_{ac}$ is a unit vector directed from the anion to the cation and in Eqs. (III.87) and (III.88) the electron coordinates in square brackets are to be measured from center n'. Also, the right hand side of Eq. (III.88) is written for the z-axis in the $\hat{r}_{ac}$ direction. More explicit expressions for $\delta_{nn'',}^{n'}$ and $\gamma_{nn'',}^{n'}$ in terms of the $\underline{s}$ and $\underline{p}$ components of the $\underline{sp}^3$ hybrids are considered in Sec. IV. In HMSB only the non-overlap terms δ_{nn}^{n} and γ_{nn}^{n} (Eq. (II.44)) are included. The tensor $\overleftrightarrow{Q}_n$ clearly has the same form as Eq. (III.85) with $\delta_{nn'',}^{n'}$ replaced by

$$\delta_n = \theta_n \left[(1+S\tfrac{b_1}{b_2})\delta_{aa}^{n} - (1-S\tfrac{b_1}{b_2})\delta_{cc}^{n} - 2\tfrac{b_1}{b_2}\delta_{ac}^{n}\right]/(1-S^2)^{1/2} \tag{III.89}$$

and $\gamma_{nn'',}^{n'}$ replaced by

$$\gamma_n = \theta_n \left[(1+S\tfrac{b_1}{b_2})\gamma_{aa}^{n} - (1-S\tfrac{b_1}{b_2})\gamma_{cc}^{n} - 2\tfrac{b_1}{b_2}\gamma_{ac}^{n}\right]/(1-S^2)^{1/2}. \tag{III.90}$$

Writing out $\overleftrightarrow{Q}_n \cdot \overleftrightarrow{Q}_{n'}$ in terms of δ_n and γ_n and noting that $\overleftrightarrow{\pi}\cdot\overleftrightarrow{\pi} = 2\overleftrightarrow{1} + \overleftrightarrow{\pi}$, we arrive at the final result,

$$\Delta E = -\tfrac{1}{2} \sum_{n,n'=a,c} \theta_n \theta_{n'} \vec{I}_n \cdot \left[\Gamma_e^{nn'} \overleftrightarrow{1} + \Gamma_{Pd}^{nn'} \overleftrightarrow{\pi}\right] \cdot \vec{I}_{n'} , \tag{III.91}$$

where

$$\Gamma_e^{nn'} = \mu_B^2 \hbar^2 \gamma_n \gamma_{n'} \left[\frac{1}{18} \delta_n \delta_{n'} + \frac{9}{25} \beta_n \beta_{n'} \right] / E_0 \ , \qquad \text{(III.92)}$$

and

$$\Gamma_{Pd}^{nn'} = \mu_B^2 \hbar^2 \gamma_n \gamma_{n'} \left[\frac{1}{10} (\delta_n \beta_{n'} + \delta_{n'} \beta_n) + \frac{9}{50} \beta_n \beta_{n'} \right] / E_0 \ . \qquad \text{(III.93)}$$

Equations (III.91)-(III.93) have the same analytic structure as the corresponding results obtained in HMSB, Eqs. (II.45) and (II.46), with all effects of two-electron correlation and overlap being absorbed into the quantities δ_n, β_n and E_0. We identify $\Gamma_e = \Gamma_e^{ac}$ and $\Gamma_{Pd} = \Gamma_{Pd}^{ac}$ as the nuclear exchange and pseudo-dipolar coefficients, respectively. We normally expect δ_n and β_n and consequently Γ_e and Γ_{Pd} to be positive quantities, as is observed experimentally, since

$$0 \leq b_1 / b_2 < 1/5 \qquad \text{(III.94)}$$

and

$$\begin{aligned} \delta_{nn}^{n} &> \delta_{nn'}^{n} > \delta_{n'n}^{n'} \\ \beta_{nn}^{n} &> \beta_{nn'}^{n} > \beta_{n'n}^{n'} \end{aligned} \qquad \text{(III.95)}$$

for $n \neq n'$. The lower limit in Eq. (III.89) is for homopolar solids where $a_{4M} = a_{5M}$. We find that the inequalities Eqs. (III.94) and (III.95) are obeyed for all group IV and III-V binary compounds. Finally, we observe Eqs. (III.92) and (III.93) are similar to the earlier results obtained by Clough and Goldberg[25] with a cruder model. For the case of

tetrahedrally bonded solids, the essential differences between our results and theirs are (i) what we call E_0^{-1} is an arbitrary, unspecified constant 2λ in their treatment, (ii) they do not distinguish between either δ_a and δ_c or ρ_a and ρ_c, (iii) the term involving $(\delta_a\rho_c + \delta_c\rho_a)$ in Eq. (III.93) is a factor of 2 larger than the corresponding term in their Eq. (24), and (iv) they do not have a finite overlap integral S.

In the FH limit, Eqs. (III.84) and (III.85) simplify to

$$\delta_n = \theta_n \left[\delta_{aa}^n - \delta_{cc}^n \right] / (1-S^2)^{1/2} ,$$

and

$$\rho_n = \theta_n \left[\rho_{aa}^n - \rho_{cc}^n \right] / (1-S^2)^{1/2} . \qquad \text{(III.96)}$$

The coupling constant E_0^{-1} can be shown to be, in this case,

$$E_0^{-1} = (1/4V_2)\,\xi , \qquad \text{(III.97)}$$

where

$$\xi = 64(Q+X-4S)^2(1-S^2)/\{Q(Q+X)[4-S(Q-X)]^2[2Z-X(1+S^2) + Q(1-S^2)]\} . \qquad \text{(III.98)}$$

We have $\xi > 0$ for $Z > 0$ or $X > 0$, and $\xi = 1$ for $X = Z = 0$. If V_2^{HC} and V_2 are related by Eq. (III.60), then the HC value of E_0^{-1} is enhanced by the factor

$$\xi' = V_2^{HC}\,\xi / V_2 = \tfrac{1}{4}\left[2Z + X(1-3S^2) + Q(1-S^2)\right]\xi/(1-S^2) , \qquad \text{(III.99)}$$

which unlike β', is a function of S and Z as well as X. In Fig. (3), we have plotted ξ' vs X for Z = 0 and several values of S. One can see from the figure that ξ' is a sensitive function in the region of physical

interest: $S \sim 0.6$, $X \sim 1.0$. This sensitivity results primarily from the energy denominator in Eq. (III.97), $(E_T - E_G)$, which can vanish for sufficient large X.

In the Harrison limit δ_n becomes

$$\delta_n = \theta_n \left\{ \left[(1-S^2)^{1/2} + S(\alpha_p/\alpha_c) \right] \delta^n_{aa} - \left[(1-S^2)^{1/2} - S(\alpha_p/\alpha_c) \right] \delta^n_{cc} - 2(\alpha_p/\alpha_c)\delta^n_{ac} \right\} / (1-S^2) \tag{III.100}$$

with a similar expression for γ_n. We also recover Eq. (II.49)

$$E_0^{-1} = \tfrac{1}{4} V_2^2 / (V_2^2 + V_3^2)^{3/2} . \tag{III.101}$$

But note that for the conditions $\delta^a_{cc} = \delta^c_{aa} = \delta^a_{ac} = \delta^c_{ac} = 0$ and $S \neq 0$ we do not recover the formula in HMSB for $\Gamma_e^{nn'}$ and $\Gamma_{pd}^{nn'}$ in the Harrison limit. All terms involving S cannot simply be absorbed into V_3 and V_2. Both $\Gamma_e^{nn'}$ and $\Gamma_{pd}^{nn'}$ are multiplied instead by the factor $[1 - S^2(\alpha_p/\alpha_c)^2 / (1-S^2)]/(1-S^2)$. Hence the factor C in Eq. (II.51) has to be multiplied by $(1-S^2)^2 / [(1-S^2) - S^2(\alpha_p/\alpha_c)^2]$.

4. Cohesive energy

To obtain the cohesive energy, one needs both the binding energy of the (two) bond electrons in an anion-cation pair and the binding energy of the (eight) valence electrons in separated atoms. The latter can be written as

$$E_{atom} = \begin{cases} 2(\varepsilon^{HF}_{sa} + \varepsilon^{HF}_{sc}) + (2+\Delta Z)\varepsilon^{HF}_{pa} + (2-\Delta Z)\varepsilon^{HF}_{pc}, & \Delta Z = 0,1,2 \\ 2\varepsilon^{HF}_{sa} + \varepsilon^{HF}_{sc} + 5\varepsilon^{HF}_{pa}, & \Delta Z = 3, \end{cases} \tag{III.102}$$

where ΔZ_{iso} for group IV, is 1 for III-V, is 2 for II-VI, and is 3 for I-VII elements. Also in Eq. (III.102) ε_{sn}^{HF} and ε_{pn}^{HF} are defined as the binding energies of the s and p electrons of atom n. We use the superscript HF here because in practice it is convenient to take ε_{sn}^{HF} and ε_{pn}^{HF} to be Hartree-Fock free-atom eigenvalues, although in principle this need not be assumed. The corresponding binding energy of two bond electrons is just the ground-state energy E_G plus the electrostatic energy of the corresponding nuclei:

$$\begin{aligned} E_{bond} &= E_G + e^2/d \\ &= \varepsilon_a^{HF} + \varepsilon_c^{HF} + E_{ol} + E_G^{\circ} \quad , \end{aligned} \tag{III.103}$$

where we have defined the hybrid energies

$$\varepsilon_n^{HF} = \tfrac{1}{4}\left(\varepsilon_{sn}^{HF} + 3\,\varepsilon_{pn}^{HF}\right) \quad , \qquad n = a, c \quad , \tag{III.104}$$

and the electrostatic overlap energy

$$E_{ol} = -K + e^2/d + \Delta\varepsilon_a + \Delta\varepsilon_c \quad , \tag{III.105}$$

with

$$\Delta\varepsilon_n \equiv \varepsilon_n - \varepsilon_n^{HF} \quad . \tag{III.106}$$

Both Harrison[5] and HC neglected E_{ol} in their treatments of the cohesive energy. However, for the case of large overlap this is not justified, since we expect $\Delta\varepsilon_n$ to be negative and K is significantly larger than e^2/d.

Using Eq. (III.102) and (III.103), the cohesive energy (per atom pair) is

$$E_{coh} = E_{atoms} - 4E_{bonds} = -4E_G^o - 4E_{ol} - E_{pro} - E_{trans} , \tag{III.107}$$

where E_{pro} is the promotion energy defined by Harrison[5]

$$E_{pro} = \begin{cases} (4+\Delta Z)\, V_1^c + (4-\Delta Z)\, V_1^a , & \Delta Z = 0, 1, 2 \\ 3\, V_1^c + V_1^a , & \Delta Z = 3 \end{cases} \tag{III.108}$$

with

$$V_1^n = \tfrac{1}{4}\left(\varepsilon_{pn}^{HF} - \varepsilon_{sn}^{HF} \right) , \qquad n = a, c , \tag{III.109}$$

and E_{trans} is the transfer energy

$$E_{trans} = \Delta Z \left(\varepsilon_c^{HF} - \varepsilon_a^{HF} \right) . \tag{III.110}$$

Both Harrison[5] and HC took the transfer energy to be $2\Delta Z\, V_3$. From Eqs. (III.21), (III.30) and (III.106), however, one can see that this is only formally valid if $U_a = U_c$, $\Delta\varepsilon_a = \Delta\varepsilon_c$ and $S = 0$. In the FH limit with $E_{trans} = 0$ and $E_{pro} = 8V_1^n$, one has

$$E_{coh} = 4\left[\sqrt{4V_2^2 + V_4^2} - 2S V_2 - V_4 + V_6 \right] - 4E_{ol} - 8\, V_1^n . \tag{III.111}$$

In the Harrison limit on the other hand, one obtains

$$E_{coh} = 4\left[2\sqrt{V_2^2 + V_3^2} - 2S V_2 \right] - 4E_{ol} - E_{pro} - E_{trans} . \tag{III.112}$$

For $E_{ol} = 0$ and $E_{trans} = 2\Delta Z\, V_3$, this result agrees with Eq. (34) of HC.

Physically, we may interpret the various contributions to E_{coh} as follows. The promotion energy is the energy required to promote each valence electron from its atomic s or p orbital to an sp^3 hybrid orbital. The transfer energy is the energy required to transfer ΔZ electrons from the anion to the cation at infinite separation, so that the four hybrid orbitals on each atom contain one electron. The atoms are then brought together and bond-orbitals are formed from the overlapping hybrids. Occupation of the bond orbitals returns an energy $-(E_G + E_{o\ell})$ per bond. Equation (III.107) thus correctly includes all intrabond contributions to the cohesive energy. To be sure, there are neglected interbond contributions, as there are to all properties one calculates with the bond-orbital model, but we certainly expect these to be of lesser importance. In HC the possible improtance of the Van der Waals interaction between bonds was argued, but this was introduced in an ad-hoc fashion to explain their calculated negative values of E_{coh}. In contrast, our calculations suggest that there is no particular difficulty in understanding the origin of the cohesive energy of tetrahedrally-bonded solids in terms of Eq. (III.107) alone.

IV. QUANTITATIVE APPLICATIONS

A. Parameters of the Two Electron Bond-Orbital Model

We now consider a detailed application of the formalism described above to real semiconductors. We seek to understand quantitatively both the relative importance of the various parameters that enter the two-electron theory and the effect of overlap and correlation on the predictions of the one-electron theory. We must first establish a procedure for evaluating the basic parameters of the two-electron model. We are guided here both by the experience of HC and the fundamental limitations of a bond-orbital approach. One must recognize the approximate nature of any bond-orbital theory, so that the difficult task of a complete first-principles analysis is not really warranted. On the other hand, one can reasonably expect the theory to produce correct orders of magnitude and significant trends for a wide range of physical properties. Thus it seems desirable to fit only enough parameters to provide a proper scaling to experiment.

Of the various parameters that enter our two-electron model, one may separate out those that depend self-consistently on the full Hamiltonian of the crystal, and consequently are difficult to calculate accurately, and those that depend only on the specification of the hybrid wave functions. In the former category are the quantities V_{20}, $\Delta\mathcal{E}_a$ and $\Delta\mathcal{E}_c$. Both V_{20} and $\Delta\mathcal{E}_a + \Delta\mathcal{E}_c$ enter the covalent energy V_2, while the polar

energy V_3 depends upon the difference $\Delta\varepsilon_c - \Delta\varepsilon_a$. Following HC, we fit V_2 to the principal optical-absorption peak E_2 for each of the group IV elements. From Eq. (III.60) with $V_6 = 0$ one finds:

$$V_2 = \tfrac{1}{2}\left\{\left[2V_2^{HC} - V_4(1-3S^2)/(1-S^2)\right]^2 - V_4^2\right\}^{1/2}, \qquad \text{(IV.1)}$$

which is easily evaluated once S and V_4 are specified. It is then assumed that V_2 is constant for an isoelectronic sequence (e.g. Ge, GaAs, etc.) and that values for skew compounds are given by the appropriate geometric means of the group IV values.

The quantity V_3^{HC} was fit by HC to the experimental dielectric constant of each binary compound through Eq. (III.63). This is less convenient in the present case because V_3 enters our theory through the rather complicated cubic equation (III.27). We have chosen instead to make the assumption

$$\Delta\varepsilon_c - \Delta\varepsilon_a = 0 , \qquad \text{(IV.2)}$$

and then to calculate V_3 as

$$V_3 = \tfrac{1}{2}\left[(\varepsilon_c^{HF} - \varepsilon_a^{HF}) - \tfrac{1}{2}(U_a - U_c)\right] / (1-S^2)^{1/2}. \qquad \text{(IV.3)}$$

The validity of Eq. (IV.2) is not known <u>a priori</u>, but we can treat Eq. (IV.3) as an additional approximation to be tested by comparison with experiment. Since $|\Delta\varepsilon_n/\varepsilon_n|$ is small one may reasonably expect Eq. (IV.3) to be a good approximation. From Eq. (III.18) it is clear that the term $\frac{1}{2}(U_a - U_c)$ will reduce the magnitude of V_3, so that normally $V_3 < \frac{1}{2}(\varepsilon_c^{HF} - \varepsilon_a^{HF})$, as was found empirically by HC. Interestingly the

two exceptions to Eq. (III.18), namely BP and BAs, are the compounds for which HC inferred negative values of V_3^6 from their fitting procedure. From Table I it can be seen that the quantity $\frac{1}{2}(\mathcal{E}_c^{HF} - \mathcal{E}_a^{HF})$ does become much smaller for BP and BAs than for the rest of the III-V compounds. However, this effect is offset by the change in sign of the term $\frac{1}{2}(U_a - U_c)$, so that normal positive values of V_3 result from Eq. (IV.3).

The remaining parameters V_4, V_5 and V_6 are functions of the one-center integrals U_n and the two-center integrals S, K, H_n and J. All of these integrals depend only on the hybrid wavefunctions $\phi_n(\vec{r})$, so that we also choose to calculate these quantities directly. In the spirit of the bond-orbital model, we construct our hybrid from the appropriate Hartree-Fock free-atom ground state s and p wavefunctions. We shall not entertain the very difficult question of exactly which atomic orbitals constitute an optimum basis set, but rather we treat our choice as an additional assumption to be tested. Choosing $\hat{r}_{ac} = \hat{z}$, one can write

$$\phi_n(\vec{r}_n) = \frac{1}{2\sqrt{4\pi}}\left[R_{sn}(r_n) + 3\Theta_n R_{pn}(r_n)\frac{z_n}{r_n}\right], \qquad \text{(IV.4)}$$

where $\vec{r}_n$ is the electron coordinate measured relative to the center n and $R_{sn}(r_n)$ and $R_{pn}(r_n)$ are measured to be positive as $r_n \to \infty$. Free-atom Hartree-Fock s and p radial wavefunctions $r_n R_{sn}(r_n)$ and $r_n R_{pn}(r_n)$, as well as the corresponding term values $\mathcal{E}_s^{HF}$ and $\mathcal{E}_p^{HF}$, have been calculated and tabulated by Mann[26] for the entire Periodic Table. The use of such atomic tables is convenient but it does restrict one to consideration of compounds formed out of group III, IV and V elements, since the

p states of elements in groups I and II are unoccupied and are not usually calculated.

The details of evaluating U_n, S, K, H_n and J in terms of the hybrids defined by Eq. (IV.4) are discussed in the Appendix. Briefly, U_n can be written as a sum of the F and G integrals defined and calculated by Mann:[26]

$$U = \frac{1}{16}\left[F^0(n_0;n_0) + 6\,F^0(n_0;n_1) + 4\,G^1(n_0;n_1) + 9\,F^0(n_1;n_1) + \frac{36}{25}\,F^2(n_1;n_1)\right], \tag{IV.5}$$

where n is the principal quantum number and $\ell = 0$ and $\ell = 1$ are the orbital momentum quantum numbers of the s and p wave functions. As a test of our numerical procedures, we have also evaluated these F and G integrals directly from Mann's wavefunctions. Both calculated values of U_n are listed in Table I. The agreement is better than 0.1%.

The two-center integrals S and H_n, on the other hand, are most easily calculated by expanding the sp^3 hybrid from one site in terms of spherical harmonics centered on the second site. Similarly, K can be evaluated by expanding the Coulomb potential arising from one hybrid electron density about the second site. In both cases, this procedure leads to a finite series of one-dimensional integrals. This same type of expansion method applied to the exchange integral J, however, leads to an infinite series of terms, which must be truncated. Tests of our procedures in the case of hydrogen 1s orbitals, where exact results are known,[24] suggest that we calculate S, H_n and K to an accuracy of better than 1% (see Table XV), but that we may underestimate J by a few percent. Also, the

overlap integrals S calculated by Sundfors[9] using Clementi's analytic Hartree-Fock wavefunctions[27] agree with our results to better than 1% (see Table II).

Values of S, K and V_4 that we have computed for the twengy group IV elements and group IV and III-V binary compounds are listed in Table II, together with values of V_2 obtained from Eq. (IV.1) and V_3 obtained from Eq. (IV.3). The two-center Coulomb integral K decreases with increasing bond length, as expected. The overlap integral S, on the other hand, tends to be constant, although AlN, GaN and InN have somewhat smaller values than the rest. For the solids listed in Table II, one has approximately, $K \cong (1+S)\frac{e^2}{d} \sim 1.6\frac{e^2}{d}$. The constancy of S and the simple dependence of K on bond length give V_4 its expected covalent behavior. For S = 0, Eq. (IV.1) demands that $V_2 < V_2^{HC}$; but in our case $S^2 > \frac{1}{3}$ and we calculate $V_2 > V_2^{HC}$. For group IV elements the ratio $X = 2V_4/V_2$ is 0.77 for C, is 1.08 for Si, is 1.10 for Ge, and is 1.13 for Sn.

As mentioned in Sec. III, our calculated values of V_5 and V_6 (see Table III) always turn out to be small in comparison with V_3 and V_4, respectively. Specifically, we find

$$0.11 \geq V_5 \geq -0.02 \quad eV$$
$$|V_5/V_3| < 0.075 \qquad \text{(IV.6)}$$

and

$$0.27 \geq V_6 \geq -0.02 \quad eV$$
$$|V_6/V_2| < 0.11 \qquad \text{(IV.7)}$$

for all twenty solids considered here. In view of the large overlap of the $\underline{sp}^3$ hybrids, the uniformly small magnitude of V_5 and V_6 is indeed remarkable, and we have found no simple explanation for these results. The magnitudes of V_5 and V_6 are actually comparable to the numerical uncertainty in these quantities. For the sake of conceptual simplicity we shall set $V_5 = V_6 = 0$ in our subsequent analysis. Note that with V_2 fit to experiment and V_5 and V_6 set to zero, values for the integral H_n and J are no longer required.

Having established values for the basic parameters of our two-electron model, we may quantitatively solve the cubic equation, Eq. (III.27) for the singlet-state eigenvalues. We have done this and the values of E_M^0, defined by Eq. (III.26), are given in Table IV, together with the triplet-state eigenvalues

$$E_T^0 = 2 S V_2 - 2 S^2 V_4 / (1 - S^2) \qquad \text{(IV.8)}$$

for the twenty solids under consideration. The corresponding eigenstate expansion coefficients a_{4m}, a_{5m} and a_{6m}, as calculated from Eqs. (III.35)-(III.37), are listed in Table V.

Also, in Table IV we compare our theoretical values for the principal optical-absorption peak $E_2 = E_{IV}^0 - E_{VI}^0$ with both the HC predictions, $E_2^{HC} = 2[(V_2^{HC})^2 + (V_3^{HC})^2]^{1/2}$, and the experimental E_{2A} and E_{2B} sub-peaks as given by Phillips.[28] Because E_2 for the group IV elements is used to fit V_2, only the results for the binary compounds offer a test of the theory. Both our E_2 and E_2^{HC} for these latter materials agree with the available experimental data to within 12%. Our E_2 values

tend to agree best with E_{2B}, and E_2^{HC} agree best with E_{2A}, but the differences do not appear to be significant. It is important to stress, however, that our E_2, in contrast to E_2^{HC}, includes no direct experimental data for the binary compounds.

B. Computed Properties

With the information given in Table I-V, we may systematically study the physical properties discussed in Section III. We begin with the dielectric constant, for which we need the additional quantities γ, δ_a, δ_c and δ_{ca}. All of these parameters are readily calculable from the hybrid wavefunctions, Eq. (IV.4). The values we have obtained are given in Table VI. For the group-IV elements, the dielectric constant is given directly in terms of γ, V_2^{HC} and β' by Eqs. (III.57) and (III.61). From Table II we calculate β' to be 1.23 for C, 1.35 for Si, 1.36 for Ge, and 1.37 for Sn. For the binary compounds, the coupling matrix elements $\langle G|U_\xi^\circ|M\rangle$ must be computed from Eq. (III.52) (see Table VII). As remarked in Sec. III, the term $|\langle G|U_\xi^\circ|\text{IV}\rangle|^2/(E_G-E_{\text{IV}})$ dominates the sum in Eq. (III.52) for the susceptibility χ. We find

$$|(E_G-E_{\text{IV}})/(E_G-E_V)||\langle G|U_\xi^\circ|V\rangle/\langle G|U_\xi^\circ|\text{IV}\rangle|^2 < 0.01| \qquad \text{(IV.9)}$$

in all cases. Finally, we scale our calculated values of χ for the group-IV elements in the manner of HC. Specifically, we replace γ in Eq. (III.57) by $\lambda_n\gamma$ and determine a λ_n for each row of the Periodic Table by fitting ϵ to experiment. We obtain λ_n to be 2.02 for C, 2.22 for Si, 2.56 for Ge, and 3.10 for Sn. For the binary compounds, we multiply our calculated

χ by $\lambda_a \lambda_c$, where λ_a and λ_c are the appropriate values of λ_n for the anion and cation rows. As in the optical-absorption peak calculation and in contrast to HC, we do not use any direct experimental data for the binary compounds in determining the dielectric constant for these materials. The results are listed in Table VIII. Also, in Fig. (4), we have plotted our theoretical dielectric constants versus the best available experimental values[29] for the twenty materials under consideration here. The agreement with experiment is within 12% for the binary compounds and, together with our results for E_2, lends strong support to our method of determining parameters.

We next consider the valence-electron density and the polarity of the bond. We have made a full evaluation of the single bond electron density, as given by Eq. (III.66), in the cases of Ge and GaAs. These results are plotted in Fig. (5) and (6), respectively. There is a broad peak in the electron density at the center of the bond in Ge and a somewhat sharper peak near the As site in GaAs. In both cases the electron density in the bonding region is elongated perpendicular to the bond axis. The remaining peaks and valleys in the core regions result from the oscillations in the s and p atomic wavefunctions due to their orthogonality to the inner core states.

We have also repeated these calculations in the Harrison limit using Eqs. (III.72) and (III.73) with $\alpha_c = \alpha_c^{HC}$ and $\alpha_p = \alpha_p^{HC}$, the HC values of the covalency and the polarity. Interestingly, the results obtained are very close to those of the full calculation in the bonding region. The difference in both cases is on the order of 1%. This is

consistent with the fact that we calculate $\alpha_p^G \cong \alpha_p^{HC}$ for GaAs as well as for Ge (see Table VI), and suggests that the electron-density coefficients u_a, u_c and u_{ac} are determined primarily by the polarity. As can be seen from Eqs. (III.72) and (III.73), the latter is exactly true in the Harrison limit.

To obtain the total electron density in the crystal, one must superimpose the individual single-bond densities. We have done this along a bond axis in both Ge and GaAs and the results are plotted in Fig. (7) and (8). The density near the center of the bond is increased only slightly by adding the electron density from neighboring bonds, but there is a significant increase in the back-bonding regions. For comparison we have also plotted in Figs. (7) and (8) the corresponding results of Walter and Cohen[30] obtained via the local-empirical-pseudopotential method.[31] Their calculated densities are quantitatively similar to ours in the bonding and back-bonding regions, although clearly they find a higher electron density in the center of the bond than do we.

An accurate experimental determination of the valence-electron density has been made in the case of Si,[32] although not in either Ge and GaAs. It has been pointed out that the Walter and Cohen[33] calculation for Si yields the magnitude of the central peak to within 7% of experiment. In view of Fig. (7), it is of interest to consider what modifications in our sp^3 hybrids are required to increase $\rho(\vec{r})$ in the center of the bond. From Eqs. (III.66), (III.72), (III.73) and (IV.4) the electron density at the midpoint of the bond in a group IV element is given to a good approximation by

$$\rho(d/2) = \frac{1}{4\pi}\left[R_s(d/2) + 3R_p(d/2)\right]^2/(1+s)\,. \qquad \text{(IV.10)}$$

Free-atom wavefunctions lead to a value of 0.063 a.u. for $\rho(d/2)$ in Si, as compared with the value 0.102 a.u. found experimentally.[31] However, by smoothly contracting the tails of $R_s(r)$ and $R_p(r)$ beyond r = d/2, one can easily increase $\rho(d/2)$ to the required height,[34] as we have verified in a computer experiment. This is done by calculating the relevant parameters S, U, K, H, J, etc., for two different atomic configurations, $\underline{s}^2\underline{p}^2$ and $\underline{s}^1\underline{p}^3$, and two different approximate exchange potentials, the Herman-Skillman[35] and the Kohn-Sham[36] approximations to a full free atom Hartree-Fock calculation. The results for Si are listed in Table IX. We find that U_n, S, K, H_n, and J are not very sensitive to the different approximations while β^n_{nn} and ρ^n_{nn} on the other hand are sensitive. We also plot in Figs. (9) and (10) the electron density along the bonding axis for two cases, the Hartree-Fock-$\underline{s}^2\underline{p}^2$ configuration and the Kohn-Sham-$\underline{s}^1\underline{p}^3$ configuration wavefunctions. The electron density shapes are a little different but the central peaks are about the same height. We also artificially contract and expand the atomic radial wavefunction by adding to the atomic potential a spherically symmetric potential. The potential for a contraction is of the form

$$V_1'(r) = \begin{cases} 0 & , \ r < d/2 \\ V_0\, e^2\left[(2r/d) - 1\right]^2 \ \text{eV} & , \ r > d/2 \ , \end{cases} \qquad \text{(IV.11)}$$

and for an expansion is of the form

$$V_2'(r) = \left\langle -e^2 Z_A\, e^{-\lambda'}/|\vec{r} - \vec{d}| \right\rangle_{\Omega_r} \ \text{eV} \ , \qquad \text{(IV.12)}$$

where V_0, Z_A, and λ' are adjustable parameters. In Eq. (IV.12), the symbol $\langle\ \rangle_{\Omega_r}$ means a spherical average about an ion site. After averaging, the potential $V_2'(r)$ is then:

$$V_2'(r) = \begin{cases} -e^2\,(e^{-\lambda' d}/d)(\sinh\lambda' r/\lambda' r), & r < d \\ -e^2\,(e^{-\lambda' r}/d)(\sinh\lambda' d/\lambda' d), & r > d \end{cases} \qquad \text{(IV.13)}$$

In Table X we list examples of some calculated quantities. The effect on the electron density of contracting the radial wavefunctions is immediately seen in Fig. (11), where we plot the electron density along the bond for $V_0 = 2.5$.

Comparing Figs. (10) and (11), it is evident that the shape and height of the central peak can be brought closer to the experimental result by contracting the wavefunction. Decarpigny and Lanoo[7] reach a similar conclusion. They needed to contract their free atom Slater-type wavefunctions to fit the calculated F_{222} structure factor to experiment. It seems that valuable information about the shape of the hybrids can be extracted from an accurate knowledge of the electron density in the bonding region.

Our defined polarity α_p^G has been evaluated for each of the sixteen binary compounds considered here and these results, together with the corresponding values of α_p^{HC}, are given in Table VI. For the non-nitride Al, Ga and In compounds, we find α_p^G approximately constant (0.51 to 0.56), which is roughly in accord with α_p^{HC} (0.44 to 0.54). For the corresponding nitride compounds, however, we consistently calculate $\alpha_p^G \sim \frac{1}{2}\,\alpha_p^{HC}$. In addition, we find $\alpha_p^G < \alpha_p^{HC}$ for SiC and BN and

$\alpha_p^G > \alpha_p^{HC}$ for BP and BAs. These trends can be qualitatively understood in terms of our computed values of V_3 and V_4. Generally speaking, α_p^G increases with increasing V_3 and decreases with increasing V_4. We calculate $V_3 < V_3^{HC}$ and $V_3 < V_4$, and consequently relatively small values of α_p^G, for SiC and all the nitride compounds. For the remaining compounds, on the other hand, we obtain $V_3 > V_3^{HC}$ and $V_4 \cong V_3$ for BP and BAs and $V_3 < V_4$ for the others.

For comparison with α_p^G and α_p^{HC}, we have also listed in Table V our calculated values of Z_p, as defined by Eq. (III.76). Generally, there does not seem to be a simple correlation between Z_p and either α_p^G or α_p^{HC}. We find $Z_p \cong \alpha_p^G$ for SiC and the nitrides, but $Z_p < \alpha_p^G$ for the rest. Interestingly, however, there is a qualitative correlation between $(\delta_c - \delta_a)$ and α_p^{HC}. In particular, the trend of decreasing α_p^{HC} with increasing mean atomic number in the B, Al, Ga and In series (except for AlSb) are all reflected in $(\delta_c - \delta_a)$. In this regard, note that $(\delta_c - \delta_a)$ measures the relative spacial extent of the cation and anion hybrids, while α_p^G measures the relative weighting of these hybrids in the electron density.

Let us now move on to consider the nuclear exchange and pseudodipolar coefficients. To evaluate Eqs. (III.92) and (III.93) for Γ_e and Γ_{pd}, one needs values for the matrix elements $\delta_{nn'}^{n''}$ and $\rho_{nn'}^{n''}$. Equation (III.87), for $\delta_{nn'}^{n''}$, is easily evaluated in terms of the hybrids defined by Eq. (IV.4);

$$\delta_{nn''}^{n'} = \begin{cases} [R_{sn}(0)]^2 & , n = n' > n'' , \\ R_{sn}(0)\,[R_{sn''}(d) + 3R_{pn''}(d)] & , n = n' \neq n'' , \\ [R_{sn}(d) + 3R_{pn}(d)]^2 & , n = n'' \neq n' . \end{cases} \quad \text{(IV.14)}$$

For free-atom wavefunctions $R_{sn}(0) >> [R_{sn}(d) + 3 R_{pn}(d)]$ and consequently $s^{n}_{nn} >> s^{n}_{nn'} >> s^{n'}_{nn}$. Specifically, we find

$$|s^{n}_{nn'} / s^{n}_{nn}| < 0.10$$

and (IV.15)

$$|s^{n'}_{nn} / s^{n}_{nn}| < 0.01$$

in all cases. The situation for $p^{n'}_{nn'}$ is slightly more complicated. Only p^{n}_{nn} has a simple formula in terms of the hybrids

$$p^{n}_{nn} = \int_0^\infty R_{pn}^2(r) \frac{dr}{r} . \tag{IV.16}$$

To evaluate the overlap terms one must use the wavefunction-expansion techniques discussed in the appendix. Specific formulas for $p^{n}_{nn'}$ and $p^{n'}_{nn}$ are given there. Quantitatively, we find

$$|p^{n}_{nn'} / p^{n}_{nn}| < 0.27$$

and (IV.17)

$$|p^{n'}_{nn} / p^{n}_{nn}| < 0.18 ,$$

although the upper limits are only approached in the case of BN. Typically the ratios are much smaller. For completeness we have included all four overlap terms, $s^{n}_{nn'}$, $s^{n'}_{nn}$, $p^{n}_{nn'}$, and $p^{n'}_{nn}$ (values are listed in Table XI) in calculating Γ_e and Γ_{pd}. These have been determined both in the Harrison limit, using V_2^{HC} and V_3^{HC} to evaluate Eqs. (III.100) and (III.101), and with the full theory, using the data listed in Table IV and VI to evaluate b_1, b_2 and E_0. These results are presented in Table XII together with the best available experimental data. Note that the values of Γ_e and Γ_{pd} in the Harrison limit are larger (except for InN) than the corresponding ones calculated in HMSB. This is due primarily to the

appearance of the overlap matrix elements in Eq. (III.100). As expected from Sec. III, the effect of two-electron correlation is to enhance Γ_e and Γ_{pd} in all cases. The magnitude of the enhancement, however, shows rather complicated trends depending both on bond length and polarity. In the group IV elements, ζ' is 2.04 for C, is 3.30 for Si and Ge, and is 3.53 for Sn.

We have not included any additional scaling factors in the theoretical numbers listed in Table XII. This does not appear to be important in the case of Γ_{pd}, but clearly we overestimate the magnitudes of Γ_e, although the trends are correct.

We have made an approximate least-squares fit of Γ_e^{eff} to the six non-zero Γ_e experimental values using the form:

$$\Gamma_e^{eff} = \Lambda_a \Lambda_c \Gamma_e \quad , \tag{IV.18}$$

where Λ_a and Λ_c are constants that depend only on row number in the Periodic Table, and the Γ_e are the full-theory values given in Table XII. We have thereby determined scaling factors Λ_n appropriate to each row. Λ_n is found to be 0.19 for the Si row, 0.37 for the Ge row, and 0.64 for the Sn row. As with the scaling factor λ_n in the dielectric constant, Λ_n increases with increasing atomic number. Note, however, that $\lambda_n > 1$ while $\Lambda_n < 1$.

As noted in Sec. II, there is a relationship between the dielectric constant and the nuclear exchange coefficient in the Harrison limit, Eq. (II.50). This motivated a plot[22] of experimental values of $(\epsilon - 1)$ against the known experimental values of $\Gamma_e / \Gamma_{dd} d^4 = \Gamma_e / (\gamma_a \gamma_c \hbar d)$,

and it revealed a rather striking linear relationship in the series InP, InAs and InSb. Subsequently, experiments[37] on the Ga series displayed the linear relationship for those compounds as well. Both sets of experimental data are shown in Fig. (12). Using the calculated values of ϵ from Table VIII and the full-theory values of Γ_e from Table XII, we have plotted in Fig. (13) the theoretical equivalent to Fig. (12) for all the III-V compounds. Approximate linear trends can be seen in the In and Ga series, as well as the Al series, for the heaviest three compounds. To examine the origin of this behavior, we repeated the calculation in the Harrison limit. In this case, the linear behavior was improved slightly in the In series, worsened slightly in the Ga series and was destroyed in the Al series.

Rewriting Eq. (II.51) by keeping only the dominant terms in $\delta^{n'}_{nn''}$ and $\beta^{n'}_{nn''}$, and applying the multiplicative factor discussed in Sec. III, one has

$$\hbar\gamma_c\gamma_a C \sim \left[\frac{\lambda_c\lambda_a}{\delta^a_{aa}\delta^c_{cc}\beta'}\right]\left[\frac{18\sqrt{3}\,(\gamma e)^2\,(1-S^2)^2}{(1-S^2)-S^2(\alpha_p^{Hc}/\alpha_c^{Hc})^2}\right], \qquad \text{(IV.19)}$$

where by construction, $(\lambda_a\lambda_c/\beta')^{1/2}\gamma$ is the HC fitted value of γ^{Hc}. For the heavier Ga and In compounds, β', γ, S, α_p^{Hc} and α_c^{Hc} are rather constant. This implies that for a given cation series

$$\lambda_a/\delta^a_{aa} \sim \text{constant}. \qquad \text{(IV.20)}$$

Evaluation of Eq. (IV.20) gives 0.0155 for Sb, 0.0163 for As, and 0.0311 for P. The higher value for P is consistent with Fig. (13), where the

points for AlP, GaP and InP all lie above the straight line defined by corresponding As and Sb compounds.

It seems clear that Γ_{pd}/Γ_e is dominated by the ratio ρ^n_{nn}/β^n_{nn}, which in turn is a direct property of the s and p wavefunctions that make up the hybrid. We have to bring this ratio close to the experimental value in order that Γ_{pd} and Γ_e will reconcile with experiment simultaneously. Interestingly, we have found in the case of Si that the latter ratio can be increased if the tails of the free-atom wavefunctions are contracted in the manner necessary to account for the electron density in the center of the bond.

As our final application, we turn to the cohesive energy. For the group IV elements, it is instructive to rewrite Eq. (III.111) as

$$E_{Coh} = 8(1-S)V_2^{HC} - 4E_{corr} - 4E_{ol} - E_{pro}\,, \qquad \text{(IV.21)}$$

where $-4E_{corr}$ is the explicit contribution of two-electron correlation to the cohesive energy. Using Eq. (IV.1) and comparing Eqs. (III.111) and (IV.21), one has (with $V_6 = 0$)

$$E_{corr} = 2(1-2S^2)V_4/(1-S^2) - 2S(V_2^{HC} - V_2)\,. \qquad \text{(IV.22)}$$

As desired, one finds $E_{corr} = 0$ for $V_4 = 0$, since then $V_2^{HC} = V_2$. Unfortunately, a complete evaluation of Eq. (IV.21) requires the uncertain quantity $\Delta\varepsilon_a + \Delta\varepsilon_c$. Because an accurate evaluation of $\Delta\varepsilon_n$ is quite difficult, we calculate only the remaining terms. Specifically, we replace E_{ol} in Eq. (IV.21) with

$$E_{o\ell}^{o} = -K + e^2/d \ , \qquad \text{(IV.23)}$$

and use our calculated values of V_1^n, V_2, V_4, S and K to evaluate E_{coh} and its components. The results are listed in Table XIII together with the experimental values of the cohesive energy. Note that our calculated E_{coh} is less than experiment but positive in each case. This is consistent with the small negative values of $\Delta\mathcal{E}_n$ that we expect theoretically. Also note that $-4\ E_{o\ell}^{o}$ makes a large positive contribution and $-4\ E_{corr}$ a smaller, but non-negligible, negative contribution to E_{coh}. We may contrast this with the calculation of E_{coh} made by HC. They, of course, neglected both $E_{o\ell}$ and E_{corr}. Quantitatively, these omissions were partly compensated for by their use of smaller values of S (a constant value of 0.5) and a scaling factor of 0.8 multiplying E_{pro}. Their prescription gives a rather fortuitous value of E_{coh} - 11.1 eV for C, but negative values of -2.72 eV for Si, -3.94 eV for Ge and -3.01 eV for Sn.

We have determined empirical values of $\Delta\mathcal{E}_n$ for each group IV element by fitting to the experimental cohesive energy:

$$\Delta\mathcal{E}_n^{fit} = (E_{coh} - E_{coh}^{expt})/8 \ . \qquad \text{(IV.24)}$$

As can be seen from Table XIII, the magnitudes of the $\Delta\mathcal{E}_n^{fit}$ are reasonable. The irregular variation from element to element is questionable and no doubt partly reflects the fact that our theoretical model is best for a large band gap material like C. In any case, we have used Eq. (IV.2) to extend the calculation of E_{coh} to the binary compounds. We

have assumed that $\Delta\varepsilon_\alpha + \Delta\varepsilon_c$ is a covalent quantity and have used the appropriate arithmetic mean of the group IV values for each compound together with a direct calculation of the remaining terms in Eq. (III.107). The results are listed in Table XIV and also plotted against the known experimental cohesive energies in Fig. (14). The comparison is not as favorable as with E_2 and ϵ , but positive values are found in all cases except for InN.

V. CONCLUSION

The full formal theory of the two-electron bond-orbital model has been presented and the applications have been extended. It has also been extensively compared and contrasted with Harrison's one-electron bond-orbital model. Both the analytic formulas given in Sec. III and the parameters listed in Tables I - XIV can be used to treat many additional physical properties, including those considered by Harrison and other workers using the one-electron model.

It has been shown from Eqs. (III.57), (III.61), (III.97), (III.99), (IV.21) and (IV.22) that two-electron correlation effects are significant in the dielectric constant, the nuclear exchange and pseudo-dipolar coefficients, and the cohesive energy. However, by comparing the valence electron density plots in the full theory with those in the Harrison limit, one finds the difference is almost invisibly small. Thus, in this case the polarity and the shape of the $\underline{sp}^3$ hybrid wavefunctions are the dominant quantities, rather than electron correlation.

In $\epsilon - 1$, Γ_e , and Γ_{Pd} the effect of correlation is essentially multiplicative. In particular, with the fitting procedure used here the calculated values of the electric susceptibility χ characteristically decrease by about 30% from the values in Harrison limit. On the other hand, both Γ_e and Γ_{Pd} characteristically increase by about 300% (see in Table XII, the values in parenthesis and those under full theory). This relative insensitivity of χ is because the energy difference between singlet states IV and VI that enters into χ from second

order perturbation theory is fixed to the E_2 peak. Hence, the energy denominator does not change when correlation is included. However, the energy of the triplet states is decreased relative to state IV when correlation is present. As a consequence, the calculated values for Γ_e and Γ_{Pd} are more sensitive to electron correlation, since the energy denominator that enters in a calculation of Γ_e and Γ_{Pd} is the difference between the triplet and the ground state energies.

The correlation corrections can be hidden to some extent if scaling factors are used to achieve quantitative agreement with experiment as did HC. It is especially encouraging that we have successfully predicted results that agree with experiments while actually fitting fewer parameters to experiment than did HC. For example, in predicting the principal optical absorption peak E_2, and the dielectric constant ϵ, there are only 8 parameters fitted to experimental values, while 24 fitted parameters were needed in HC for the twenty semiconductors considered here. Also, by including the overlap energy E_{ol} and correlation energy E_{corr}, positive cohesive energies are predicted for all the compounds treated except InN.

An interesting and potentially important area for additional work is in optimizing the $\underline{sp}^3$ hybrid wavefunctions and determining the impact this has on calculated parameters such as V_3, V_4, δ_{nn}^{n} and ρ_{nn}^{n}. A better way to determine V_2 is also desired, so that one can eliminate any fitting procedure. A set of optimized $\underline{sp}^3$ hybrid wavefunctions can probably be obtained by requiring them to reproduce the measured valence electron density or equivalently the atomic form factors. The formulas

for $\epsilon \sim 1$, Γ_e, and Γ_{pd} can then be used as a sensitive check on these wavefunctions since they each separate into two multiplicative parts: one depends only on the intrabond parameters, and the other depends only on the intraatomic parameters. Moreover, the dependence on the intrabond parameters is the same in Γ_e and Γ_{pd}. Thus the ratio Γ_{pd}/Γ_e provides a very sensitive test to the hybrid wavefunctions. If wavefunctions can be found that meet these tests, they will be an improvement over free atom wavefunctions.

To complete this procedure, local field and d-state corrections to ϵ need to be examined. The inherent errors in all the calculated quantities caused by the bond-orbital approximation must also be determined. Also, the influence of the core polarization effect on Γ_e and Γ_{pd} must be examined in semiconductors. For example, in case of Fe and some other magnetic materials,[38] the spin of the valence electron can polarize the core s-state electrons through the exchange interaction. This effect changes the sign of the contact interaction and hence significantly modifies the contact interaction.

Finally, these calculations can be extended to the II-VI and I-VII compounds. The additional problems of semiconductor alloys, amorphous materials and surface effects can be treated in this framework as well.

APPENDIX

One way to carry out the two center integrals discussed in Sec. III and IV is by the α -expansion method of Löwdin.[38] In this method a function on one center c of the form

$$\begin{aligned} \phi_c(\vec{r}_c) &= \phi_c(n_c \ell_c m_c \mid \vec{r}_c) \\ &= R_{n_c \ell_c}(r_c)\, Y_{\ell_c m_c}(\Omega_c), \end{aligned} \tag{A.1}$$

where $Y_{\ell_c m_c}(\Omega_c)$ is the usual spherical harmonic and $R_{n_c \ell_c}(r_c)$ is a function that depends only on the radial coordinate, is expanded in spherical harmonics centered on the other site a. One has

$$\phi_c(n_c \ell_c m_c \mid \vec{r}_c) = \sum_{\ell=0}^{\infty} \sum_{m=-\ell}^{\ell} \alpha_{\ell m}(n_c \ell_c m_c \mid d, r_a)\, Y_{\ell m}(\Omega_a), \tag{A.2}$$

where d is the distance between the two centers. The expansion coefficient $\alpha_{\ell m}$ can be determined by taking advantage of the orthogonality of the spherical harmonics

$$\alpha_{\ell m}(n_c \ell_c m_c \mid d, r_a) = \int \phi_c(n_c \ell_c m_c \mid \vec{r}_c)\, Y_{\ell m}(\Omega_a)\, d\Omega_a . \tag{A.3}$$

One can without a loss of generality choose a coordinate system in which the two sets of coordinates share the same z-axis, and the center c is located at displacement $+d\hat{z}$ from the center a. Then in Eq. (A.3) only the $m = m_c$ component contributes, because the azimuthal angle is the same for centers a and c. There is an additional simplification that arises because only $m_a = m_c = 0$ enter the calculations. Hence

the important spherical harmonics can be expressed in terms of the Legendre polynomials

$$Y_{l0}(\Omega) = \sqrt{\frac{2l+1}{4\pi}}\, P_l(\cos\theta) . \tag{A.4}$$

Equation (A.3) then simplifies to

$$\alpha_l(n_c l_c | d, r_a) = \tfrac{1}{2}\sqrt{2l_c+1}\sqrt{2l+1}\int_0^{\pi} R_{n_c l_c}(r_c) P_{l_c}(\cos\theta_c) \cdot P_l(\cos\theta_a)\sin\theta_a\, d\theta_a . \tag{A.5}$$

The geometric relations between the two sets of coordinates are

$$r_c^2 = d^2 + r_a^2 - 2 d r_a \cos\theta_a , \tag{A.6a}$$

$$r_a^2 = d^2 + r_c^2 + 2 d r_c \cos\theta_c , \tag{A.6b}$$

$$-r_c\cos\theta_c + r_a\cos\theta_a = d , \tag{A.6c}$$

$$r_c \sin\theta_c = r_a \sin\theta_a . \tag{A.6d}$$

If r_a and d are treated as fixed parameters, then one can switch the integration variable from θ_a to r_c by using Eq. (A.6a). One has the result

$$\sin\theta_a\, d\theta_a = \frac{r_c}{r_a d}\, dr_c , \tag{A.7}$$

θ_a varies between the limits 0 and π, so r_c varies between $|d - r_a|$ and $(d + r_a)$. Finally one has

$$\alpha_\ell(n_c \ell_c | d, r_a) = \frac{1}{2 r_a d} \sqrt{2\ell_c+1}\sqrt{2\ell+1} \int_{|d-r_a|}^{(d+r_a)} R_{n_c \ell_c}(r_c) \cdot P_{\ell_c}\left(\frac{r_a^2 - d^2 - r_c^2}{2 d r_c}\right) P_\ell\left(\frac{r_a^2 + d^2 - r_c^2}{2 d r_a}\right) r_c \, dr_c \quad . \tag{A.8}$$

It can be shown that when $r_a \to 0$, α_ℓ has the limiting form

$$\alpha_\ell(n_c \ell_c | d, r_a) \underset{r_a \to 0}{=} (-1)^{\ell_c} R_{n_c \ell_c}(d) \frac{r_a^\ell}{\ell^2+1} \quad . \tag{A.9}$$

So α_ℓ goes to zero proportional to r_a^ℓ .

The two center integrals then become a series of one center integrals that will either terminate or converge rapidly. This can be established by using the following identities of Legendre polynomials:

$$\int_{-1}^{1} P_{\ell'}(x) P_\ell(x) \, dx = \frac{2}{2\ell+1} \delta_{\ell\ell'} \, , \tag{A.10a}$$

$$\int_{-1}^{1} x P_{\ell'}(x) P_\ell(x) \, dx = \begin{cases} \dfrac{2(\ell+1)}{(2\ell+1)(2\ell+3)} \delta_{\ell', \ell+1} \\ \dfrac{2\ell}{(2\ell-1)(2\ell+1)} \delta_{\ell', \ell-1} \, , \end{cases} \tag{A.10b}$$

$$\int_{-1}^{1} x^2 P_{\ell'}(x) P_\ell(x) \, dx = \begin{cases} \dfrac{2(\ell+1)(\ell+2)}{(2\ell+1)(2\ell+3)(2\ell+5)} \delta_{\ell', \ell+2} \\ \dfrac{2(2\ell^2+2\ell-1)}{(2\ell-1)(2\ell+1)(2\ell+3)} \delta_{\ell', \ell} \, , \end{cases} \tag{A.10c}$$

where in Eq. (A.10) $\ell' \geq \ell$ is assumed.

Central to the evaluation of two-electron repulsive integrals is the standard expansion

$$\frac{1}{|\vec{r} - \vec{r}'|} = 4\pi \sum_{\ell=0}^{\infty} \sum_{m=-\ell}^{\ell} \frac{1}{2\ell+1} \frac{r_<^\ell}{r_>^{\ell+1}} Y_{\ell m}^*(\Omega) Y_{\ell m}(\Omega') \, , \tag{A.11}$$

where $r_<$ ($r_>$) is the lesser (greater) of r and r'. In terms of the Legendre polynomials $P_\ell(x)$, the $\underline{sp}^3$ hybrid wavefunctions have the form

$$\phi_n(\vec{r}) = \frac{1}{2\sqrt{4\pi}} \left[R_{sn}(r) P_0(\cos\theta) + 3\theta_n R_{pn}(r) P_1(\cos\theta) \right] , \quad \text{(A.12)}$$

where $P_0(x) = 1$, $P_1(x) = x$, and again $\theta_a = +1$ and $\theta_c = -1$. Using Eqs. (A.11) and (A.12), the Coulomb potential arising from an $\underline{sp}^3$ hybrid electron density can be written

$$\begin{aligned} V_n(\vec{r}) &= \int \phi_n(\vec{r}') \frac{e^2}{|\vec{r} - \vec{r}'|} \phi_n(\vec{r}')\, d\vec{r}' \\ &= \frac{1}{4} \left[Z^0_{ss}(r) + 9 Z^0_{pp}(r) + 2\theta_n Z^1_{sp}(r) P_1(\cos\theta) \right. \\ &\qquad \left. + \frac{6}{5} Z^2_{pp}(r) P_2(\cos\theta) \right] \frac{e^2}{r} , \end{aligned} \quad \text{(A.13)}$$

where

$$\begin{aligned} Z^k_{\ell\ell'}(r) &= \int_0^r R_{\ell n}(r') \left(\frac{r'}{r}\right)^k R_{\ell' n}(r') r'^2 dr' \\ &\quad + \int_r^\infty R_{\ell n}(r') \left(\frac{r}{r'}\right)^{k+1} R_{\ell' n}(r') r'^2 dr' . \end{aligned} \quad \text{(A.14)}$$

From Eqs. (A.12) and (A.13) one then has

$$\begin{aligned} U_n &= \int \phi_n(\vec{r})\, V_n(\vec{r})\, \phi_n(\vec{r})\, d\vec{r} \\ &= \frac{1}{16} \left[F^0_{ss} + 9 F^0_{pp} + 6 F^0_{sp} + 4 G^1_{sp} + \frac{36}{25} F^2_{pp} \right] , \end{aligned} \quad \text{(A.15)}$$

where $F^k_{\ell\ell'}$ and $G^k_{\ell\ell'}$ are the integrals defined by Mann:[26]

$$F^k_{\ell\ell'} = \int_0^\infty R_{\ell n}(r) \frac{e^2 Z^k_{\ell\ell'}(r)}{r} R_{\ell n}(r) r^2 dr , \quad \text{(A.16)}$$

$$G^k_{\ell\ell'} = \int_0^\infty R_{\ell n}(r) \frac{e^2 Z^k_{\ell\ell'}(r)}{r} R_{\ell' n}(r) r^2 dr , \quad \text{(A.17)}$$

and we have derived Eq. (IV.5).

To evaluate K, one can expand $V_c(\vec{r}_c)$ in spherical harmonics centered on the anion. Again only the m = 0 component of the expansion is required and one can write

$$V_c(\vec{r}-\vec{d}) = \frac{1}{4}\sum_{k=0}^{\infty} B_c^k(d,r)\, P_k(\cos\theta), \tag{A.18}$$

where $\vec{r}$ is measured from the anion and

$$B_c^k(d,r) = \beta_{sso}^k(d,r) + 9\beta_{ppo}^k(d,r) - 2\beta_{sp1}^k(d,r) + \frac{6}{5}\beta_{pp2}^k(d,r), \tag{A.19}$$

with

$$\beta_{ll'k'}^k(d,r) = \frac{2k+1}{2dr}\int_{|d-r|}^{d+r} \frac{e^2}{r'} Z_{ll'}^{k'}(r')\, P_{k'}\left(\frac{r^2-r'^2-d^2}{2dr'}\right) \cdot P_k\left(\frac{r^2-r'^2+d^2}{2dr}\right) r'\,dr'. \tag{A.20}$$

Then K is

$$\begin{aligned} K &= \int \phi_a(\vec{r})\, V_c(\vec{r}-\vec{d})\, \phi_a(\vec{r})\, d\vec{r} \\ &= \frac{1}{16}\int_0^{\infty}\Big\{[R_{sa}(r)]^2 B_c^o(d,r) + R_{sa}(r)R_{pa}(r)\, B_c^1(d,r) \\ &\quad + [R_{pa}(r)]^2\left[9B_c^o(d,r) + \frac{6}{5}B_c^2(d,r)\right]\Big\} r^2\,dr. \end{aligned} \tag{A.21}$$

To compute the remaining integrals, one must use an expansion for the $\underline{sp}^3$ hybrid wavefunction.

$$\phi_n(\vec{r}+\phi_n d) = \frac{1}{2}\sum_{k=0}^{\infty}\sqrt{\frac{2k+1}{4\pi}}\, A_n^k(d,r)\, P_k(\cos\theta), \tag{A.22}$$

where

$$A_n^k(d,r) = \alpha_{sn}^k(d,r) + \sqrt{3}\,\theta_n\,\alpha_{pn}^k(d,r) \quad , \tag{A.23}$$

with

$$\alpha_{\ell n}^k(d,r) = \frac{2\pi}{dr}\sqrt{\frac{2k+1}{4\pi}}\sqrt{\frac{2\ell+1}{4\pi}}\int_{|d-r|}^{d+r} R_{\ell n}(r')\,P_\ell\left(\frac{r^2-r'^2-d^2}{2dr'}\right) \cdot P_k\left(\frac{r^2-r'^2+d^2}{2dr}\right) r'\,dr' . \tag{A.24}$$

Formulas for S, H_n, δ_{ca} and β_{nn}^n in terms of the $A_n^k(d,r)$ follow immediately.

$$S = \frac{1}{4}\int_0^\infty \left[R_{sa}(r)\,A_c^0(d,r) + \sqrt{3}\,R_{pa}(r)\,A_c^1(d,r)\right] r^2\,dr, \tag{A.25}$$

$$\begin{aligned} H_n = \frac{1}{32}\int_0^\infty \Big\{ & R_{sn}(r)\Big[2\left(Z_{ss}^0(r) + 9\,Z_{pp}^0(r)\right)A_{n'}^0(d,r) \\ & + \frac{4\sqrt{3}}{3}\theta_n\,Z_{sp}^1(r)\,A_{n'}^1(d,r) + \frac{12\sqrt{5}}{5}\,Z_{pp}^2(r)\,A_{n'}^2(d,r)\Big] \\ & + R_{pn}(r)\Big[2\sqrt{3}\,\theta_n\left(Z_{ss}^0(r) + 9\,Z_{pp}^0(r)\right)A_{n'}^0(d,r) \\ & + 6\,Z_{sp}^1(r)\left(\frac{4\sqrt{5}}{15}A_{n'}^2(d,r) + \frac{2}{3}A_{n'}^0(d,r)\right) \\ & + \frac{18}{5}\theta_n\,Z_{pp}^2(r)\left(\frac{18\sqrt{7}}{35}A_{n'}^3(d,r) + \frac{4\sqrt{3}}{15}A_{n'}^1(d,r)\right)\Big]\Big\} r^2\,dr, \end{aligned} \tag{A.26}$$

$$\begin{aligned} \delta_{ca} = & \frac{1}{2}S - \frac{1}{4d}\int_0^\infty \Big\{\frac{\sqrt{3}}{3}R_{sa}(r)\,A_c^1(d,r) + R_{pa}(r) \\ & \cdot\left[A_c^0(d,r) + \frac{2\sqrt{5}}{5}A_c^2(d,r)\right]\Big\} r^3\,dr \quad , \end{aligned} \tag{A.27}$$

and

$$\begin{aligned} \beta_{nn'}^n = & \int_0^\infty \Big\{\frac{\sqrt{5}}{6}R_{sn}(r)\,A_{n'}^2(d,r) + \theta_n R_{pn}(r)\Big[\frac{\sqrt{3}}{3}A_{n'}^1(d,r) \\ & + \frac{3\sqrt{7}}{14}A_{n'}^3(d,r)\Big]\Big\}\frac{dr}{r} . \end{aligned} \tag{A.28}$$

Finally a formula for $\rho_{nn}^{n'}$ may be derived by making two expansions of the form of Eq. (A.22)

$$\rho_{nn}^{n'} = \frac{1}{8} \sum_{k,k'} \sqrt{2k+1}\sqrt{2k'+1} \int_0^\infty A_{n'}^{k}(d,r)\, A_{n'}^{k'}(d,r)\, \frac{dr}{r} \cdot \int_{-1}^{1} P_2(x)\, P_k(x)\, P_{k'}(x)\, dx \quad . \tag{A.29}$$

In this case an infinite but rapidly convergent series is obtained. For each value of k there are from one to three values of k' according to Eq. (A.10), that give finite contributions to the series. In our calculations we have accumulated terms up to k = 3 and k' = 3.

In the case of J a double expansion like Eq. (A.29) is required. We have to replace one of the functions $\phi_n(\vec{r})$ in Eq. (A.13) by a series of functions $A_n^k(d,r)$. Then we can obtain an expression similar to Eq. (A.26) for H_n with the Z's properly replaced. Once again we kept all the terms up to ℓ or k = 3.

REFERENCES

1. G. G. Hall, Philos. Mag. 43, 338 (1952).
2. G. Lehman and J. Friedel, J. Appl. Phys. 33, 281 (1962).
3. C. A. Coulson, L. R. Redei and D. Stocker, Proc. Roy. Soc. 270, 357 (1962).
4. D. Weaire and M. F. Thorpe, Phys. Rev. B 4, 2508 (1971), also, M. F. Thorpe and D. Weaire, Phys. Rev. B 4, 3518 (1971), M. F. Thorpe, D. Weaire and R. Alben, Phys. Rev. B 7, 3777 (1973).
5. W. A. Harrison, Phys. Rev. B 8, 4487 (1973).
6. W. A. Harrison and S. Ciraci, Phys. Rev. B 10, 1516 (1974).
7. J. N. Decarpigny and M. Lanoo, Phys. Rev. B (to be published).
8. W. A. Harrison and J. Ch. Phillips, Phys. Rev. Lett 33, 410 (1974).
9. R. K. Sundfors, Phys. Rev. B 10, 4244 (1974).
10. W. A. Harrison, Phys. Rev. B 10, 767 (1974).
11. M. Lanoo and J. N. Decarpigny, Phys. Rev. B 8, 5704 (1973).
12. G. Lucovsky, R. M. Martin and E. Burstein, Phys. Rev. B 4, 1367 (1971).
13. R. M. Martin, Phys. Rev. B 5, 1607 (1972).
14. D. J. Chadi, R. M. White and W. A. Harrison, Phys. Rev. Lett. 35, 1372 (1975).
15. V. P. Sukhatme and P. A. Wolff, Phys. Rev. Lett. 35, 1369 (1975).

16. S. T. Pantelides and W. A. Harrison, Phys. Rev. B 11, 4049 (1975).

17. I. P. Batra and S. Ciraci, Phys. Rev. Lett. 34, 1337 (1975).

18. P. E. Gregory, W. E. Spicer, S. Ciraci and W. A. Harrison, App. Phys. Lett. 25, 511 (1974).

19. S. T. Pantelides and W. A. Harrison, Phys. Rev. B 11, 3006 (1975).

20. J. Tejeda and N. J. Shevchik, Phys. Rev. B (to be published, March 15, 1976).

21. S. T. Pantelides and W. A. Harrison, Phys. Rev. B (to be published, March 15, 1976).

22. C. Huang, J. A. Moriarty, A. Sher, and R. K. Breckenridge, Phys. Rev. B 12, 5395 (1975).

23. L. M. Falicov and R. A. Harris, J. Chem. Phys. 51, 3153 (1969).

24. J. C. Slater, "Quantum Theory of Molecules and Solids, Vol. I", (McGraw-Hill, New York, 1965).

25. S. Clough and W. I. Goldberg, J. Chem. Phys. 45, 4080 (1966). They consider an orbital with arbitrary amounts of s and p character of the form $a_s|s\rangle + a_p|p\rangle$. For the case of an sp^3 hybrid it is appropriate to take $a_s = 1/2$ and $a_p = \sqrt{3}/2$ in their equation.

26. J. B. Mann, Los Alamos Scientific Laboratory Reports Nos. LA-3690 and LA-3691 (1967) (unpublished).

27. C. Roetti and E. Clementi, J. Chem. Phys. 61, 2062 (1974).

28. J. C. Phillips, "Bands and Bonds in Semiconductors" (Academic, New York, 1973) p. 169.

29. J. A. Van Vechten, private communication. A refined version of Table III in the paper J. A. Van Vechten, Phys. Rev. 182, 891 (1969).

30. J. P. Walter and M. L. Cohen, Phys. Rev. B 4, 1877 (1971).

31. In this method only the pseudo-electron density is calculated and all structure in the core region is consequently absent.

32. Y. W. Yang and P. Coppens, Solid State Commun. 15, 1555 (1975).

33. J. R. Chelikowsky and M. L. Cohen, Phys. Rev. Lett. 33, 1339 (1974). These authors also report that non-local pseudopotential corrections to the method of Ref. (30) are necessary to explain the detailed shape of the experimental bond density in Si.

34. This is consistent with the experience of quantum chemists on simple diatomic molecules such as H_2. See for example Ref. (24).

35. F. Herman and S. Skillman, "Atomic Structure Calculations" (Prentice-Hall, Englewood Cliffs, N. J. 1963).

36. W. Kohn and L. J. Sham, Phys. Rev. 140, A1133 (1965).

37. M. K. Cueman and J. F. Soest, Phys. Rev. B (to be published).

38. R. E. Watson and A. J. Freeman, "Hartree-Fock Theory of Electric and Magnetic Hyperfine Interaction in Atoms and Magnetic Compounds" edited by A. J. Freeman and R. B. Frankel (Academic Press, New York, 1967).

39. P. O. Löwdin, Adv. Phys. 5, 1 (1956).

Fig. 1. A diamond or zinc blende lattice. In the diamond structure all the atoms are the same, while zinc blende structure the two components are located at the bigger or smaller spheres respectively. The four nearest neighbors to each site form a tetrahedron.

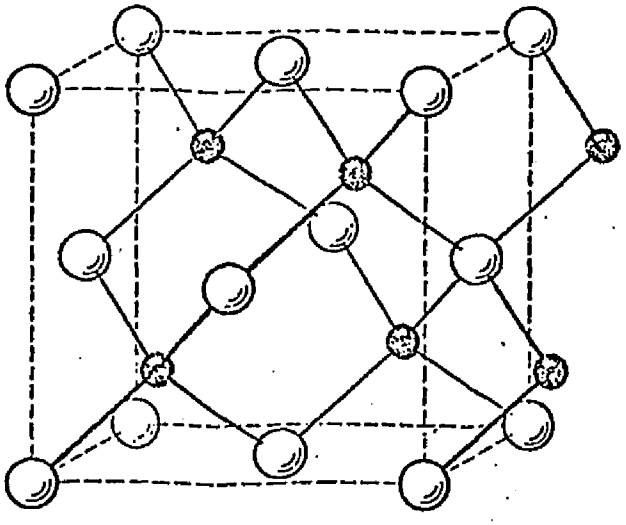

Fig. 2. Energy levels of Harrison's one-electron bond-orbital model and the present two-electron bond-orbital model in the Harrison and Falicov-Harris limits. Note that the six two-electron states derive from the six unique ways (including spin) that two electrons can occupy E_b and $E_{\bar{b}}$. Also in this figure $E_{IV} - E_{VI}$ = const. is maintained in all cases.

HARRISON
ONE ELECTRON

HARRISON
TWO ELECTRON

FALICOV-HARRIS
TWO ELECTRON
$S = 0$

FALICOV-HARRIS
TWO ELECTRON
$S \neq 0 \quad V_6 = 0$

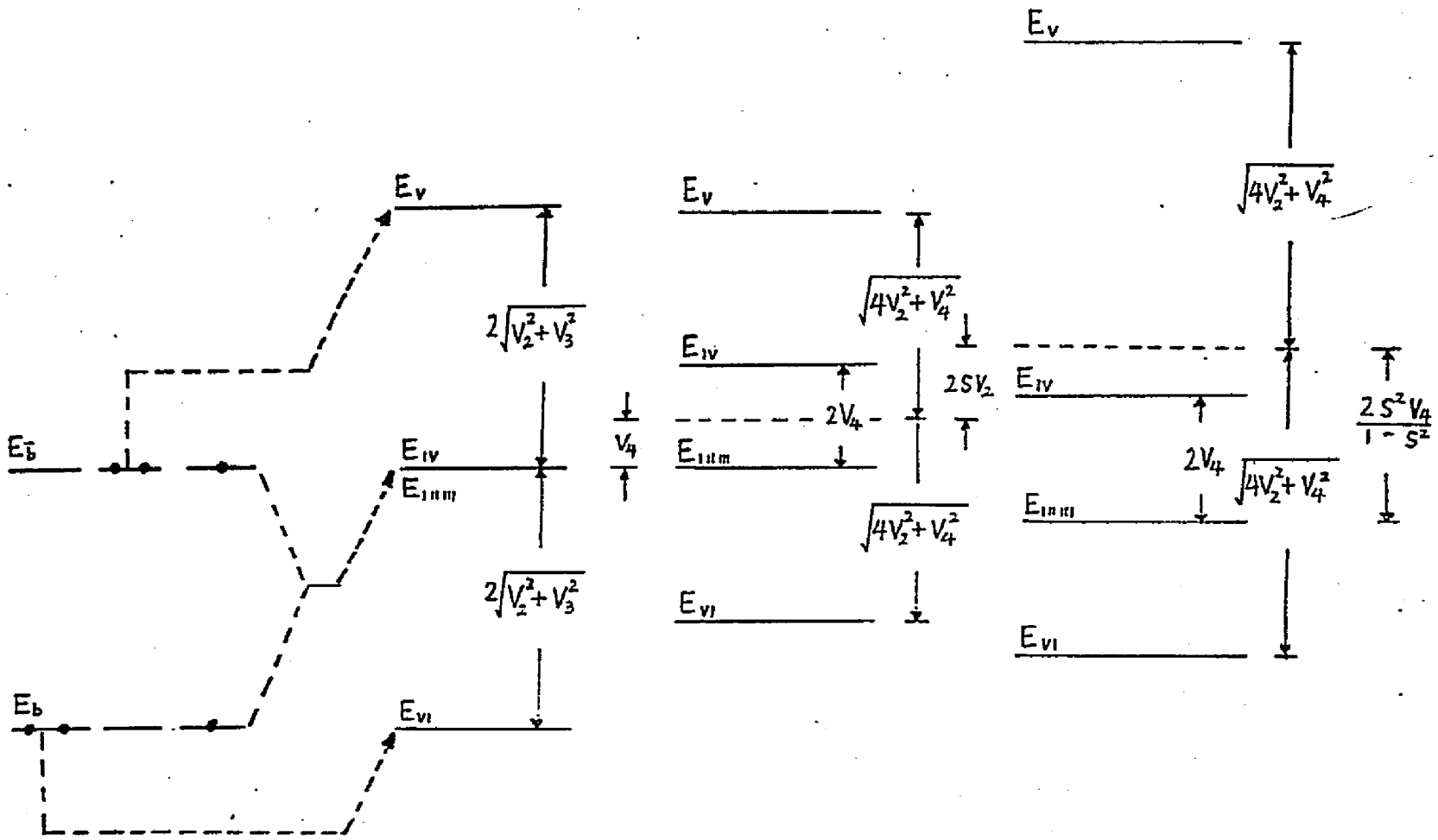

Fig. 3. Correlation enhancement factor ξ' defined by Eq. (III.99) for the nuclear exchange and pseudodipolar coefficients of homopolar solids as a function of $X = 2V_4/V_2$ with $V_6 = 0$.

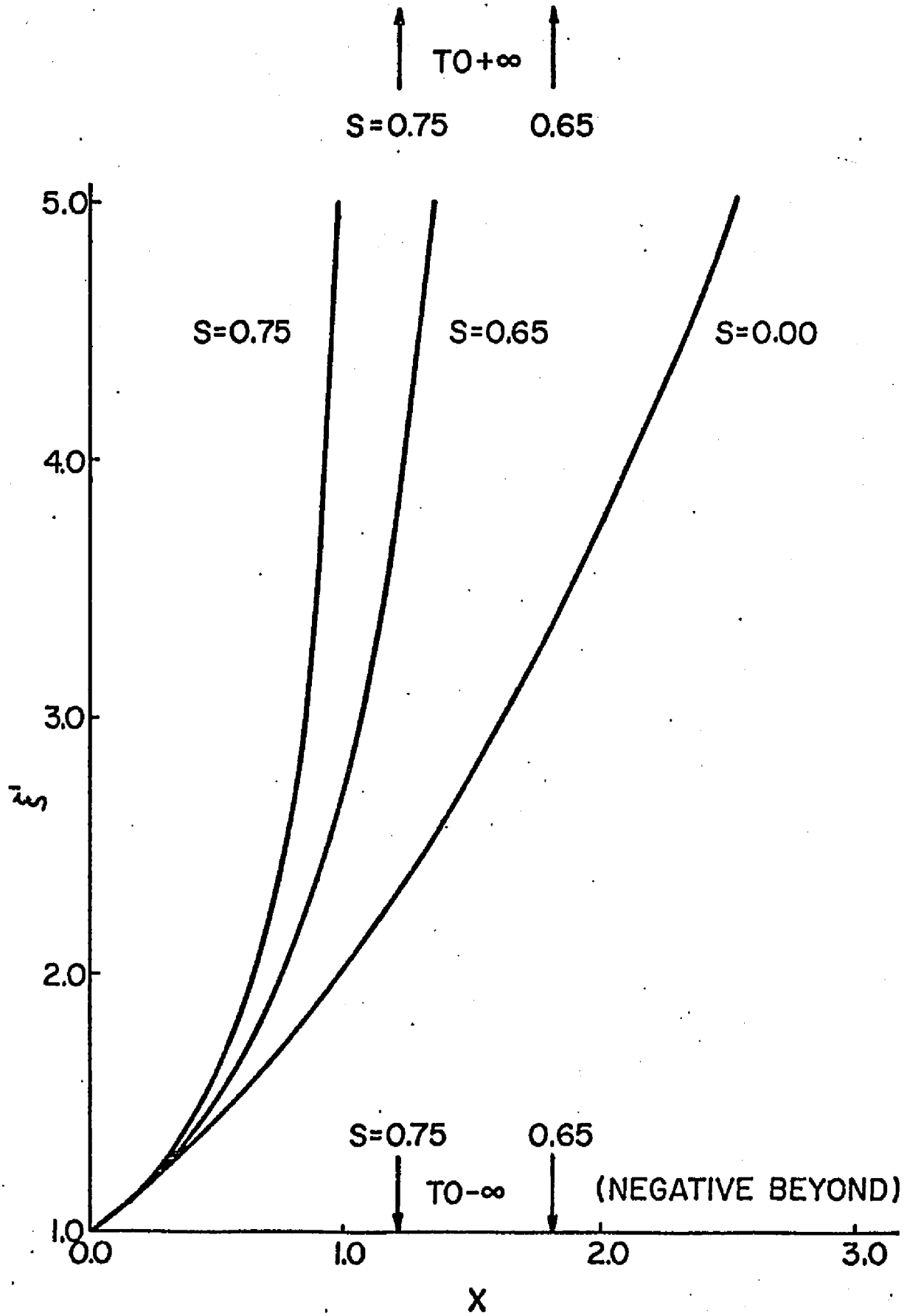
T0+∞
S=0.75
0.65
5.0
4.0
3.0
2.0
1.0
S=0.75
S=0.65
S=0.00
S=0.75
0.65
T0-∞
(NEGATIVE BEYOND)
0.0
1.0
2.0
3.0
X

Fig. 4. Two-electron bond-orbital model values of the dielectric constant ϵ for sixteen binary compounds, plotted against the best available experimental values (Ref. 29). No experimental data exist for BP, BAs or InN, and the estimates of Van Vechten (Ref. 29) has been used instead.

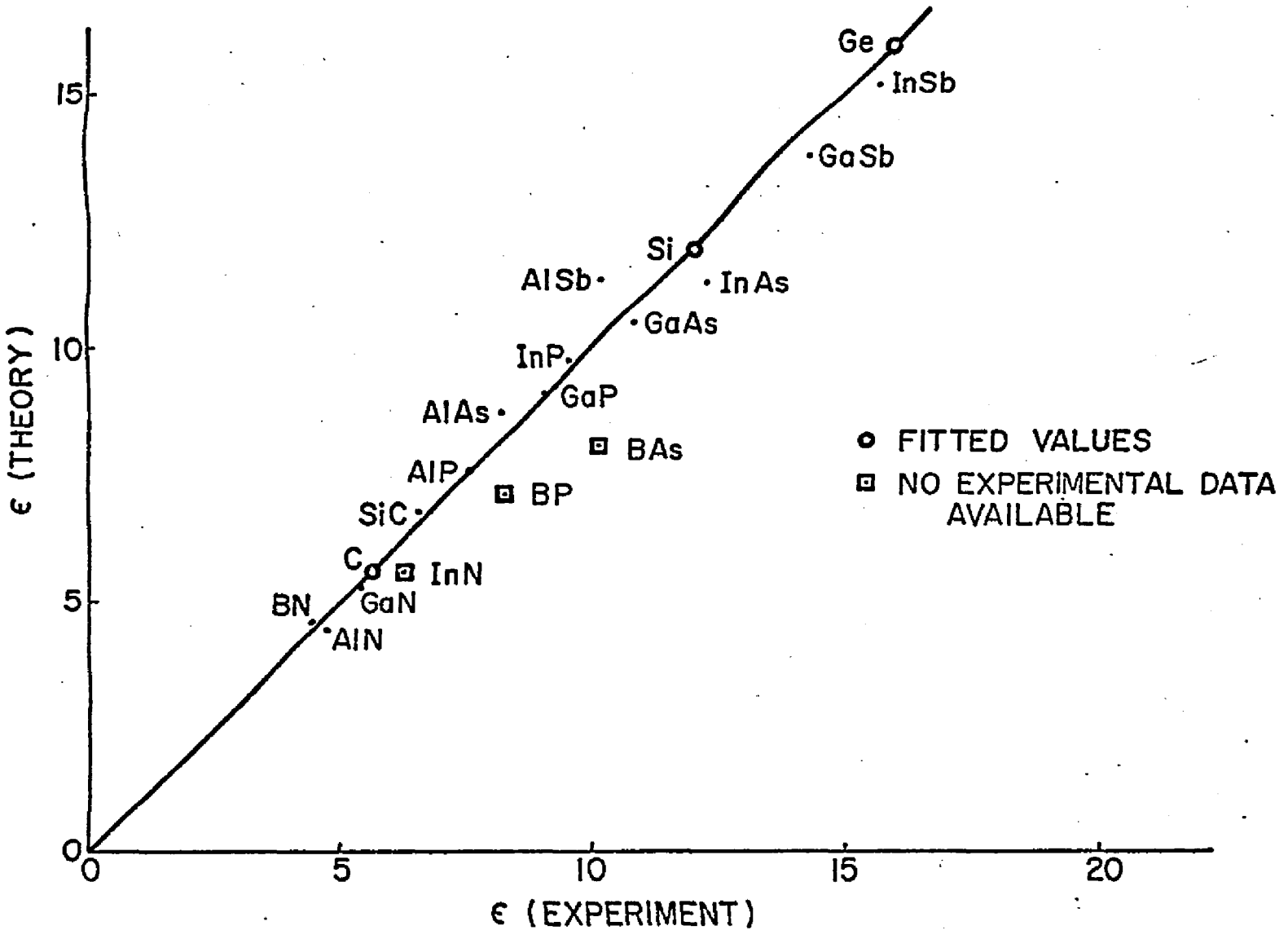
Ge
InSb
GaSb
Si
AlSb
InAs
GaAs
InP
GaP
AlAs
BAs
AlP
BP
SiC
C
InN
BN
GaN
AlN
FITTED VALUES
NO EXPERIMENTAL DATA AVAILABLE
ϵ (THEORY)
ϵ (EXPERIMENT)
0
5
10
15
20

Fig. 5. Single-bond electron density for Ge as calculated from Eq. (III.66) using Hartree-Fock free-atom wavefunctions and the a_{iG} given in Table V.

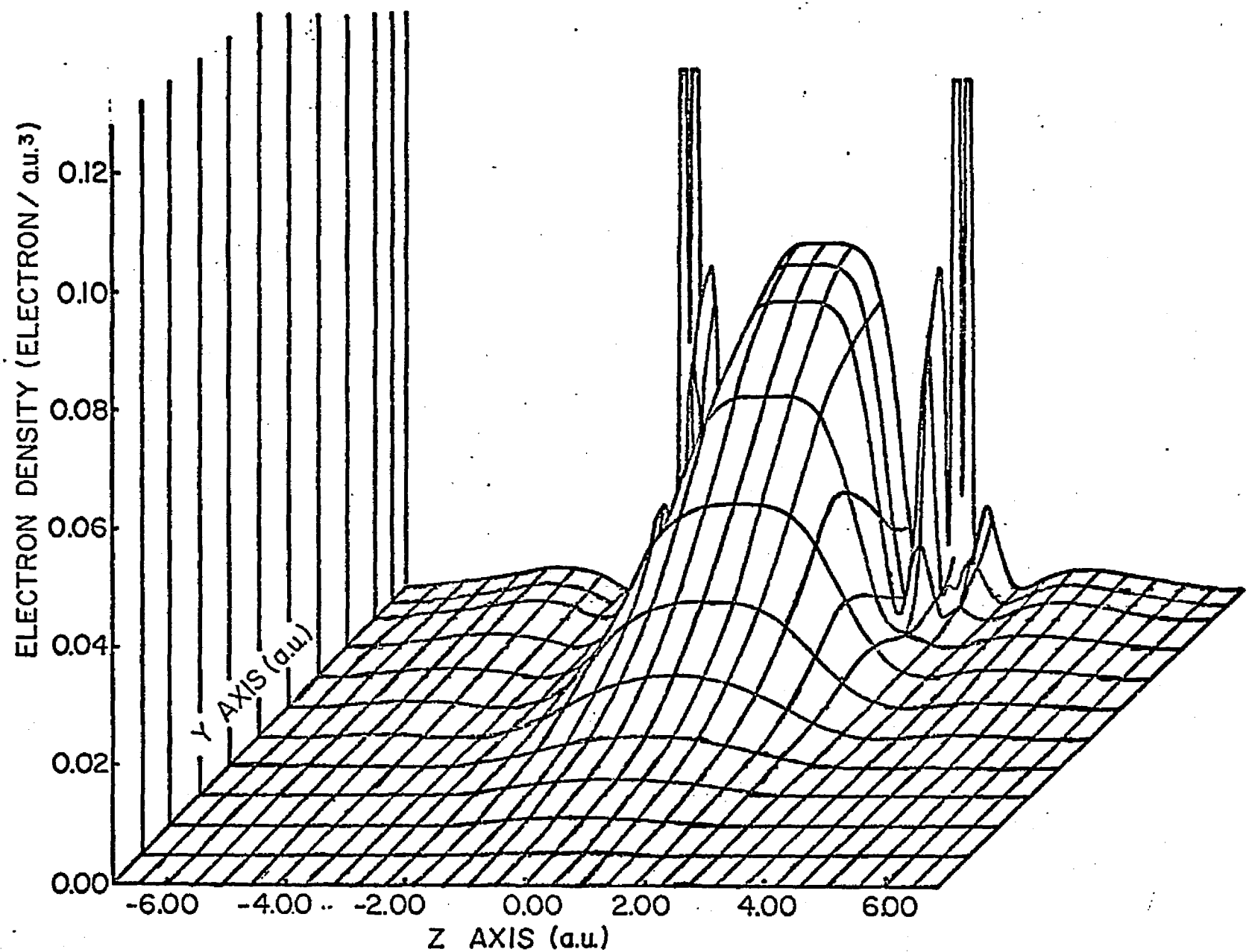
ELECTRON DENSITY (ELECTRON / a.u.³)
0.12
0.10
0.08
0.06
0.04
0.02
0.00
Y AXIS (a.u)
-6.00
-4.00
-2.00
0.00
2.00
4.00
6.00
Z AXIS (a.u.)

Fig. 6. Single-bond electron density for GaAs as calculated from Eq. (III.66) using free-atom Hartree-Fock wavefunctions and the a_{iG} given in Table V. The As nucleus is on the right.

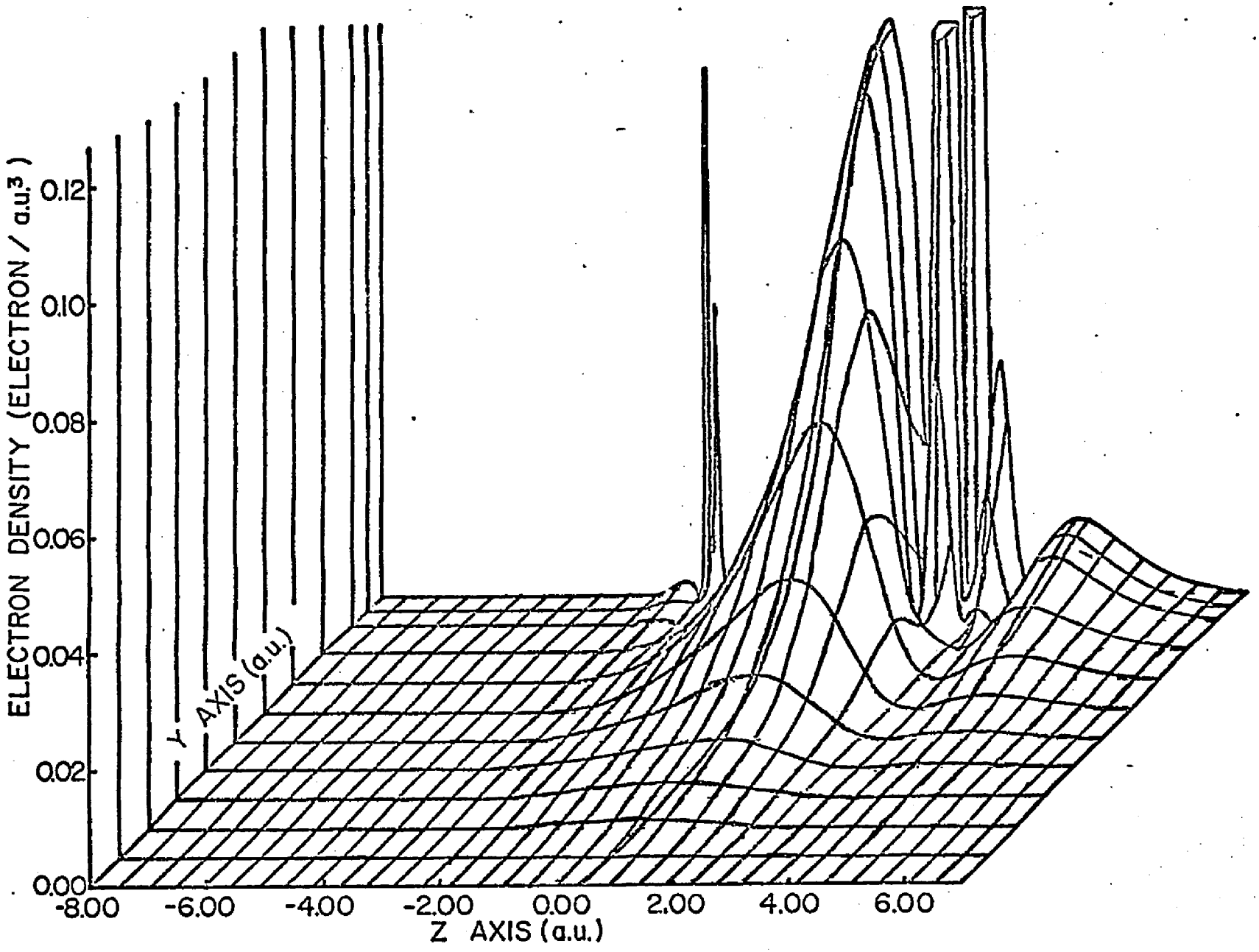
ELECTRON DENSITY (ELECTRON / a.u.^{3})
0.12
0.10
0.08
0.06
0.04
0.02
0.00
Y AXIS (a.u.)
-8.00
-6.00
-4.00
-2.00
0.00
2.00
4.00
6.00
Z AXIS (a.u.)

Fig. 7. Profile of the total valence electron density in Ge along a bond axis, obtained by superimposing single-bond densities (Fig. (5)) in the solid. The corresponding local-empirical-pseudopotential calculation of Walter and Cohen (Ref. 30) is shown in dash line for comparison. The small arrows on the z-axis indicate the positions of the nuclei.

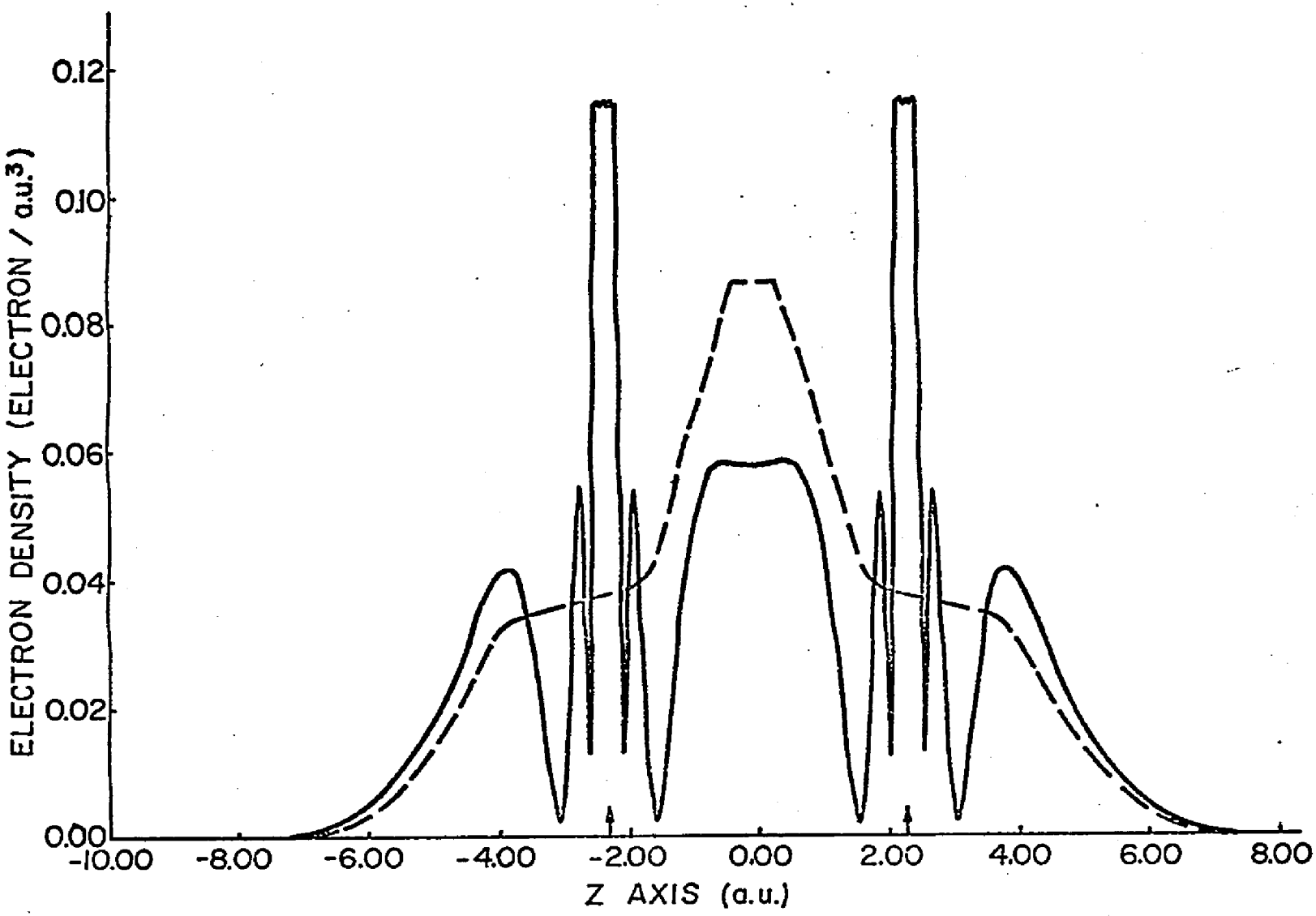
0.12
0.10
0.08
0.06
0.04
0.02
0.00
ELECTRON DENSITY (ELECTRON / a.u.³)
-10.00
-8.00
-6.00
-4.00
-2.00
0.00
2.00
4.00
6.00
8.00
Z AXIS (a.u.)

Fig. 8. Profile of the total valence electron density in GaAs along a bond axis, obtained by superimposing single-bond densities (Fig. (6)) in the solid. The corresponding local-empirical-pseudopotential calculation of Walter and Cohen (Ref. 30) is shown in dash line for comparison. The small arrows on the z-axis indicate the positions of the nuclei with As on the right.

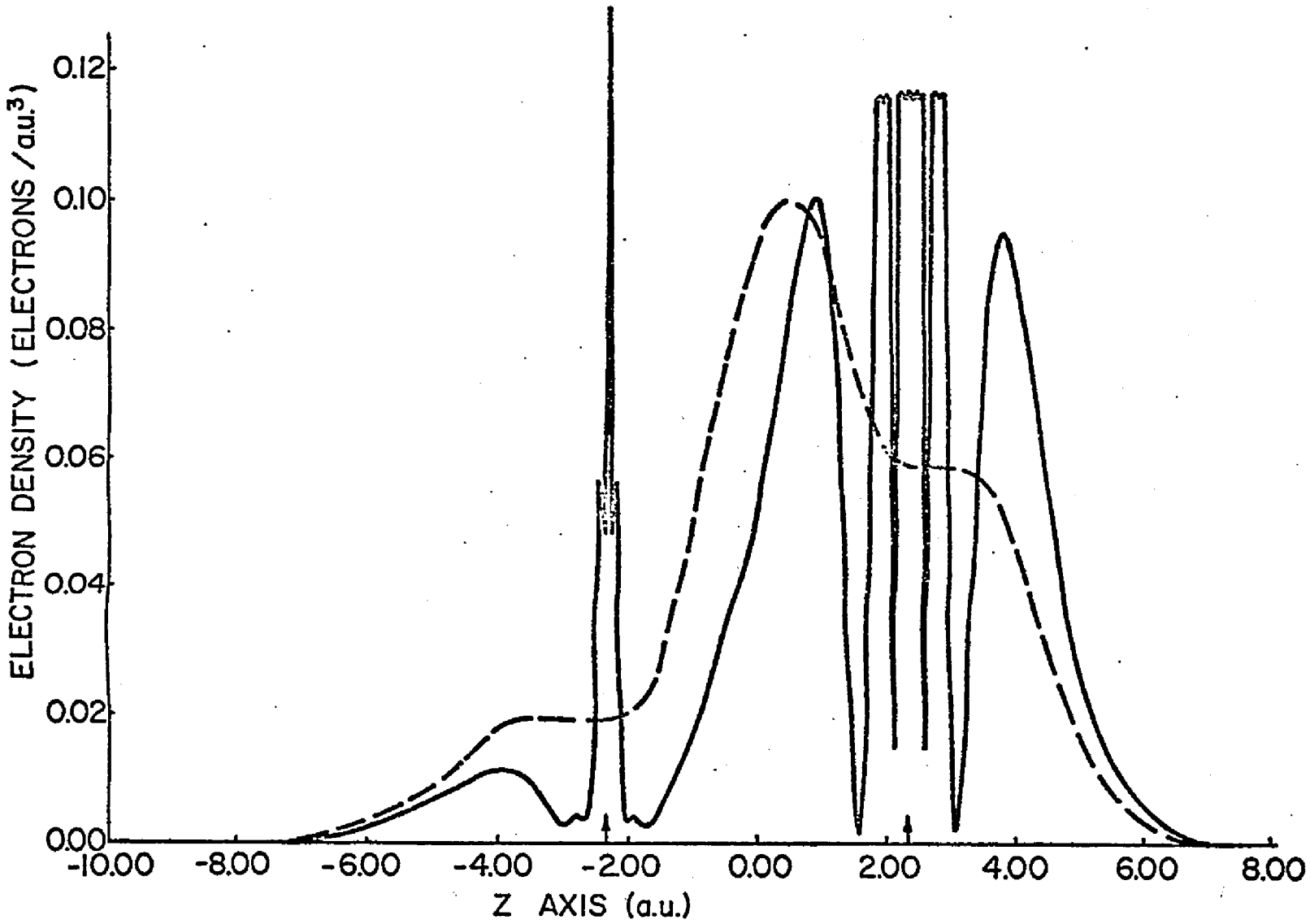
ELECTRON DENSITY (ELECTRONS /a.u.³)
0.12
0.10
0.08
0.06
0.04
0.02
0.00
-10.00
-8.00
-6.00
-4.00
-2.00
0.00
2.00
4.00
6.00
8.00
Z AXIS (a.u.)

Fig. 9. Profile of the total valence electron density in Si along a bond axis, using Hartree-Fock $\underline{s}^2\underline{p}^2$ wavefunctions. The corresponding local-empirical-pseudopotential calculation of Walter and Cohen (Ref. 30) is shown for comparison (denoted by **X**). The small arrows on the z-axis indicate the positions of the nuclei.

ELECTRON DENSITY (ELECTRONS/Å³)
0.00
0.02
0.04
0.06
0.08
0.10
0.12
SIGMA-2
-10.00
-8.00
-6.00
-4.00
-2.00
0.00
2.00
4.00
6.00
8.00
10.00
(a.u.)

Fig. 10. Profile of the total valence electron density in Si along a bond axis, using Kohn-Sham $\underline{s}^1\underline{p}^3$ wavefunctions (see text). The corresponding local-empirical-pseudopotential calculation of Walter and Cohen (Ref. 30) is shown for comparison (denoted by X). The small arrows on the z-axis indicate the positions of the nuclei.

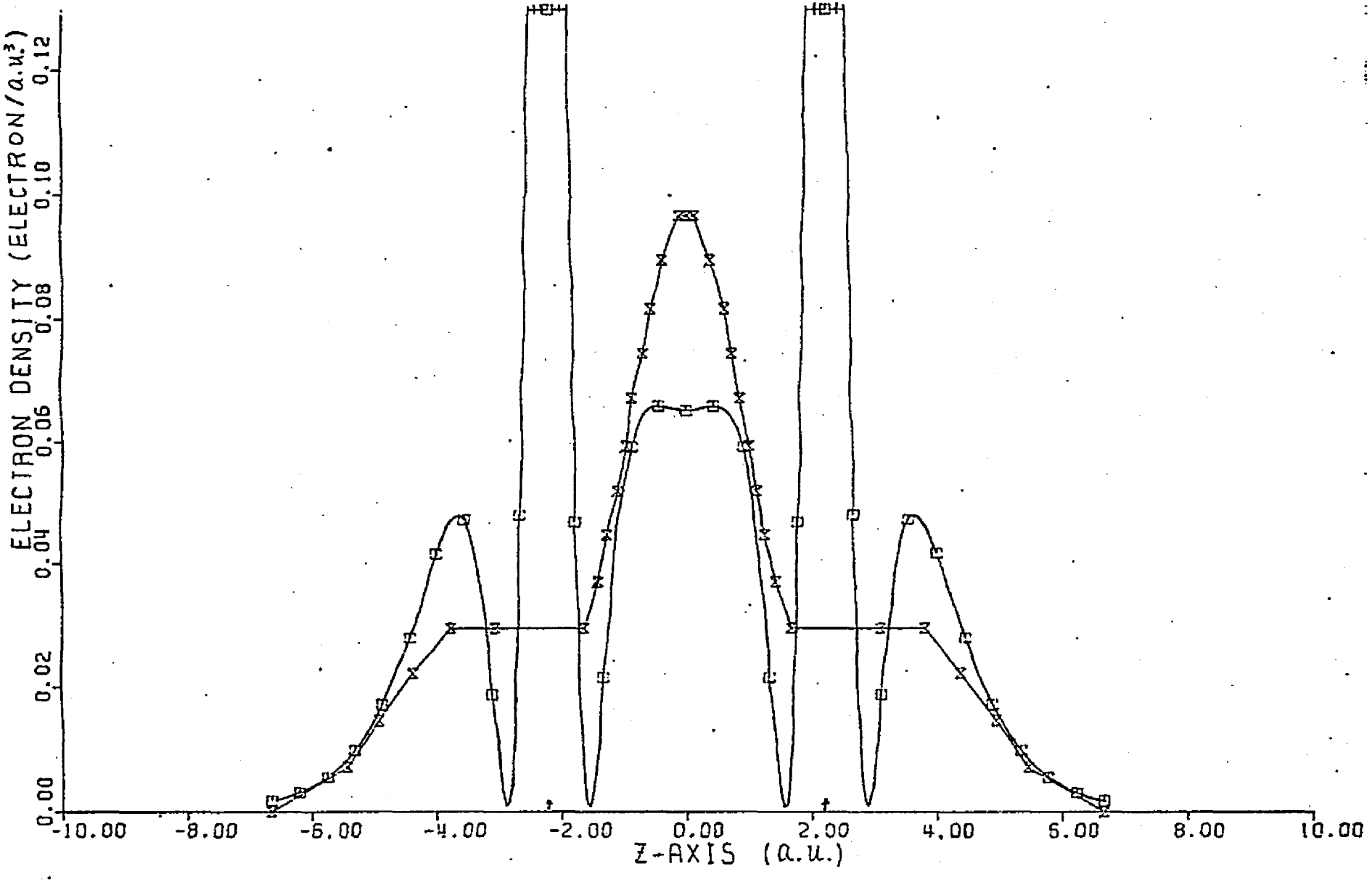
ELECTRON DENSITY (ELECTRON/a.u.³)
0.00
0.02
0.04
0.06
0.08
0.10
0.12
-10.00
-8.00
-6.00
-4.00
-2.00
0.00
2.00
4.00
6.00
8.00
10.00
Z-AXIS (a.u.)

Fig. 11. Profile of the total valence electron density in Si along a bond axis, using contracted Kohn-Sham $\underline{s}^1\underline{p}^3$ wavefunctions. An artificial potential $V_1'(r)$ (see Eq. (IV.11)) is added to the free-atom potential. The corresponding local-empirical-pseudopotential calculation of Walter and Cohen (Ref. 30) is shown for comparison (denoted by **X**). The small arrows on the z-axis indicate the positions of the nuclei.

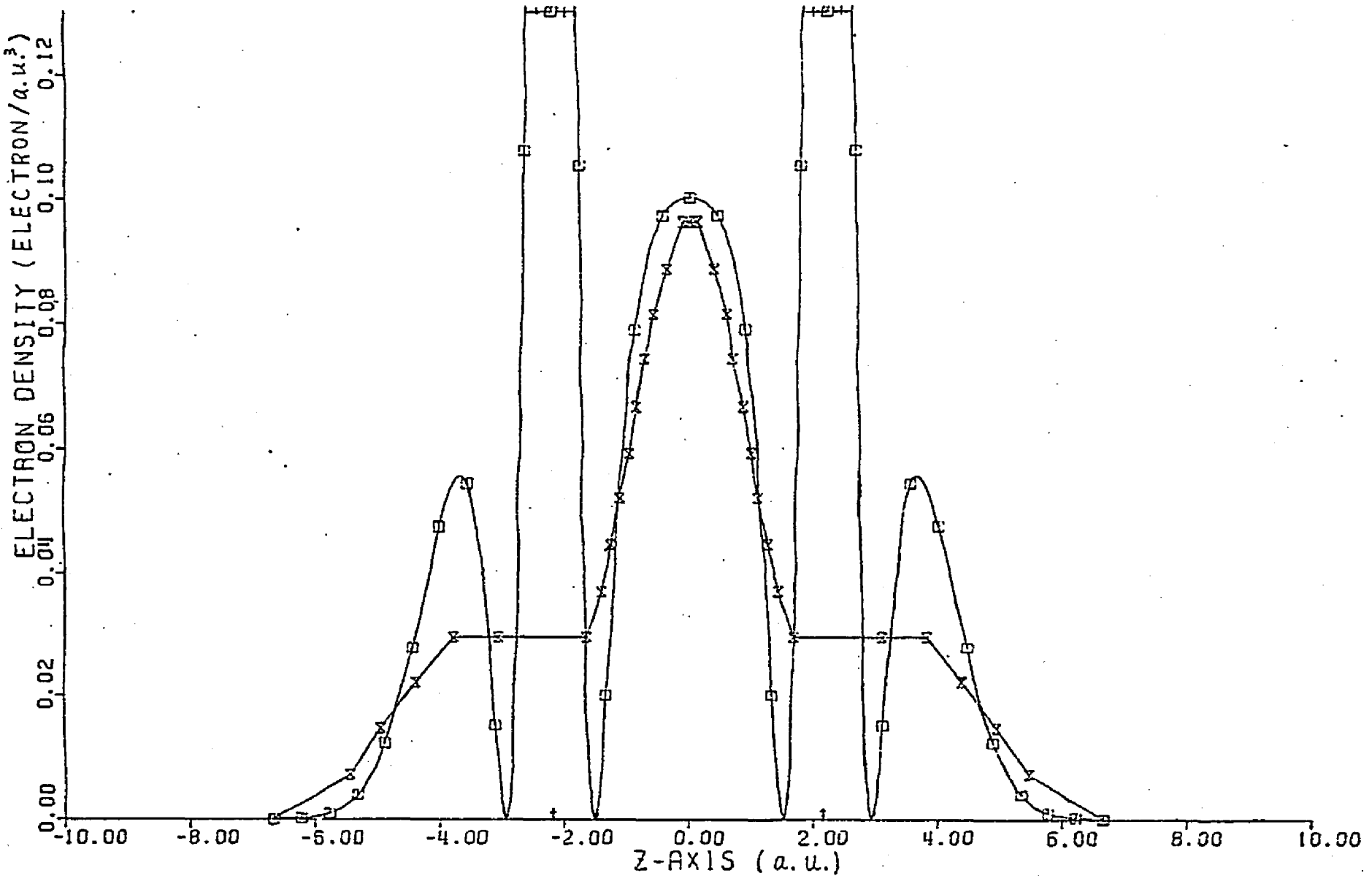
ELECTRON DENSITY (ELECTRON/a.u.³)
0.00
0.02
0.04
0.06
0.08
0.10
0.12
-10.00
-8.00
-6.00
-4.00
-2.00
0.00
2.00
4.00
6.00
8.00
10.00
Z-AXIS (a.u.)

Fig. 12. Experimental values of ϵ_1 vs experimental values of $\Gamma_e / \Gamma_{dd} d^4$ for the seven III-V compounds for which data are available. The linear trends in the Ga and In series are to be compared against the theoretical predictions shown in Fig. (13).

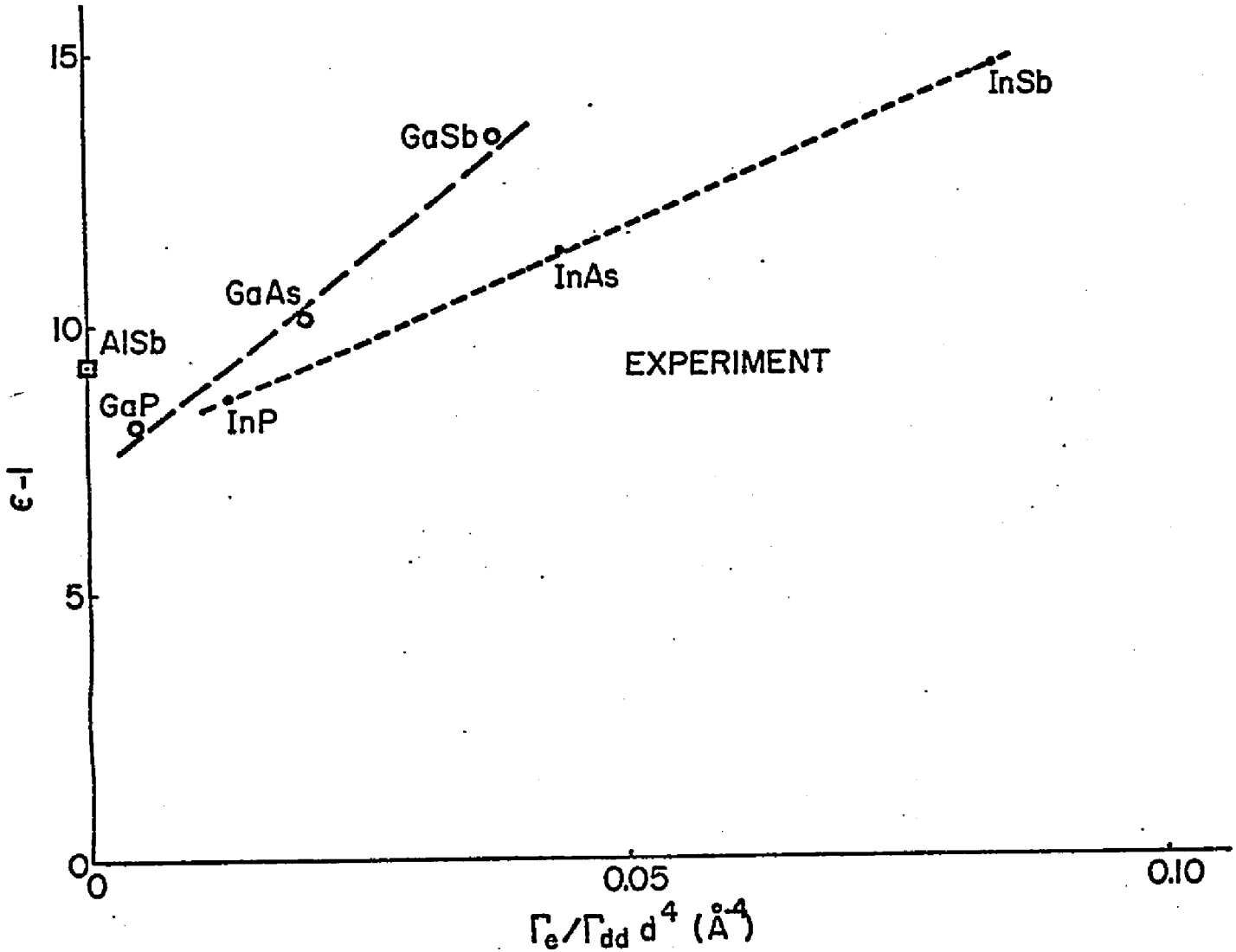
15
10
5
0
0
0.05
0.10
ε-1
$\Gamma_e/\Gamma_{dd}\, d^4$ (Å^{-4})
GaSb
InSb
GaAs
InAs
AlSb
GaP
InP
EXPERIMENT

Fig. 13. Theoretical values of $\epsilon - 1$ vs theoretical values of $\Gamma_e / \Gamma_{dd} d^4$ for fifteen III-V compounds, as calculated from the two-electron bond-orbital model. The corresponding experimental results are plotted in Fig. (12).

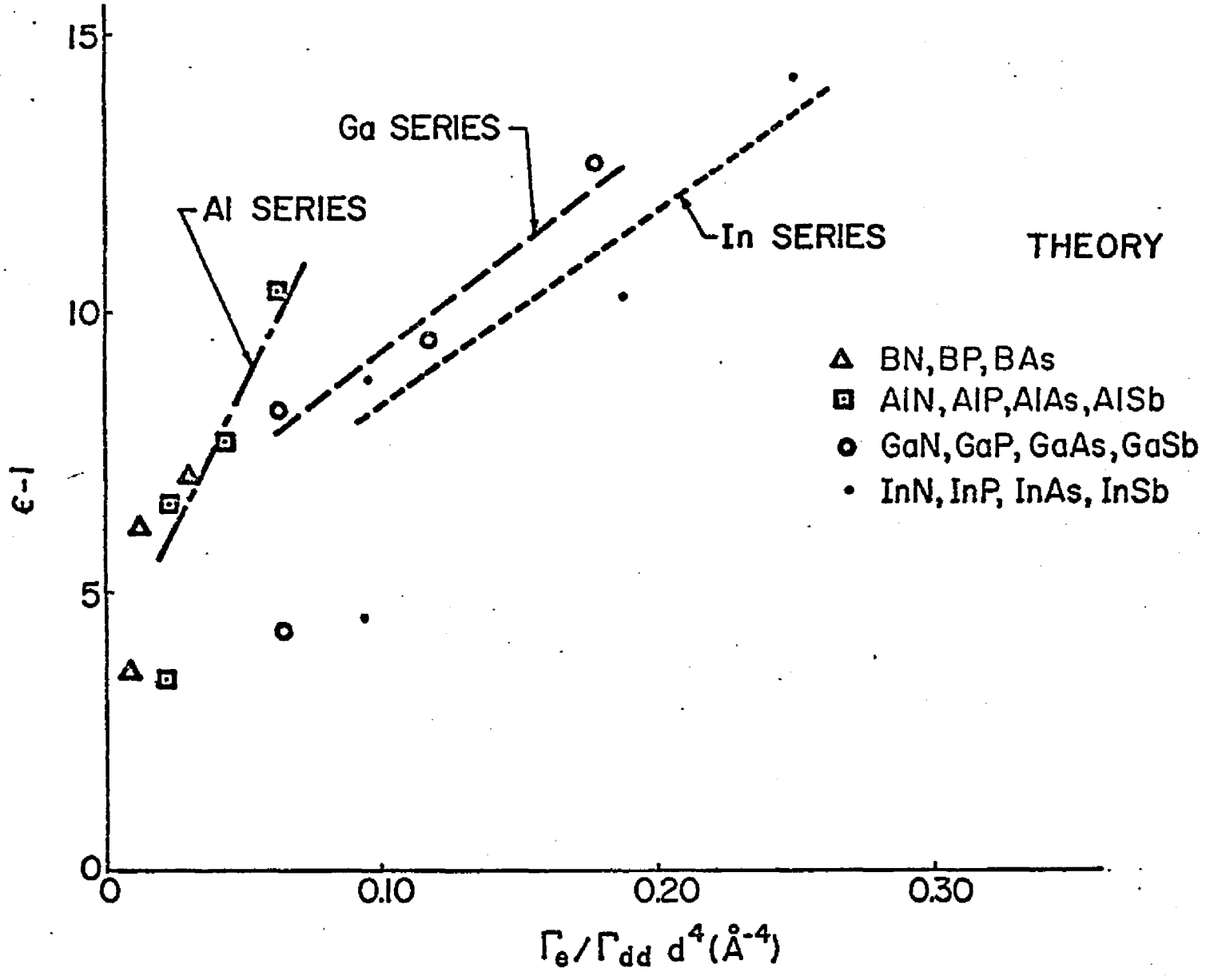
15
10
5
0
0
0.10
0.20
0.30
ε-1
Γe/Γdd d4(Å-4)
Ga SERIES
Al SERIES
In SERIES
THEORY
BN, BP, BAs
AlN, AlP, AlAs, AlSb
GaN, GaP, GaAs, GaSb
InN, InP, InAs, InSb

Fig. 14. Two-electron bond-orbital model values of the cohesive energy E_{coh} for sixteen binary compounds plotted against the known experimental values. References to the experimental data are given in Table XIV.

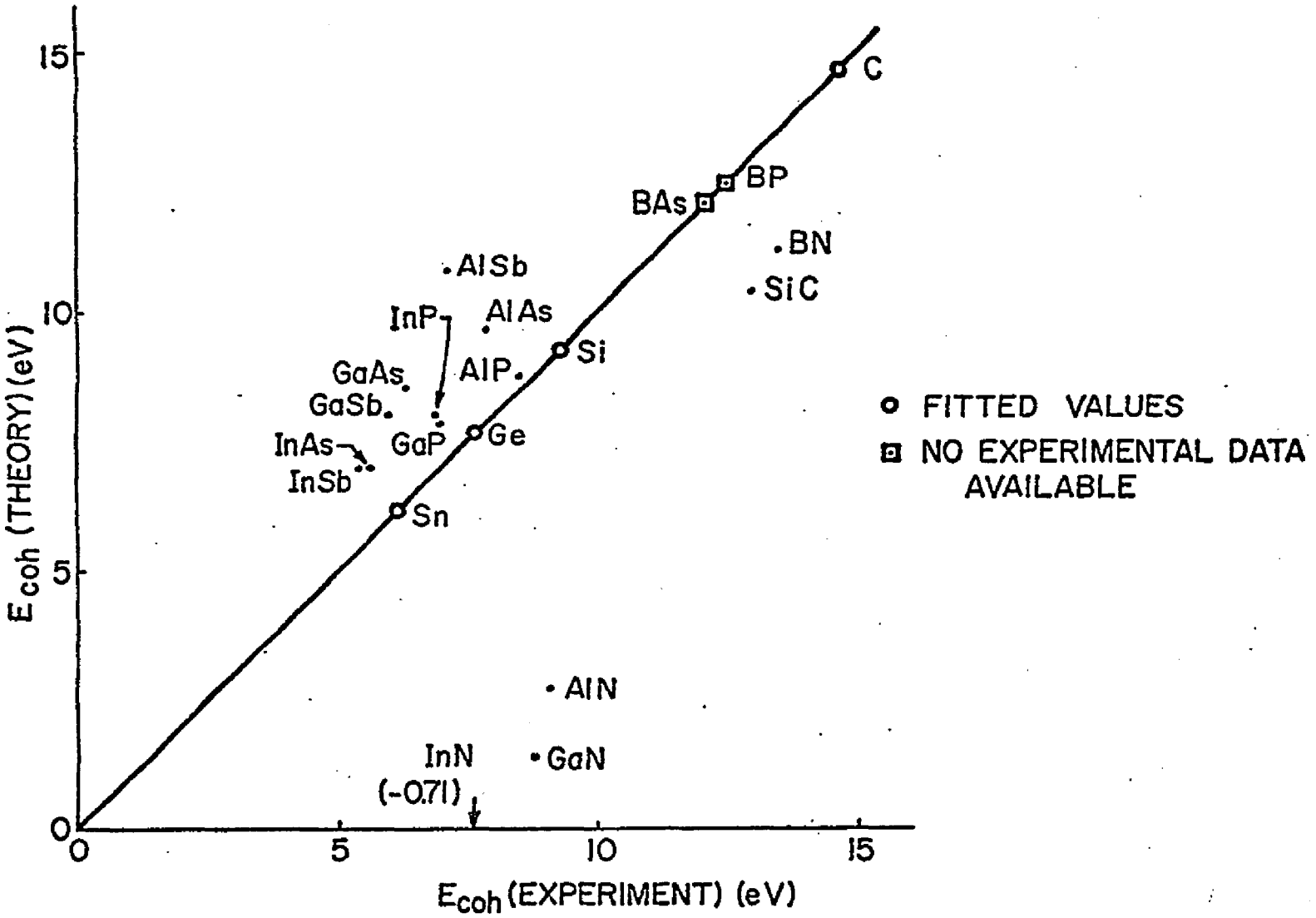
15
10
5
0
0
5
10
15
E_{coh} (THEORY) (eV)
E_{coh} (EXPERIMENT) (eV)
C
BP
BAs
BN
SiC
AlSb
InP
AlAs
Si
AlP
GaAs
GaSb
InAs
InSb
GaP
Ge
Sn
AlN
InN
(-0.71)
GaN
FITTED VALUES
NO EXPERIMENTAL DATA AVAILABLE

Table I. Intra-atomic parameters for the group - III, -IV and V elements obtained from free atom Hartree-Fock term values and wavefunctions of Mann (Ref. 27). Energies are given in eV, while δ^n_{nn} and $\wp^n_{nn}$ are given in a.u. The values in the parenthesis of U_n are from HMSB calculated from Mann's F and G functions.

Element	$-\epsilon_n^{HF}$	V_1^n	U_n		δ^n_{nn}	$\wp^n_{nn}$
B	9.68	1.26	13.95	(13.96)	17.7	0.776
Al	6.96	1.25	9.27	(9.27)	29.6	1.09
Ga	7.14	1.47	9.37	(9.37)	87.2	2.89
In	6.56	1.19	8.43	(8.43)	123	4.46
C	13.14	2.08	17.62	(17.62)	35.0	1.66
Si	9.38	1.80	11.34	(11.34)	48.1	2.03
Ge	9.28	1.96	10.96	(10.96)	120	4.73
Sn	8.33	1.57	9.63	(9.63)	160	6.75
N	16.92	3.09	21.22	(21.20)	60.5	2.02
P	11.95	2.42	13.27	(13.27)	71.3	3.27
As	11.46	2.48	12.36	(12.36)	157	6.85
Sb	10.11	1.97	10.66	(10.67)	200	9.23

Table II. Intrabond parameters for the group - IV elements and the group - IV and III-V binary compounds. The quantity V_2 was obtained by fitting to experiment, while S, K, V_3 and V_4 were calculated using Hartree-Fock free-atom term values and wavefunctions, as described in the text. All energies are given in eV; the bond length d is given in Å and the values of S in the parenthesis are those calculated by Sundfors (Ref. 9) using Clementi's analytic Hartree-Fock atomic wavefunctions. Also V_2^{HC} and V_3^{HC} are listed for comparison.

Material	d	S		K	V_2	V_3	V_4	V_2^{HC}	V_3^{HC}
C	1.54	0.648		17.70	6.54	0.0	2.52	6.10	0
Si	2.35	0.668		9.83	2.53	0.0	1.36	2.20	0
Ge	2.44	0.659		9.46	2.42	0.0	1.33	2.15	0
Sn	2.80	0.661		8.37	1.99	0.0	1.12	1.76	0
SiC	1.88	0.627		11.95	4.07	0.40	2.08	3.66	1.54
BN	1.57	0.608		14.18	6.54	2.27	2.70	6.10	2.76
BP	1.97	0.663		11.65	4.07	1.74	1.75	3.66	0
BAs	2.07	0.656		11.14	3.98	1.71	1.77	3.62	0
AlN	1.89	0.517		11.27	4.07	2.33	2.71	3.66	2.68
AlP	2.36	0.633		9.58	2.53	1.93	1.41	2.20	1.18
AlAs	2.43	0.645		9.34	2.47	1.93	1.26	2.18	1.06
AlSb	2.66	0.659	(0.659)	8.68	2.24	1.63	1.14	1.97	1.26

Table II. (cont'd.)

GaN	1.94	0.513		11.13	3.98	2.25	2.83	3.62	1.33
GaP	2.36	0.629	(0.627)	9.58	2.47	1.84	1.44	2.18	0.94
GaAs	2.45	0.637	(0.635)	9.28	2.42	1.83	1.25	2.15	1.21
GaSb	2.65	0.654	(0.657)	8.70	2.19	1.54	1.15	1.94	0.94
InN	2.15	0.470		10.16	3.61	2.25	2.99	3.27	2.75
InP	2.54	0.602	(0.600)	8.96	2.24	1.86	1.48	1.97	1.41
InAs	2.61	0.617	(0.611)	8.75	2.19	1.86	1.33	1.94	1.22
InSb	2.81	0.644	(0.642)	8.24	1.99	1.59	1.12	1.76	1.04

Table III. Intrabond parameters that are hidden in the theory of this text for group - IV elements and the group - IV and III-V binary compounds. All are calculated using Hartree-Fock free-atom wavefunctions in units of eV.

Material	H_c	H_a	J	V_5	V_6
C	11.11	11.11	8.07	0.0	0.27
Si	7.64	7.64	5.78	0.0	0.07
Ge	7.31	7.31	5.48	0.0	0.08
Sn	6.44	6.44	4.82	0.0	0.07
SiC	7.96	9.88	6.42	0.03	0.11
BN	9.31	11.35	7.19	0.11	0.21
BP	9.07	8.86	6.69	-0.01	0.14
BAs	8.78	8.28	6.30	-0.01	0.17
AlN	5.96	9.11	4.70	-0.04	0.11
AlP	6.57	7.86	5.29	-0.02	0.01
AlAs	6.60	7.62	5.30	-0.02	-0.02
AlSb	6.45	6.91	5.03	0.00	0.01
GaN	5.90	8.94	4.56	0.00	0.17
GaP	6.57	7.83	5.25	-0.02	0.03
GaAs	6.53	7.52	5.17	-0.02	0.02
GaSb	6.46	6.88	4.99	0.00	0.02

Table III. (cont'd.)

InN	4.92	7.98	3.67	-0.03	0.19
InP	5.78	7.32	4.61	-0.05	0.05
InAs	5.85	7.13	4.66	-0.04	0.03
InSb	5.87	6.62	4.62	-0.02	0.01

Table IV. Relative singlet and triplet eigenvalues $E_M^0 = E_M-(\epsilon_a+\epsilon_c-K)$ for the twenty solids considered in the text, where $E_G^0 = E_{V.I}^0$ and $E_T^0 = E_{I,II,III}^0$. Also listed are the theoretical predictions of the E_2 optical-absorption peak both from the present work, $E_2 = E_{IV}^0 - E_G^0$, and from the work of Harrison and Ciraci (Ref. 6), E_2^{HC}. All energies are in eV.

Material	E_G^0	E_T^0	E_{IV}^0	E_V^0	Theory $E_2^0=E_{IV}^0-E_G^0$	Theory E_2^{HC}	Experiment[a] E_{2A}	Experiment[a] E_{2B}
C	-2.32	4.82	9.87	24.32	12.2 [b]	12.2 [c]	12.2	12.2
Si	-0.50	1.19	3.91	9.98	4.41[b]	4.40[c]	4.40	4.40
Ge	-0.50	1.15	3.81	9.54	4.31[b]	4.30[c]	4.3	4.3
Sn	-0.38	0.89	3.13	7.88	3.52[b]	3.52		
SiC	-1.25	2.33	6.56	15.63	7.80	7.98	8.3	
BN	-3.33	4.78	9.95	24.87	13.3	13.4		
BP	-1.81	2.65	6.04	16.22	7.85	7.32	6.9	
BAs	-1.78	2.55	5.96	15.89	7.73	7.24		
AlN	-2.46	2.23	6.69	17.08	9.32	9.07		
AlP	-1.72	1.32	3.80	11.28	5.52	4.99		
AlAs	-1.80	1.39	3.64	10.96	5.44	4.85		
AlSb	-1.46	1.20	3.30	9.83	4.76	4.68	4.25	4.6
GaN	-2.26	2.06	6.92	16.90	9.18	9.26		
GaP	-1.59	1.22	3.76	11.02	5.35	5.11	5.27	5.74
GaAs	-1.71	1.38	3.60	10.65	5.30	4.93	4.85	5.33
GaSb	-1.36	1.14	3.26	9.57	4.61	4.31	4.1	4.5

Table IV. (cont'd.)

InN	-2.13	1.70	6.61	15.96	8.74	8.54		
InP	-1.56	1.02	3.48	10.41	5.04	4.84	4.8	5.1
InAs	-1.64	1.07	3.31	10.12	4.95	4.58	4.5	5.0
InSb	-1.39	0.98	2.97	9.01	4.36	4.09[c]	4.08	

[a] Reference 28

[b] Fit to E_2^{HC}, as described in the text.

[c] Fit to experimental E_{2A}.

Table V. Expansion coefficients entering Eq. (III 34) for the singlet eigenstates M = VI (the ground state), M = IV and M = V of the twenty semiconductors considered in the text.

Material	M=VI			IV			V		
	a_{4M}	a_{5M}	a_{6M}	a_{4M}	a_{5M}	a_{6M}	a_{4M}	a_{5M}	a_{6M}
C	0.167	0.167	0.736	0.928	-0.928	0	-1.44	-1.44	2.33
Si	0.100	0.100	0.841	0.950	-0.950	0	-1.53	-1.53	2.47
Ge	0.103	0.103	0.838	0.940	-0.940	0	-1.49	-1.49	2.39
Sn	0.097	0.097	0.847	0.942	-0.942	0	-1.50	-1.50	2.41
SiC	0.198	0.084	0.781	0.990	-0.817	-0.200	-1.30	-1.43	2.15
BN	0.402	0.020	0.653	1.11	-0.574	-0.642	-1.06	-1.48	1.97
BP	0.465	-0.061	0.635	1.23	-0.512	-0.865	-1.21	-1.71	2.33
BAs	0.459	-0.058	0.641	1.22	-0.508	-0.855	-1.17	-1.68	2.27
AlN	0.448	-0.015	0.658	1.10	-0.357	-0.814	-0.680	-1.32	1.38
AlP	0.643	-0.120	0.494	1.26	-0.218	-1.24	-0.889	-1.65	1.92
AlAs	0.680	-0.121	0.451	1.27	-0.202	-1.30	-0.920	-1.70	2.00
AlSb	0.659	-0.131	0.480	1.30	-0.238	-1.28	-1.00	-1.75	2.14
GaN	0.428	-0.017	0.678	1.10	-0.358	-0.800	-0.675	-1.31	1.36
GaP	0.619	-0.121	0.520	1.25	-0.231	-1.21	-0.886	-1.63	1.89
GaAs	0.655	-0.113	0.476	1.26	-0.224	-1.25	-0.904	-1.66	1.95
GaSb	0.632	-0.128	0.508	1.29	-0.259	-1.24	-0.998	-1.72	2.11

Table V. (cont'd.)

InN	0.420	-0.010	0.695	1.07	-0.310	-0.789	-0.563	-1.26	1.16
InP	0.626	-0.118	0.516	1.22	-0.179	-1.22	-0.761	-1.55	1.67
InAs	0.667	-0.122	0.471	1.24	-0.163	-1.28	-0.796	-1.60	1.76
InSb	0.674	-0.134	0.466	1.28	-0.188	-1.31	-0.911	-1.69	1.98

Table VI. Calculated parameters related to the dielectric constant and the polarization of the bond, as discussed in the text. The quantity α_p^{HC} is the value of polarity assigned by Harrison and Ciraci (Ref. 6).

Material	δ_c	δ_a	$\delta_c-\delta_a$	$2\delta_{ca}$	γ	Z_p	α_p^G	α_p^{HC}
C	0.279	0.279	0.0	0.0	0.581	0.0	0.0	0.0
Si	0.265	0.265	0.0	0.0	0.633	0.0	0.0	0.0
Ge	0.257	0.257	0.0	0.0	0.646	0.0	0.0	0.0
Sn	0.259	0.259	0.0	0.0	0.643	0.0	0.0	0.0
SiC	0.331	0.229	0.102	0.098	0.565	0.14	0.08	0.39
BN	0.334	0.228	0.116	0.053	0.539	0.24	0.27	0.41
BP	0.274	0.275	-0.001	-0.040	0.602	0.20	0.35	0.0
BAs	0.261	0.275	-0.014	-0.057	0.615	0.19	0.35	0.0
AlN	0.390	0.189	0.201	0.110	0.492	0.34	0.34	0.59
AlP	0.312	0.229	0.083	0.054	0.593	0.39	0.53	0.47
AlAs	0.303	0.234	0.069	0.037	0.606	0.40	0.55	0.44
AlSb	0.277	0.251	0.026	0.004	0.628	0.36	0.54	0.54
GaN	0.363	0.184	0.179	0.114	0.528	0.33	0.32	0.62
GaP	0.299	0.229	0.070	0.050	0.607	0.38	0.51	0.52
GaAs	0.288	0.233	0.055	0.034	0.621	0.38	0.54	0.50
GaSb	0.266	0.252	0.014	-0.001	0.638	0.34	0.52	0.44

Table VI. (cont'd.)

InN	0.372	0.166	0.206	0.156	0.523	0.36	0.31	0.64
InP	0.315	0.213	0.102	0.097	0.591	0.41	0.52	0.58
InAs	0.307	0.218	0.089	0.080	0.604	0.42	0.56	0.53
InSb	0.285	0.237	0.048	0.044	0.625	0.39	0.56	0.51

Table VII. List of the matrix elements $\langle G|U_\varepsilon^0|M\rangle$ for M = IV, V, G in calculating the dielectric constant.

Material	$\langle G\|U_\varepsilon^0\|G\rangle$	$\langle G\|U_\varepsilon^0\|IV\rangle$	$\langle G\|U_\varepsilon^0\|V\rangle$
C	0	-0.621	0
Si	0	-0.987	0
Ge	0	-1.042	0
Sn	0	-1.185	0
SiC	-0.285	-0.712	-0.00246
BN	-0.413	-0.587	-0.00951
BP	-0.437	-0.790	0.0429
BAs	-0.433	-0.845	0.0428
AℓN	-0.710	-0.606	-0.0518
AℓP	-1.001	-0.858	0.0682
AℓAs	-1.053	-0.897	0.0814
AℓSb	-1.038	-1.009	0.116
GaN	-0.707	-0.651	-0.0469
GaP	-0.965	-0.873	0.0728
GaAs	-1.024	-0.927	0.0805
GaSb	-0.982	-1.021	0.116
InN	-0.851	-0.692	-0.0613
InP	-1.133	-0.895	0.0640
InAs	-1.195	-0.932	0.0813
InSb	-1.196	-1.389	0.119

Table VIII. The dielectric constant of binary compounds. ϵ^{calc} and ϵ^{scaled} are the calculated values and the values after multiplication by the scaling factors λ_n (see text). ϵ^{expt} is from Ref. (28).

Material	ϵ^{expt}	ϵ^{calc}	$\epsilon^{scale}=1+\lambda_a\lambda_c(\epsilon^{calc}-1)$	% error
SiC	6.6	2.288	6.78	+ 2.7
BN	4.5	1.883	4.60	+ 2.2
BP	8.2*	2.372	7.15	-12.8
BAs	10.2*	2.370	8,08	-20.8
AlN	4.8	1.769	4.45	- 5.2
AlP	7.6	2.237	7.59	- 0.1
AlAs	8.2	2.262	8.74	+ 6.6
AlSb	10.2	2.504	11.4	+11.8
GaN	5.4	1.835	5.32	- 1.4
GaP	9.1	2.431	9.13	+ 0.3
GaAs	10.9	2.457	10.5	- 3.7
GaSb	14.4	2.605	13.7	- 4.9
InN	6.3*	1.729	5.56	-11.7
InP	9.6	2.279	9.80	+ 2.1
InAs	12.3	2.302	11.3	- 8.1
InSb	15.7	2.475	15.2	- 3.2

*Values not available experimentally are predicted by J. A. Van Vechtor see Ref. (29).

Table IX. Sensitivity of various parameters of Si to small changes in atomic s and p wave functions making up the sp^3 hybrid. The symbols HF, HS and KS denote results of Hartree-Fock, Herman-Skillman calculations and Herman-Skillman calculation with Kohn-Sham exchange potential respectively. Values of energies are given in eV. The rest of the quantities are in a.u.

configuration	HF $3s^2\ 3p^2$	HS $3s^2\ 3p^2$	HS $3s^1\ 3p^3$	KS $3s^2\ 3p^2$	KS $3s^3\ 3p^1$
S	0.668	0.620	0.610	0.649	0.644
U	11.34	11.78	12.16	11.11	11.48
K	9.83	9.78	9.90	9.63	9.78
H	7.64	7.26	7.26	7.36	7.43
J	5.78	5.13	5.02	5.51	5.45
V_4	1.36	1.62	1.80	1.28	1.45
V_6	0.07	0.18	0.24	- 0.02	0.11
$\delta=\sqrt{3}\ \bar{x}/d$	0.265	0.249	0.245	0.262	0.257
γ	0.633	0.639	0.642	0.626	0.635
$(\wp^n_{nn})^{1/2}$	6.94	8.02	8.15	7.67	7.82
(p^n_{nn})	2.03	2.69	2.90	2.34	2.55
$R=\frac{9}{5}p^n_{nn}/\wp^n_{nn}$	0.0759	0.0753	0.0787	0.0716	0.751
$-\varepsilon_s$	14.78	13.57	14.25	9.77	10.52
$-\varepsilon_p$	7.58	6.530	7.034	3.20	3.76
$-\varepsilon$	9.58	8.29	8.84	4.84	5.45
V_1	1.81	1.76	1.804	1.64	1.69

Table X. Changes of parameters and values of wavefunction introduced by artificially adding an extra potential V(r). The effect for $V(r) = V_1'(r)$ (see Eq. (IV.11)) is to contract the tail of the wavefunction. While the effect for $V(r) = V_2'(r)$ (see Eq. (IV.12)) is to extend the tail. The experimental value of $\rho^{expt}(d/2)$ is 0.102 (Ref. 32) and the value of $\rho^{wc}(d/2)$ calculated by Walter and Cohen[30] is 0.097.

Exchange Configuration V	$3s^1{}^{KS}3p^3$ 0	$3s^1{}^{KS}3p^3$ $V_1'(V_0=5)$	$3s^1{}^{KS}3p^3$ $V_1'(V_0=2.5)$	$3s^1{}^{KS}3p^3$ $V_1'(V_0=1)$	$3s^1{}^{KS}3p^3$ $V_2'(Z_A=14,\lambda'=1)$
$P_{3S}(d/2)$	0.675	0.722	0.719	0.709	0.548
$P_{3p}(d/2)$	0.622	0.761	0.750	0.725	0.392
$Q_{out}(d/2)$	2.27	1.24	1.47	1.73	3.30
S	0.644	0.335	0.422	0.525	0.806
U	11.48	15.58	14.86	12.95	8.48
K	9.78	10.38	10.49	10.53	8.35
H	7.43	4.93	5.95	7.00	7.14
J	5.45	2.04	2.97	4.20	6.37
V_1	1.69	2.18	2.06	1.94	0.99
V_4	1.45	2.93	2.66	2.36	0.19
V_6	0.11	0.11	0.22	0.34	- 0.81
δ	0.257	0.207	0.216	0.227	0.349
γ	0.635	0.622	0.626	0.642	0.510
$\mathcal{S}^n_{nn}$	61.2	77.5	71.8	66.3	33.41
$\mathcal{P}^n_{nn}$	2.55	5.04	4.45	3.83	0.71
$R = \frac{9}{5}\mathcal{P}^n_{nn}/\mathcal{S}^n_{nn}$	0.0751	0.117	0.112	0.103	0.0383

Table X. (cont'd.)

$R_S(0)$	7.8236	8.8034	8.4735	8.1425	5.78
$\rho(d/2)$	0.063	0.109	0.100	0.088	0.031

Table XI. A list of $\mathcal{S}^{n'}_{nn'}$, and $\mathcal{P}^{n'}_{nn'}$, values in a.u.

Material	$\mathcal{S}^{a}_{ac}$	$\mathcal{S}^{c}_{ca}$	$\mathcal{S}^{a}_{cc}$	$\mathcal{S}^{c}_{aa}$	$\mathcal{P}^{a}_{ac}$	$\mathcal{P}^{c}_{ac}$	$\mathcal{P}^{c}_{aa}$	$\mathcal{P}^{a}_{cc}$
C	-2.890	-2.890	0.239	0.239	0.269	0.269	0.161	0.161
Si	1.735	1.735	0.0625	0.0625	0.036	0.036	0.034	0.034
Ge	-2.552	-2.552	0.0538	0.0538	0.055	0.055	0.030	0.030
Sn	2.311	2.311	0.0331	0.0331	0.027	0.027	0.018	0.018
SiC	-2.825	1.818	0.228	0.0686	0.177	0.056	0.067	0.076
BN	-4.683	-1.436	0.362	0.116	0.279	0.206	0.136	0.136
BP	2.760	-1.419	0.107	0.113	0.053	0.142	0.076	0.062
BAs	-3.563	-1.343	0.0812	0.102	0.079	0.129	0.059	0.050
AlN	-4.217	0.936	0.294	0.0296	0.164	0.047	0.053	0.051
AlP	2.785	0.968	0.109	0.0317	0.032	0.035	0.031	0.031
AlAs	-3.825	0.996	0.0936	0.0335	0.055	0.033	0.029	0.028
AlSb	3.328	0.936	0.0557	0.0296	0.028	0.028	0.022	0.021
GaN	-3.960	-1.457	0.259	0.0243	0.162	0.066	0.046	0.051
GaP	2.709	-1.663	0.103	0.0317	0.033	0.052	0.031	0.031
GaAs	-3.613	-1.644	0.0835	0.0310	0.055	0.049	0.027	0.027
GaSb	3.271	-1.644	0.0538	0.0310	0.028	0.043	0.026	0.021
InN	-3.501	1.121	0.203	0.0102	0.132	0.036	0.026	0.035
InP	2.549	1.487	0.0913	0.0176	0.028	0.030	0.021	0.024
InAs	-3.488	1.520	0.0778	0.0188	0.048	0.029	0.020	0.022
InSb	3.299	2.597	0.0547	0.0193	0.025	0.026	0.017	0.017

Table XII. Nuclear exchange and pseudodipolar coefficients, Γ_e and Γ_{pd}, for the twenty solids considered in the text, in units of the direct dipole-dipole interaction coefficient Γ_{dd}. The theoretical results refer to our calculations done in both the Harrison limit (values in parenthesis are for S = 0 in HMSB) and with the full two-electron formalism described in the text.

Material	Γ_e/Γ_{dd}			Γ_{pd}/Γ_{dd}			Γ_{pd}/Γ_e		
	Theory		Expt.	Theory		Expt	Theory		Expt
	Harrison	Full		Harrison	Full		Harrison	Full	
C	0.043(0.0253)	0.087		0.0068(0.00444)	0.0139		0.160(0.175)	0.160	
Si	0.846(0.473)	2.79		0.130 (0.0735)	0.427		0.153(0.155)	0.153	
Ge	6.00 (3.35)	19.8		0.860 (0.487)	2.84		0.143(0.145)	0.143	
Sn	19.7 (11.1)	69.5		3.04 (1.72)	10.7		0.154(0.155)	0.154	
SiC	0.120(0.0828)	0.435		0.0187(0.0137)	0.0681		0.155(0.165)	0.157	
BN	0.022(0.0177)	0.055		0.0034(0.00307)	0.0076		0.154(0.173)	0.137	
BP	0.161(0.0909)	0.203		0.0254(0.0151)	0.0386		0.158(0.166)	0.190	
BAs	0.404(0.234)	0.568		0.0628(0.0379)	0.103		0.155(0.162)	0.180	
A&N	0.077(0.0596)	0.273		0.0087(0.00958)	0.0322		0.113(0.160)	0.118	
A&P	0.412(0.296)	0.684		0.0619(0.0451)	0.102		0.150(0.152)	0.150	

Table XII. (cont'd.)

AlAs	1.20 (0.768)	1.54		0.170 (0.114)	0.214		0.142(0.148)	0.139	
AlSb	1.56 (1.17)	3.15	~0.0 [a]	0.233 (0.180)	0.469		0.149(0.154)	0.149	
GaN	0.185(0.174)	0.917		0.0218(0.0267)	0.107		0.118(0.153)	0.117	
GaP	0.913(0.807)	1.97	0.14[b]	0.140 (0.118)	0.303	0.20[b]	0.154(0.146)	0.154	1.43
GaAs	2.69 (2.12)	4.26	0.73[b]	0.388 (0.301)	0.623	0.65[b]	0.144(0.142)	0.146	0.89
GaSb	5.07 (4.17)	8.08	1.89[b]	0.768 (0.610)	1.36		0.151(0.146)	0.154	
InN	0.277(0.347)	2.01		0.0325(0.0554)	0.246		0.117(0.160)	0.122	
InP	1.50 (1.35)	4.00	~0.55[c]	0.228 (0.205)	0.608	~1.0 [c]	0.152(0.152)	0.152	~1.8
InAs	4.71 (3.64)	8.72	2.06[a]	0.673 (0.538)	1.24		0.143(0.148)	0.143	
InSb	9.18 (6.82)	15.6	5.88[a]	1.38 (1.04)	2.33		0.150(0.152)	0.149	

[a] Ref. (9)

[b] Ref. (37)

[c] M. Engelsberg and R. E. Norberg, Phys. Rev. B 5, 3395 (1972).

Table XIII. Cohesive energy per atom pair and its components for the group - IV elements in eV. The quantities E^0_{coh} and E_{coh} are our calculated values of the cohesive energy without and with the correlation energy E_{corr}, respectively, as discussed in the text. The quantity $\Delta\varepsilon_n^{fit}$ is the value of $\Delta\varepsilon_n$ necessary to fit E_{coh} to E_{coh}^{expt}.

Material	$8(1-S)V_2^{HC}$	$-4\ E_{corr}$	$-4\ E^0_{o\ell}$	$-E_{pro}$	E^0_{coh}	E_{coh}	E_{coh}^{expt}	$\Delta\varepsilon_n^{fit}$
C	17.18	-7.88	21.44	-16.64	22.0	14.1	14.7 [k]	-0.075
Si	5.84	-3.84	14.84	-14.40	6.28	2.44	9.28[k]	-0.855
Ge	5.87	-3.87	14.24	-15.68	4.43	0.56	7.74[k]	-0.898
Sn	4.77	-3.23	12.92	-12.56	5.13	1.90	6.24[k]	-0.542

[k] C. Kittel, "Introduction to Solid State Physics" (Wiley, New York 1971)

Table XIV. Cohesive energy of the binary compounds, using E_G^0 from the full theory, the fitted values of $(\Delta\varepsilon_a+\Delta\varepsilon_c)$ (see text and Table X). All quantities are given in eV.

Material	$-4\,E_G^0$	$-4\,E_{o\ell}^0$	$-4(\Delta\varepsilon_a+\Delta\varepsilon_c)$	$-E_{pro}$	$-E_{trans}$	E_{coh}	E_{coh}^{expt}
SiC	5.00	17.20	3.72	-15.53	0.0	10.4	~13.0 (HC)
BN	13.33	20.08	0.60	-15.58	- 7.24	11.2	~13.5 (HC)
BP	7.25	17.40	3.72	-13.56	- 2.28	12.5	
BAs	7.11	16.76	3.89	-13.74	- 1.78	12.2	
AℓN	9.83	14.64	3.72	-15.52	- 9.96	2.71	9.09 (WB)
AℓP	6.88	13.92	6.84	-13.51	- 4.99	8.84	~ 8.5 (HC)
AℓAs	7.20	13.68	7.01	-13.69	- 4.50	9.70	7.89 (WB)
AℓSb	5.85	13.08	7.18	-12.16	- 3.15	10.8	7.16 (WB)
GaN	9.06	14.84	3.89	-16.62	- 9.78	1.39	~ 8.80 (WB)
GaP	6.36	13.92	7.01	-14.61	- 4.81	7.87	7.02 (WB)
GaAs	6.83	13.64	7.18	-14.79	- 4.32	8.54	6.33 (WB)
GaSb	5.42	13.08	5.76	-13.26	- 2.98	8.02	5.98 (WB)
InN	8.52	13.88	2.47	-15.22	-10.36	- 0.71	~ 7.59 (WB)
InP	6.24	13.20	7.18	-13.21	- 5.39	8.02	6.89 (WB)
InAs	6.55	12.96	5.76	-13.39	- 4.90	6.98	5.64 (WB)
InSb	5.58	12.48	4.34	-11.86	- 3.55	6.99	5.50 (WB)

(WB) N.N. Sirato, "Semiconductors and Semimetals" edited by R. K. Willardson and A. C. Beer (Academic, New York, 1968) Vol. 4.

(HC) Fig. (11) of HC, Ref. (6).

Table XV. Parameters calculated from the expansion method in the appendix, compared with Slater's values (Ref. 24) for H_2 as a function of interatomic distances. d is given in a.u. and the energies are in eV.

	Slater			This Work		
d	K	H	J	K	H	J
0.5	16.47	16.08	15.45	16.47	16.08	15.29
1	15.09	13.80	11.88	15.09	13.80	11.48
1.5	13.34	11.03	8,077	13.34	11.03	7.575
2	11.59	8.383	5.011	11.59	8.386	4.557
2.5	10.02	6.139	2.901	10.03	6.142	2.562
3	8.702	4.374	1.592	8.705	4.378	1.367
4	6.736	2.095	0.4245	6.739	2.096	0.3475